

**In vivo Evaluation of Tissue Engineered  
Islets Derived from Stem Cells Aided by  
Development of Functionalised 3D Scaffold  
Systems and a Nanoporous  
Immunoprotection Device**

**JIJO WILSON J**

**Ph.D. THESIS**

**2023**



**SREE CHITRA TIRUNAL INSTITUTE FOR MEDICAL  
SCIENCES AND TECHNOLOGY  
THIRUVANANTHAPURAM  
INDIA**

**In vivo Evaluation of Tissue Engineered  
Islets Derived from Stem Cells Aided by  
Development of Functionalised 3D Scaffold  
Systems and a Nanoporous  
Immunoprotection Device**

A THESIS PRESENTED BY

**JIJO WILSON J**

TO

SREE CHITRA TIRUNAL INSTITUTE FOR MEDICAL

SCIENCES AND TECHNOLOGY

THIRUVANANTHAPURAM

INDIA

IN PARTIAL FULFILMENT OF THE REQUIREMENTS

FOR THE AWARD OF

**DOCTOR OF PHILOSOPHY**

**2023**

## DECLARATION

I, **Jijo Wilson J**, hereby certify that I had personally carried out the work depicted in the thesis entitled, “**In vivo evaluation of tissue engineered islets derived from stem cells aided by development of functionalised 3D scaffold systems and a nanoporous immunoprotection device**”, except where due acknowledgement has been made in the text. No part of the thesis has been submitted for the award of any other degree or diploma prior to this date.



Thiruvananthapuram

03/11/2023

**Jijo Wilson J**

Reg. No: PhD/2017/10

**SREE CHITRA TIRUNAL INSTITUTE FOR MEDICAL SCIENCES &  
TECHNOLOGY**

THIRUVANANTHAPURAM – 695012, INDIA  
(An Institute of National Importance under Govt. of India)  
Phone-(91)0471-2520242 Fax-(91)0471-2341814  
Email- [vdnair70@gmail.com](mailto:vdnair70@gmail.com) Web site – [www.sctimst.ac.in](http://www.sctimst.ac.in)



**Dr. Prabha D. Nair**

Scientist G, Senior grade (RTD)

Division of Tissue Engineering and Regeneration Technologies

BMT Wing, SCTIMST

Thiruvananthapuram

This is to certify that **Ms. Jijo Wilson J** in the **Division of Tissue Engineering and Regeneration Technologies** of this Institute has fulfilled the requirements prescribed for the Ph.D. degree of the Sree Chitra Tirunal Institute for Medical Sciences and Technology, Thiruvananthapuram. The thesis entitled **“In vivo evaluation of tissue engineered islets derived from stem cells aided by development of functionalised 3D scaffold systems and a nanoporous immunoprotection device”** was carried out under my direct supervision. No part of the thesis was submitted for the award of any degree or diploma prior to this date. Clearance was obtained from the Institutional Animal Ethics Committee for carrying out the study.

03/11/2023

Thiruvananthapuram

**Dr. Prabha D. Nair**

Research Guide



The thesis entitled

**In vivo evaluation of tissue engineered islets derived from stem cells  
aided by development of functionalised 3D scaffold systems and a  
nanoporous immunoprotection device**

Submitted by

**Jijo Wilson J**

for the degree of

**Doctor of Philosophy**

Of

**SREE CHITRA TIRUNAL INSTITUTE FOR MEDICAL SCIENCES AND TECHNOLOGY,**

**Thiruvananthapuram**

Is evaluated and approved by

Dr. Prabha D. Nair

(Research Guide)

Prof. Sarita Gupta

(Thesis examiner)

## **ACKNOWLEDGEMENT.**

*I would never have been able to finish my dissertation without the guidance, help, support and encouragement of numerous people around me. I would like to thank all those who made this thesis possible and it is a pleasant task to express my thanks to all those who contributed in many ways to the success of this study.*

*At this moment of accomplishment, first of all I express my sincere and deepest gratitude to my guide Dr. Prabha D. Nair. This work would not have been possible without her guidance, support and encouragement. Under her guidance I successfully overcame many difficulties. She taught me how to become an independent researcher. I thank her and I am indebted to her for the patience, motivation and enthusiasm shown to me in my failures and difficulties.*

*I am grateful to the present Director, former Directors of this Institute and also The Head, BMT Wing for giving me the opportunity as well as for providing the facilities to carry out my research in this Institute.*

*I would like to thank my Doctoral Advisory Committee members, Dr. Ramesh P, Dr. Rekha M.R and Prof. S Kannan for their valuable suggestions throughout my study.*

*I thank the Deputy Registrar, Academic Division and Project Cell for their help in academic affairs. I acknowledge UGC-JRF for providing financial assistance in the form of research fellowship throughout the tenure.*

*Most of the results described in this thesis would not have been obtained without the support and help of many Scientists and staff of SCTIMST. I am grateful to Dr. Hari krishnan from DLAS for playing a major role in my animal experiments and the surgical implantation of the device. I thank Mr. Manoj, Mr. Sunil and all staff of DLAS for their help in through out my animal experiments. I am thankful to Dr. Renjith. S and Mrs. Radhakumary. C, Common Analytical Facility for the TGA Analysis. I expressed my sincere gratitude to Dr. T V Anil Kumar, Dr. Geetha and Mr. Pratheesh from experimental pathology for their help in histological*

*analysis. I thank Mr.Nishad, Bioceramics Laboratory for the SEM imaging. I also thank Dr.Lissymol P.P, Dr. Deepu D. R, Dental Products Laboratory for the mechanical testing experiments. I also thank Dr. P.R. Anilkumar for helping me with the ELISA plate shaker. I Thank Dr. Rekha M.R and all staff of BST for helping e with nanodrop measurements, Dr. Jayasree and all members of BPI for allowing me to use cold centrifuge. I express my gratitude to the entire faculty who took effort in spending their valuable time and sharing their knowledge in the course work conducted.*

*I also extend my gratitude to The Director, Rajiv Gandhi Centre for Biotechnology, for giving the permission to use the confocal microscope facility and FACS analysis.*

*I immensely thank my Mphil guide Dr. Neethu Mohan from molecular cardiology, SCTIMST for her support and suggestions throughout my study.*

*On a personal note, I would like to thank every member of the Division of Tissue Engineering and Regeneration Technologies (DTERT). Most of all I sincerely thank Dr. Lynda and Dr. Babitha for the support well as for their expert advice, help and friendship. I thank my senior Dr. Rahul V.G for teaching me the basics and also for his valuable suggestions, critical comments and friendship throughout my study. I would also like to thank the former and current members of DTERT Dr. Shiny, Mrs. Nimi, Dr. Dhanesh, Dr. Rakhi, Dr. Merlin, Dr. Neelima, Dr. Sivadas, Dr. Amrita, Ms. Anjitha, Ms. Banu, Ms. Keerthana, Ms. Asha, and Ms. Rukhiya for their cooperation and help throughout my work. I warmly thank all other fellow colleagues for their care and concern. Besides this, several people have knowingly and unknowingly helped me in the successful completion of this project.*

*It's my fortune to gratefully acknowledge the support of my family. Words fail me to express my appreciation to my beloved parents, my sister who were beside me*

*during the happy and hard moments to push me and motivate me. And my friend Sam and his family for their support. I owe everything to them.*

*Last, but not the least, I thank the Almighty for the wisdom and perseverance that he has bestowed upon me during this research project and throughout my life.*

*Jijo Wilson*

# TABLE OF CONTENTS

<b>SYNOPSIS</b> .....	<b>i</b>
<b>CHAPTER 1</b> .....	<b>1</b>
<b>1 Introduction</b> .....	<b>1</b>
1.1 Diabetes mellitus .....	1
1.2 Types of diabetes .....	3
1.2.1 Type I Diabetes Mellitus .....	3
1.2.2 Type II Diabetes Mellitus .....	4
1.2.3 Gestational diabetes mellitus .....	5
1.2.4 Other types of diabetes .....	6
1.3 Treatments for diabetes mellitus .....	6
1.4 Tissue engineering approach .....	8
1.5 Hypothesis.....	11
1.6 Objectives.....	10
1.7 Significance .....	12
<b>CHAPTER 2</b> .....	<b>13</b>
<b>2 Literature review</b> .....	<b>13</b>
2.1 History of diabetes mellitus .....	13
2.2 Islet of Langerhans .....	15
2.3 Insulin hormone .....	15
2.4 Current approaches for the treatment of diabetes mellitus .....	16
2.4.1 Oral antidiabetics .....	17
2.4.2 Insulin therapy .....	17
2.4.3 Pancreas transplantation .....	19
2.4.4 Islet transplantation .....	21
2.5 Cell source for islet transplantation .....	23
2.5.1 Embryonic stem cells.....	25
2.5.2 Induced pluripotent stem cells .....	27
2.5.3 Adult stem cells .....	28
2.5.3.1 Pancreatic stem cells.....	28
2.5.3.2 Mesenchymal stem cells .....	29

2.6 Tissue engineering of islet construct .....	31
2.6.1 Three-dimensional scaffolds.....	31
2.6.2 Role of extra cellular matrix on islet survival and function .....	35
2.6.3 Immunoisolation .....	38
<b>CHAPTER 3.....</b>	<b>42</b>
<b>3 Materials and methods .....</b>	<b>42</b>
3.1 Fabrication and characterization of scaffolds .....	42
3.1.1 Fabrication of wet electrospun scaffolds.....	42
3.1.1.1 Aminolysis and collagen conjugation on scaffold .....	42
3.1.1.2 Ninhydrin assay to quantify amino group .....	43
3.1.1.3 Fourier Transform Infrared (FTIR) analysis .....	43
3.1.1.4 Atomic force microscopy (AFM) analysis .....	44
3.1.1.5 Fiber architecture and porosity measurement .....	44
3.1.1.6 Contact angle measurement .....	44
3.1.2 Fabrication of ECM protein conjugated C-DEXGEL scaffold .....	45
3.1.2.1 ECM protein conjugation on DEXGEL scaffold .....	46
3.1.2.2 Contact angle measurement.....	46
3.1.2.3 Pore architecture and porosity analysis .....	46
3.1.2.4 Fourier Transform Infrared (FTIR) analysis .....	47
3.1.2.5 Swelling test .....	47
3.1.2.6 Degradation study .....	47
3.1.2.7 <i>In vitro</i> cytotoxicity evaluation .....	48
3.2 Isolation and characterization of mesenchymal stem cells .....	49
3.2.1 Cytoskeletal organization .....	50
3.2.2 Expression of stem cell markers .....	51
3.2.3 Multilineage differentiation .....	52
3.3 Rat adipose derived mesenchymal stem cells on scaffolds .....	53
3.3.1 Differentiation of ADMSCs on 2D culture plates.....	53
3.3.2 Differentiation of ADMSCs on wet electrospun scaffold .....	54
3.3.2.1 Morphology of formed ILCs on wet electrospun scaffold .....	54
3.3.2.2 Viability assay .....	54
3.3.2.3 Gene expression studies .....	55
3.3.2.4 Immunofluorescence analysis .....	56
3.3.2.5 Glucose stimulated insulin secretion .....	56
3.3.3 Differentiation of ADMSCs on C-DEXGEL scaffold .....	57

3.3.3.1	Morphology of ILCs during differentiation .....	57
3.3.3.2	Viability assay .....	57
3.3.3.3	Insulin immunofluorescence analysis .....	58
3.3.3.4	Glucose stimulated insulin secretion .....	58
3.4	Isolation and culture of rat islet cells on 3D scaffold.....	58
3.4.1	Isolation of islet from rat pancreas .....	58
3.4.2	Diphenylthiocarbazon (DTZ) staining of rat islets .....	59
3.4.3	Viability and Immunocytochemistry of rat islets .....	59
3.4.4	Islet culture on ECM coated C-DEXGEL scaffold .....	60
3.4.5	Morphology of rat islets on scaffold.....	60
3.4.6	Viability and Immunocytochemistry of rat islets .....	60
3.5	Fabrication and characterisation of immunoprotection membrane .....	61
3.5.1	Synthesis of PU-PVP semi IPN .....	61
3.5.2	Fabrication of immunoprotection membrane .....	62
3.5.2.1	3D printing of immunoprotection membrane .....	63
3.5.2.2	Porosity analysis of 3D printed membrane.....	63
3.5.2.3	Diffusion of molecules across the membrane .....	64
3.5.3	Fabrication of immunoprotective pancreatic transplantation device...64	
3.6	In vivo studies .....	65
3.6.1	Diabetic animal model.....	65
3.6.2	Diabetes induction and metabolic monitoring .....	65
3.6.3	Implantation of tissue engineered construct .....	66
3.6.4	Intraperitoneal glucose tolerance test and serum collection .....	67
3.6.5	Histological analysis .....	67
<b>CHAPTER 4</b>	<b>.....</b>	<b>69</b>
<b>4 Results of the study</b>	<b>.....</b>	<b>69</b>
4.1	Fabrication and characterization of scaffold systems .....	69
4.1.1	Fabrication of wet electrospun scaffold .....	69
4.1.1.1	Aminolysis and collagen conjugation .....	72
4.1.1.2	Confirmation of collagen conjugation by FTIR analysis .....	74
4.1.1.3	Hydrophilicity of the scaffold .....	75
4.1.1.4	Fiber architecture and porosity of the scaffold .....	75
4.1.1.5	Surface topography by AFM .....	76
4.1.2	Fabrication and characterization of C-DEXGEL scaffold .....	77
4.1.2.1	ECM protein conjugation .....	78
4.1.2.2	Change in hydrophilicity of the scaffold .....	79
4.1.2.3	Change in porosity and pore architecture .....	80

4.1.2.4 Swelling ratio .....	80
4.1.2.5 Degradation study .....	81
4.1.2.6 <i>In vitro</i> cytotoxicity evaluation .....	82
4.2 Isolation and characterization of adipose derived mesenchymal stem cells ....	83
4.2.1 Surface marker analysis .....	84
4.2.2 Multilineage differentiation .....	86
4.3 Differentiation of ADMSCs into ILCs.....	86
4.3.1 Rat ADMSCs on wet electrospun scaffold .....	88
4.3.1.1 Differentiation of MSCs on wet electrospun scaffold .....	88
4.3.1.2 Viability of ILCs on scaffold .....	89
4.3.1.3 Hormone expression and functionality of ILCs .....	89
4.3.1.4 Gene expression of ILCs .....	90
4.3.2 Differentiation of ADMSCs on C-DEXGEL scaffold .....	91
4.3.2.1 Morphology of ILCs during differentiation.....	94
4.3.2.2 Viability assay .....	93
4.3.2.3 Hormone expression and functionality .....	94
4.4 Isolation and culture of rat islet cells on 3D scaffold .....	96
4.4.1 Isolation and characterisation of rat islets .....	96
4.4.2 Islet morphology in 3D culture .....	97
4.4.3 Viability of islets on scaffold .....	97
4.4.4 Expression of insulin hormone .....	98
4.4.5 Islet function on the scaffold .....	99
4.5 Fabrication and characterisation of immunoprotection membrane.....	101
4.5.1 Synthesis of PU-PVP semi IPN.....	101
4.5.2 Fabrication of immunoprotective membrane .....	104
4.5.2.1 3D printing of immunoprotection membrane .....	104
4.5.2.2 Diffusion of molecule across the membrane .....	106
4.5.3 Fabrication of IPTD.....	107
4.5.3.1 Viability and insulin secretion of islet/ILCs in IPTD .....	108
4.6 <i>In vivo</i> assessment of differentiated ILC .....	110
4.6.1 Blood glucose measurement .....	111
4.6.2 Response to glucose challenge .....	112
4.6.3 Architecture of the implant .....	113
<b>CHAPTER 5.....</b>	<b>117</b>
<b>5 Discussion .....</b>	<b>117</b>

5.1 fabrication and characterization of scaffolds .....	117
5.2 ADMSC isolation and characterization and differentiation into ILC on scaffolds .....	122
5.3 Islet isolation and culture on scaffolds .....	127
5.4 Fabrication and characterization of immunoprotection membrane.....	129
5.5 In vivo evaluation of tissue engineered construct.....	133
<b>CHAPTER 6</b>	<b>139</b>
<b>6 Summary and conclusion .....</b>	<b>138</b>
Future perspectives .....	141
<b>REFERENCES.....</b>	<b>142</b>

## LIST OF FIGURES

Figure 1.1	Basic principles of tissue engineering	8
Figure 2.1	Islet architecture	15
Figure 2.2	Structure of insulin	16
Figure 2.3	Schematic representation of islet transplantation	21
Figure 2.4	Cell source for the generation of insulin producing cells	25
Figure 2.5	Image explaining the basic principles of islet tissue engineering	32
Figure 2.5	Image showing the loss of extracellular matrix leads to cell death	35
Figure 2.6	Attachment of pancreatic beta cells to extracellular matrix	36
Figure 2.7	Microencapsulation (a) and macro encapsulation (b) strategies of islets	39
Figure 4.1	Schematic representation of wet electrospinning	71
Figure 4.2	Comparison between conventional electrospun sheet and wet electrospun scaffold	71
Figure 4.3	Schematic representation of aminolysis and collagen conjugation to PCL scaffold	73
Figure 4.4	Ninhydrin assay showing concentration of amino group on PCL	73
Figure 4.5	FTIR spectra of PCL, APCL and CPCL scaffolds	74
Figure 4.6	Water contact angle measurement of PCL, APCL and CPCL scaffolds	75
Figure 4.7	Showing SEM images of PCL, APCL and CPCL scaffolds	76
Figure 4.8	AFM analysis of surface topography of PCL, APCL and CPCL scaffolds	77
Figure 4.9	Schematic representation of DEXGEL scaffold fabrication.	78
Figure 4.10	Showing the conjugation of ECM molecule to the DEXGL scaffold	79
Figure 4.11	Contact measurement of DEXGEL and C-DEXGEL scaffold	79

Figure 4.12	SEM images showing porosity and pore distribution of DEXGEL and C-DEXGEL scaffolds	81
Figure 4.14	A&B Swelling and degradation of DEXGEL and C-DEXGEL scaffolds	81
Figure 4.15	Cytotoxicity evaluation of the scaffolds showing	83
Figure 4.16	Phenotypic characteristics of isolated stem cells from rat adipose tissue	84
Figure 4.17	Immunophenotype characterization of rat adipose derived cells	85
Figure 4.18	Flow cytometry analysis of rat adipose derived cells	85
Figure 4.19	Multilineage differentiation of adipose stem cells showing	86
Figure 4. 20	Generation of ILCs on tissue culture plates	87
Figure 4.21	Morphology of islet like clusters differentiated from adipose derived stem cells wet electrospun scaffolds	88
Figure 4. 22	Viability of ILCs formed on scaffold on 30 <sup>th</sup> day of culture	89
Figure 4.23	Immunophenotypic characterization of islet like clusters	90
Figure 4. 24	Quantitative analysis of pancreatic islet specific genes on adipose stem cell differentiated islet like clusters (ILC)	91
Figure 4.25	Phase contrast image of stem cell derived islet like clusters on scaffolds	92
Figure 4.26	Cytoskeletal organisation mesenchymal stem cells during differentiation	93
Figure 4.27	SEM image showing the Differentiation of rat adipose derived stem cells to islet like clusters on scaffolds	93
Figure 4.28	Viability of adipose stem cell differentiated islet like clusters	95
Figure 4.29	Qualitative and quantitative analysis of insulin hormone in generated ILCS.	95
Figure 4.31	Characterisation isolated rat islets	96
Figure 4. 32	SEM image showing the intact cluster morphology of islets	98
Figure 4.33	Viability of rat islets cultured on scaffolds	98
Figure 4.34	Immunoflourescence staining of rat islets on scaffolds	99
Figure 4.35	Functionality and viability of islet cultured on scaffolds	99

Figure 4.36	Quantitative analysis of pancreatic islet specific genes	101
Figure 4.37	showing physico-chemical characterisation of synthesised PU-PVP semi IPN	102
Figure 4.38	Cytotoxicity evaluation of PU-PVP semi IPN	103
Figure 4.39	Design for the fabrication of Immunoisolation membranes	104
Figure 4. 40	Nanopore creation by 3D printing	105
Figure 4.41	Showing phase contrast images of printed layers	105
Figure 4.41	AFM image showing the nano pores created on the surface of 3D printed membranes	106
Figure 4.42	Diffusion of molecules across the 3D printed membranes	107
Figure 4.43	Showing schematic representation of the fabrication of immunoprotective pancreatic transplantation device (IPTD)	108
Figure 4.44	Viability and functionality of islet in immunoprotective transplantation device (IPTD)	109
Figure 4.45	Blood glucose and body weight of diabetic rats transplanted with tissue engineered constructs	111
Figure 4.46	Intra peritoneal glucose tolerance test (IPGT) of animals	112
Figure 4.47	C-peptide concentration in blood serum of rats	112
Figure 4.48	Hematoxylin and eosin staining of retrieved construct	113
Figure 4.49	Trichrome staining of retrieved construct	114
Figure 4.50	Showing insulin immunofluorescence staining of retrieved constructs	115

## LIST OF TABLES

Table 2.1	Types of antidiabetic drugs	17
Table 2.2	Mechanism and action of different types of insulin	18
Table 3.1	Antibody for mesenchymal stem cell characterisation	52
Table 3.2	Trilineage differentiation media composition	52
Table 3.3	Differentiation media for the generation of islet like clusters	54
Table 3.4	3D printing parameters	63
Table 3.5	Test groups for <i>in vivo</i> experiment	67
Table 4.1	Showing contact angle measurements	77
Table 4.2	Test groups for in vivo experiment	110

## ABBREVIATIONS

2D	Two dimensional
3D	Three dimensional
ADMSCs	Adipose derived mesenchymal stem cells
BSA	Bovine serum albumin
DDA	Dextran dialdehyde
DEXGEL	Dextran gelatin
C-DEXGEL	Coated dextran gelatin
DM	Diabetes mellitus
DMEM HG	Dulbecco's Minimal Essential Medium-High glucose
ECM	Extracellular matrix
EDC	(N-ethyl-N'-(3-(dimethylamino)propyl)carbodiimide
EGF	Epidermal growth factor
ELISA	Enzyme-linked immunosorbent assay
ESC	Embryonic stem cells
FBS	Foetal bovine serum
FGF	Fibroblast growth factor
IgG	Immunoglobulin G
ILCs	Islet-like clusters
IPN	Interpenetrating network
IPGT	Intraperitoneal glucose tolerance test
IPTD	Intraperitoneal pancreatic transplantation device
ISCT	International society for cellular therapy
KRBH	Krebs-Ringer bicarbonate HEPES buffer
NHS	N-hydroxysuccinimide
PBS	Phosphate buffered saline

PCL	Polycaprolactone
PCR	Polymerase chain reaction
PU-PVP	Polyurethane-polyvinylpyrrolidone
SEM	Scanning electron microscopy
SFM	Serum free media
STZ	Streptozotocin

## SYNOPSIS

Diabetes mellitus is a chronic, heterogeneous metabolic disorder with a complex pathophysiology. It is characterised by hyperglycemia, or increased blood sugar levels, which are caused by problems in insulin secretion, action, or both. Metabolic dysfunctions related to carbohydrates, fats, and proteins are brought on by hyperglycemia, which can present itself in many different ways. Various microvascular and macro vascular problems of diabetes are frequently brought on by long-term hyperglycemia, and these complications are mostly responsible for the mortality and morbidity in diabetic patients. Globally around 573 million adults are living with diabetes in 2021 and it is expected to rise to 643 million by 2030.

A major treatment strategy for diabetes mellitus includes exogenous insulin administration after monitoring the blood glucose level, but it cannot effectively attain the same level of control achieved by endogenous insulin secretion. As a result, the patients undergoing such treatment often suffer from hypoglycemia and prolonged hyperglycemia induced diabetic retinopathy, nephropathy, neuropathy, cardiovascular diseases, diabetic foot ulcers, etc. Transplantation of pancreatic islets from the cadaveric pancreas has proven to be an effective treatment for diabetes mellitus. The first successful clinical human islet transplantation, also known as the edmonton protocol, emphasizes the importance on the use of steroid-free immunosuppressive regimen with insulin, and antioxidant therapy in conjunction with a larger transplanted islet mass ( $> 11,000$  islet equivalent (IEQ)/kg body weight). This achievement marked a major turning point in the field of islet

transplantation and promoted the opening of several centers around the globe as well as a sharp rise in the quantity of islet transplants. However, it has major disadvantages associated with the unavailability of donor islets, islet loss during transplantation, and continuous supply of immunosuppressants, etc. Additionally, neither the long-term restoration of beta cell activity nor the normalization of blood glucose have been accomplished yet. This is partially caused by the instant blood mediated inflammatory reaction (IBMIR), which is activated when the newly transplanted islets are exposed to the recipient's blood components and induces early islet graft failure. Therefore, a renewable source of beta cells, efficient methods to prevent early graft loss, and induction of allo-immune tolerance are needed to improve the success of islet transplantation procedure and extend the applicability to more patients.

In this situation, tissue engineering is a promising strategy. Tissue engineering provides a method for generating functional insulin-producing cells from progenitor cells or pluripotent stem cells that mimic native islet. The current approach in tissue engineering includes the fabrication of scaffolds from suitable biomaterials and extracellular matrix (ECM) proteins that enable complete immune protection, effective vascularization post-transplantation, and reduction of micro environmental stress of transplanted cells. In order to maintain the proper three-dimensional (3D) architecture of the islet, the scaffold also serve as a structural component. For proper cell orientation, cell adhesion, and to have effective oxygen/mass transfer properties, the scaffold should have a high surface area to volume ratio,

high pore interconnectivity, and geometry. Since islets have a diameter of 100–200  $\mu\text{m}$ , pore size of the scaffold is an important factor for islet culture and ideally, the scaffold's pore size should be higher than the islet diameter. Apart from providing structural architecture, modification of the biomaterial scaffold with ECM components could also provide added functional benefits such as enhanced viability and functionality of transplanted cells.

Another aspect of tissue engineering is to generate insulin producing islet-like clusters from human embryonic stem cells (ESCs), induced pluripotent stem cells (iPSCs), and adult stem cells like mesenchymal stem cells. In this study, we planned to generate insulin secreting islet-like clusters from adult stem cells like adipose tissue derived mesenchymal stem cells. These cells when differentiated directly *in vitro* on the appropriate scaffold systems are expected to overcome the shortage of donor islets. In order to achieve higher differentiation efficiency and maturation in mimicking glucose-stimulated insulin secretion patterns comparable to adult human islets, the potential methods have been continuously improved.

Currently, prolonged graft survival is achieved by using immunosuppressive medications. However, use of long-term immunosuppression can have a number of harmful side effects, including cancer, nephrotoxicity, opportunistic infections, and myelosuppression. Medication that suppresses the immune system is also harmful to the survival and function of transplanted cells. The benefits of islet transplantation may be greatly diminished by these severe side effects. Furthermore, long-term immunosuppressive medication usage can drastically reduce glucose tolerance and increase insulin resistance. To achieve successful islet transplantation, encapsulation

of pancreatic construct in a protective nanoporous semi permeable polymeric membrane is necessary to create a barrier between the transplanted construct and the autoantibodies of the recipient's immune system. The semi permeable membrane will facilitate the transfer of nutrients to maintain the viability and functionality of transplanted cells and also allow the transfer of insulin and glucose to maintain normoglycaemia. Apart from this, it needs to have a well-controlled pore size to exclude the penetration of immune cells, autoantibodies, and pro-inflammatory cytokines.

The main objectives of the study is to develop a suitable highly porous three dimensional scaffold system that can support the attachment and maintain the viability and functionality of pancreatic islet and support the attachment of adipose derived mesenchymal stem cells and formation of insulin producing islet like-clusters and the fabrication of a 3D printed nanoporous polymeric immunoprotection device for the safe delivery of this tissue engineered pancreatic construct which upon implantation in diabetic rat model can decrease hyperglycemia. The thesis entitled "In vivo evaluation of tissue engineered islets derived from stem cells aided by a functionalized 3D scaffold system protected by a nanoporous immunoisolation device" is divided into six chapters. In chapter 1, introduction and background of the study is elaborated which includes pathophysiology and types of diabetes mellitus, current treatment modalities, its advantages and limitations. This chapter also elaborates the importance of tissue engineering in addressing the limitations of current treatment strategies and the fabrication of tissue engineered pancreatic islet

construct using cells, scaffold and growth factors. The study hypothesis “extra cellular matrix protein conjugated 3D biomimetic scaffolds could enhance stem cell differentiation to islet-like clusters and maintain its survival and functionality when transplanted *in vivo* with 3D-printed nanoporous immunoprotection bag” is put forward in this chapter. To prove the hypothesis, major objectives are derived as follows.

- I. Selection and fabrication of scaffold for islet tissue engineering
  - a. Fabrication and protein conjugation of three-dimensional wet electrospun PCL scaffold.
  - b. Fabrication and protein conjugation of Dextran dialdehyde-gelatin scaffold.
- II. Isolation and characterisation of adipose-derived mesenchymal stem cells (ADMSCs) and pancreatic islets from rats and differentiation of mesenchymal stem cells into islet-like clusters (ILC) on 2D and on 3D polymeric scaffolds and its comparison.
- III. Fabrication and characterisation of 3D printed immunoprotection bag for transplantation studies.
- IV. In vivo assessment of the tissue-engineered pancreatic construct for the reversal of the hyperglycaemic condition.

The second chapter is the review of the literature that discusses in greater detail about the aetiology of diabetes and the function of pancreatic islets. This

chapter discusses alternative cell sources, the potential of stem cells to be used in islet transplantation, the signaling cues adopted for their differentiation to islets, and natural and synthetic scaffold systems and their importance in islet tissue engineering. The extracellular matrix (ECM) composition of islets, a review of the extracellular matrix components employed for islet culture, their beneficial effects on improving islet survival and function, as well as their signaling mechanism, are discussed. This chapter also emphasized on the various aspects of immunoisolation of islets during transplantation.

Chapter 3 deals with the experimental designs adopted in the study. First, fabrication and protein conjugation of two different scaffold systems are described. The first is the fabrication and protein conjugation of a highly porous synthetic polycaprolactone based scaffold system by wet electrospinning. To increase the cell attachment, collagen I was conjugated to the PCL scaffold. For that, PCL scaffold is aminolysed with 1,6-hexadiazine followed by collagen I conjugation by EDC-NHS method. The aminolysis and collagen conjugation was confirmed by ninhydrin assay, FTIR and AFM analysis.

Further, the second system was fabricated using two natural polymers dextran and gelatin. First, aldehyde groups were introduced into dextran by periodate oxidation followed by the crosslinking with gelatin. Two ECM proteins collagen IV and laminin were conjugated to the prefabricated scaffold by EDC-NHS method to increase the functionality and viability of cells. Protein conjugation was confirmed

by immunohistochemical analysis and further physicochemical characterisation of the scaffold was carried out to check the effect of protein modification.

In the next section 3.2, the procedure of isolation and characterisation of adipose derived mesenchymal stem cells are described. Followed by the differentiation of isolated mesenchymal stem cells into islet-like clusters (ILCs) on 2D culture system and the differentiation was confirmed by immunophenotyping. Furthermore, formation of ILCs on the two different scaffold system were carried out. The insulin protein expression was analysed by immunofluorescence staining, viability was studied by live/dead assay followed by the quantification of insulin secretion by ELISA. After comparing the insulin secretion of two scaffold systems, the second system composed for dextran aldehyde and gelatin was used for further studies.

In the section 3.4, the procedure for islet isolation and characterisation by dithizone staining and insulin immunofluorescence staining are described. The attachment, viability and functionality of the isolated pancreatic islet on the selected scaffold system is also described.

Section 3.5 describes the synthesis, physico-chemical and cytotoxic evaluation of polyurethane-polyvinyl pyrrolidone for the fabrication of Immunoisolation membrane. The design and fabrication of immunoisolation membrane by 3D printing was elaborated in the following section. Presence of nano pores was analysed by atomic force microscopy and the diffusion of molecules across the membrane was carried out. This section also emphasis on the fabrication

of immunoprotective pancreatic transplantation device (IPTD) followed by the evaluation of viability and functionality of islet and ILCs encapsulated in the IPTD.

Section 3.6 describes the induction of diabetes in rat by streptozotocin injection followed by the *in vivo* implantation of tissue engineered pancreatic construct with and without immunoprotection device in the intraperitoneal cavity of diabetic rats. Blood glucose levels and body weight of implanted rats with diabetic and nondiabetic controls were compared. *In vivo* glucose challenge assay and comparison of serum c-peptide level was also described. Construct retrieval and histological analysis was also described in the last section.

Chapter 4 deals with the results and is divided into six sections. In the first section, the results deals with the process of fabrication of two different scaffold systems. The first sub section describes the fabrication of a synthetic scaffold system by wet eletrospinning of polycaprolactone (PCL). Scanning micrographic image revealed that the wet electrospun scaffold is highly porous with a porosity ranging from 70-120  $\pm\mu\text{m}$ . Amino group introduced on the surface of PCL scaffold was quantified at 1.5 hrs. is  $\sim 1.7 \times 10^{-8}$  mol/mg. In FTIR analysis, formation of two additional peaks at  $1658\text{cm}^{-1}$ ,  $1558\text{cm}^{-1}$  confirms the conjugation of collagen I. Contact angle study shows that after collagen conjugation, the scaffold becomes highly hydrophilic favoring cell attachment.

In the second section, the second scaffold system was fabricated by the cross linking between two natural polymers dextran dialdehyde and gelatin followed by conjugation of collagen IV and laminin. The immunohistochemistry with specific

antibodies conformed the conjugation these ECM proteins on the fabricated natural scaffold. Scanning electron micrograph showed that the scaffold is highly porous and the pores are interconnected with porosity 200-400 $\mu$ m. Contact angle measurement revealed that the scaffold maintained a balance between hydrophilicity/hydrophobicity after conjugation. The scaffold showed a decrease in swelling ratio and degradation after protein conjugation.

Section 4.2 elaborates on the enzymatic isolation and characterisation of adipose derived mesenchymal stem cells (ADMSCs) from rat and its differentiation into islet-like clusters (ILCs) on 2D and on fabricated scaffold systems. The isolated cells are stained positive for cytoskeletal marker actin and vimentin and positive for surface markers CD73, CD90, CD105 and negative for CD34/45. The isolated cells also showed multi lineage differentiation potential. Upon differentiation of isolated ADMSCs into ILCs on 2D surfaces, the generated clusters stained positive for insulin hormone. The generation of ILCs on collagen I conjugated wet electrospun PCL scaffold was compared with conventional 2D electrospun sheets and the size of generated ILCs were also determined. The live dead assay showed that due to the formation of large ILCs on 2D eletrospun sheets, hypoxia induced cell death was observed and wet electrospun scaffold supported the formation of smaller ILCs which are superior in-terms of insulin secretion and viability. The second system made of two natural polymers dextran dialdehyde and gelatin modified with collagen IV and laminin also supported the generation of ILCs. The ILCs formed on natural scaffold system is in the range of 50-200  $\mu$ m diameter and showed superior insulin

secretion than ILCs on synthetic wet electrospun PCL scaffold and thus natural scaffold is selected for further studies. Islet from rat pancreas was isolated by enzymatic digestion and studied for the viability and insulin secretion of islets on the natural scaffold. The laminin and collagen IV conjugated natural scaffold secreted more insulin than the unmodified dextran dialdehyde-gelatin scaffold. Hence, for further studies collagen IV and laminin coated scaffold is selected.

Section 4.3 elaborates the results obtained from the fabrication of nanoporous immunoprotection device by 3D printing. For the fabrication of immunoprotection device, semi interpenetrating network of polyurethane-polyvinylpyrrolidone (PU-PVP) was synthesised as 90:10 compositions. After the polymer synthesis, nanoporous immunoprotection membrane was fabricated by 3D printing. The nano pores was obtained by varying the infill density during printing. AFM analysis revealed that the 3D printed membrane has a nano pores with a diameter of  $200 \pm 50$  nm. The membrane allowed the free diffusion of glucose and insulin and limited the diffusion of immunoglobulin.

In the following section, immunoprotective pancreatic transplantation device (IPTD) was fabricated by encapsulation of islets or ILCs seeded on collagen IV and laminin coated natural scaffold within 3D printed nanoporous membrane. The viability and insulin secretion of islet and stem cell derived ILCs encapsulated in fabricated IPTD was studied and compared with islets and ILCs on scaffold without IPTD. Viability and functionality of islets/ILCs were not affected when cultured within IPTD.

In the final section, tissue engineered construct with and without IPTD was implanted in diabetic rat models and compared the results with diabetic and non-diabetic control animals. Animals transplanted with ILCs on IPTD showed blood glucose reduction compared to diabetic controls, however mature rat islet on IPTD showed better results. Islet on scaffold without IPTD also showed better blood glucose correction but become hyperglycemic after one month of implantation. The histological analysis revealed that, groups transplanted without IPTD showed thick fibrotic layer formation around the construct. Fibrotic layer is very less in group transplanted with IPTD.

In chapter five, the findings of the study are discussed in detail and the results obtained are interpreted. It has shown that differentiation and formation of functional islet-like clusters are dependent on the microarchitecture and porosity of the scaffold. ECM conjugation influenced the insulin secretion and cell attachment. Diabetic animals transplanted with IPTD showed better results in attaining normoglycemia and fibrotic layer formation was also limited.

In chapter 6 the results are summarized and the limitation and future perspective for the development of a better tissue engineered construct is also described.

# CHAPTER 1 - INTRODUCTION

## *1.1 Diabetes mellitus*

Diabetes mellitus (DM) is rising to an alarming epidemic level with morbidity and mortality due to its microvascular and microvascular complications. The increase in the prevalence of DM in most regions across the globe has been parallel to the rapid economic development causing urbanization and the adoption of modern lifestyles. Diabetes mellitus is a group of chronic metabolic disorders characterized by hyperglycemia and glucose tolerance. Hyperglycemia or increased blood glucose level is caused by abnormalities either in insulin secretion or insulin action or both that affect carbohydrate, fat, and protein metabolic dysfunction causing multiple organ failure. The pathogenesis of DM is either due to the autoimmune-mediated destruction of insulin-producing pancreatic beta cells or defects in the insulin action pathway that results in hyperglycemia (Galicía-García et al., 2020).

Fasting blood glucose level of  $< 100$  mg/dl (5.6 mmol/L) followed by  $< 140$  mg/dl (7.8 mmol/L) 2 hrs. after 75 g of oral glucose is considered normal. The criteria for the diagnosis of diabetes includes, any individual with fasting blood glucose  $\geq 120$  mg/dl (7.0 mmol/L) and  $\geq 200$ mg/dl (11.1 mmol/L) two hours following a 75g of oral glucose load with symptoms of polydipsia, polyuria, polyphasic and unexpected weight loss. Additionally, many persons have other glucose-related abnormalities that exhibit either impaired fasting glucose (IFG) levels or impaired glucose tolerance (IGT), which is also referred to as “prediabetes”

with impaired fasting glucose tolerance of 100-125 mg/dl (5.6-6.9 mmol/L). The term "dysglycemia" refers to diabetes, IFG, and IGT taken as a whole. The term "metabolic syndrome" (also known as the "dysmetabolic syndrome" or "diabesity") refers to the concomitant presence of dysglycemia, obesity, dyslipidemia, and elevated blood pressure. The dysmetabolic symptoms include a number of metabolic abnormalities like, insulin resistance, acanthosis nigricans, glucose tolerance, hypertension, central obesity, dyslipidemia, increased plasma uric acid, hypercoagulability, vascular endothelial dysfunction, coronary artery disease, diabetic ketoacidosis, etc. presence of prolonged hyperglycemia leads to secondary complications like retinopathy, peripheral neuropathy, nephropathy, diabetic foot ulcers, etc. (Genuth et al., 2018) (Sapra and Bhandari, 2022).

According to the international diabetes federation (IDF) 2021 atlas, globally around 537 million adults aged between 19-72 yrs. are living with diabetes mellitus and it is projected to rise to 643 million by 2030 and 783 million by 2045. An estimated 240 million adults are living with undiagnosed DM and 90% of undiagnosed diabetes patients are in middle and low-income countries. IDF confirms that diabetes mellitus is one of the fastest-growing health emergencies of the current century with a mortality of approximately 6.1 million in 2021. Increased consumption of refined food and a sedentary lifestyle is the main reason for an increased number of diabetic patients worldwide. In India, approximately 73 million adults have diabetes and the number of undiagnosed patients is even higher India has the highest number of type 1 diabetic patients under the age of 19. This increased

number of diabetic patients causes a huge economic burden on health care cost (IDF atlas 2021).

## ***1.2 Types of diabetes***

Since DM is characterized by complex pathophysiology and diverse presentation, any classification of this disorder is therefore arbitrary, yet useful, and frequently impacted by the physiological parameters present at the time of assessment and diagnosis. The classification now in use is based on the pathogenesis and etiology of the disease and is helpful in determining the necessary therapy and clinical assessment of the disease. It is mainly categorized into Type 1 diabetes mellitus (T1DM), type 2 diabetes mellitus (T2DM), gestational diabetes mellitus (GDM), and diabetes-induced or related with particular specific illnesses, pathologies, and/or syndromes (Yau et al., 2000).

### **1.2.1 Type I Diabetes Mellitus**

T1DM, often referred to as type 1A diabetes mellitus (DM), insulin-dependent diabetes mellitus (IDDM), or juvenile-onset diabetes, accounts for around 5–10% of all diabetes cases. It is an autoimmune condition defined by the T-cell-mediated apoptosis of pancreatic beta-cells, which causes an insulin deficit and ultimately leads to hyperglycemia. Despite the fact that the pathogenesis of this autoimmunity is still not fully understood, it has been observed that both hereditary and environmental variables play a role (Paschou et al., 2017). Most often occurring in infants and children (juvenile onset), the rate of development of this pancreatic-

cell-specific autoimmunity and the condition itself is rapid. It may however occur gradually in adulthood (late onset) (Lucier and Weinstock, 2022).

Autoantibodies in particular are one of the immunological markers that distinguish T1DM from other autoimmune diseases. These autoantibodies are linked to the disease's distinctive immune-mediated cell death. Glutamic acid decarboxylase autoantibodies (GADs) such as GAD65, islet cell autoantibodies (ICAs) to cytoplasmic proteins such as islet cell antigen 512 (ICA512), tyrosine phosphatase autoantibodies (IA-2 and IA-2), insulin autoantibodies (IAAs), and autoantibodies to islet-specific zinc transporter isoform 8 (ZnT8) are among the autoantibodies. For the clinical diagnosis of this condition, at least one of these autoantibodies can be evaluated, but typically more of these immunological markers have been seen in about 85–90% of individuals with new-onset T1DM. The most significant of these autoantibodies, GAD65, is present in around 80% of all T1DM cases followed by ICAs in 60-90%, and finally IA-2 $\alpha$  in 54-75% of all T1DM patients (Hackett et al., 2010) (Van Belle et al., 2011).

### **1.2.2 Type II Diabetes Mellitus**

According to the previous nomenclature, T2DM, often referred to as non-insulin-dependent diabetes mellitus (NIDDM) or adult-onset diabetes, accounts for 90–95% of all cases of diabetes. Insulin resistance and cell dysfunction are the two primary insulin-related disorders that define this type of diabetes. Interruption in numerous cellular pathways causes insulin resistance, which reduces the sensitivity of cells in peripheral tissues, particularly those in the muscle, liver, and adipose

tissue, to insulin. Increased insulin production to maintain normoglycemia is achieved in the early stages of the disease when impaired insulin sensitivity causes cells to hyper function. Hyperinsulinemia, or increased amounts of circulating insulin, thereby prevents hyperglycemia. However, over time, the cells' enhanced insulin secretion is unable to fully offset the drop and moreover, insulin deficiency occurs due to the decreased function of beta cells. Because of this, normoglycemia cannot be sustained, and hyperglycemia emerges (Kaku, 2010). Although insulin levels are lower, the release of insulin usually suffices to stop diabetic keto acidosis (DKA). However, DKA can happen under extremely stressful circumstances, such as those brought on by infections or other pathophysiological situations. Atypical antipsychotics, corticosteroids, and sodium-glucose co-transporter-2 (SGLT2) inhibitors are a few medications that may cause DKA (second-generation antipsychotic drugs). Patients with T2DM frequently do not need insulin therapy at the time of illness start or even subsequently, throughout their lives, if there are no significant physiological stress situations (Galicia-Garcia et al., 2020).

### **1.2.3 Gestational Diabetes Mellitus**

Any degree of glucose intolerance or diabetes that is discovered early on or during pregnancy typically in the second or third trimester is referred to as gestational diabetes. This definition previously included any undiagnosed T2DM that could start before or happen at the start of pregnancy. The most recent recommendations of the International Association of the Diabetes and Pregnancy Study Groups, however, do not include diabetes diagnosed during or after pregnancy

in high-risk women, such as those who are obese, where any degree of glucose intolerance is referred to as previously undiagnosed overt diabetes rather than GDM. GDM differs from any preexisting diabetes in pregnant women and typically goes away shortly after childbirth or pregnancy termination (Plows et al., 2018).

#### **1.2.4 Other types of diabetes**

Other than T1DM, T2DM, and GDM, a number of other types have been found to be linked to a number of other illnesses, including several pathologies and/or many disorders, though in smaller percentages relative to the overall diabetic incidence scenario. The most common of these kinds of diabetes include endocrinopathies, exocrine pancreatic diseases, diabetes resulting from monogenic deficiencies in  $\beta$ -cell function, and those stemming from genetic abnormalities in insulin action. abnormalities in  $\beta$ -cell function that are monogenic and result in diabetes Only 0.6–2% of all cases of diabetes are caused by monogenic abnormalities in  $\beta$ -cell function, the majority of which are maturity-onset diabetes of the young (MODY) and neonatal diabetes, along with a few other uncommon kinds (Hoffman et al., 2022).

### ***1.3 Treatments for diabetes mellitus***

The main objective of treating diabetes is to reduce rise in glucose levels while minimizing the risk of severe hypoglycemia. Anti-diabetic medications are used to reduce blood glucose levels in patients with type II diabetes. Drugs work by either increasing pancreatic insulin secretion (e.g., sulfonylurea), increasing the sensitivity of target organs to insulin (e.g., metformin and thiazolidinediones), or decreasing the

rate at which the gastrointestinal tract absorbs glucose (eg. alpha-glucosidase inhibitor) (Bloomgarden, 2008).

Insulin therapy is crucial for people with type 1 diabetes because the condition's hallmark is an absence or almost nonexistent beta-cell activity. Insulinopenia can cause life-threatening tissue catabolism, hypertriglyceridemia, ketoacidosis, and other metabolic abnormalities in addition to hyperglycemia. Injections once or twice a day can and have mostly averted severe metabolic decompensation over the six to seven decades following the discovery of insulin. The optimal combination of effectiveness and safety for persons with type 1 diabetes has been shown to be provided by increasingly intense insulin replacement, employing numerous daily insulin injections or continuous subcutaneous administration with an insulin pump, over the past three decades (Thota and Akbar, 2022).

Successful pancreatic and islet transplantation can reduce microvascular consequences and restore glucose levels to normal in type 1 DM. To avoid transplant rejection and/or a return of autoimmune islet destruction, patients receiving these procedures must be on lifelong immunosuppression. Given the probable side effects of immunosuppressive medication, pancreas transplantation should only be performed in type 1 diabetic patients who are also receiving renal transplantation or who have severe hypoglycemia or recurrent ketoacidosis despite strict glycemic control. Shortage of donor organ or donor islets are another major shortcoming of pancreas or islet transplantation (Tiwari, 2015).

## 1.4 Tissue engineering approach

The idea of tissue engineering for diabetes therapy is to use biomaterials that offer mechanical support and an appropriate extracellular environment to preserve cell survival and function *in vitro* and *in vivo* for islets or more particularly beta cells. Tissue engineering is a multidisciplinary field that involves the application of engineering and life sciences toward the development of biological substitutes that

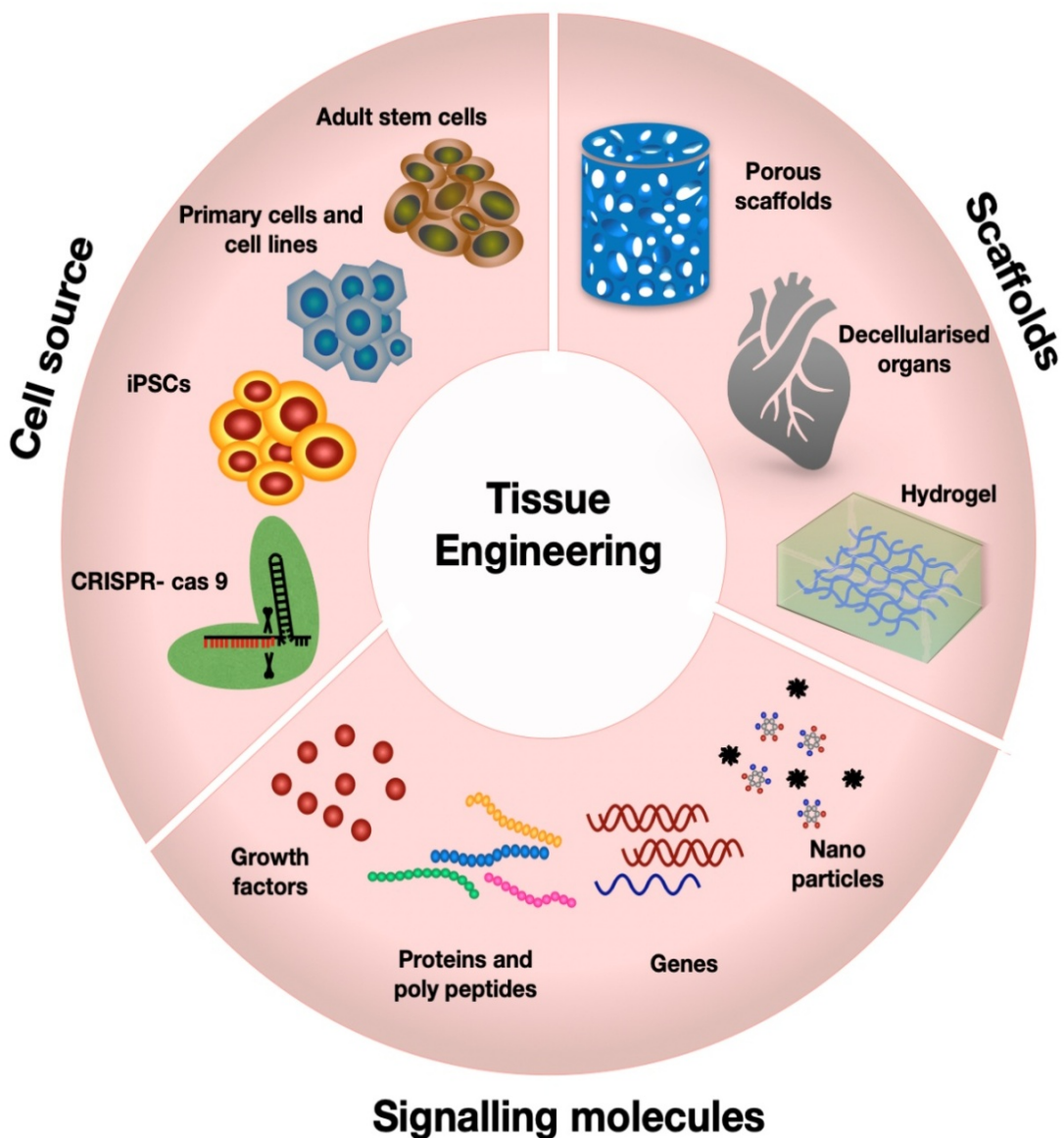


Figure 1.1: Explaining the basic principles of tissue engineering

can be utilized to repair, replace or restore the functions of damaged tissue (Amer et al., 2014). Two main strategies of tissue engineering are scaffold-free and scaffold-based approaches. Scaffold-free or bottom-up strategy involves the administration of prefabricated multi-cellular building blocks such as cell sheets, spheroids, and tissue strands that further synthesize ECM and will create better cell-cell and cell-ECM communication further leading to the development of specific tissue analog. Scaffold based tissue engineering approach is also known as the top-down approach. In this strategy, a 3D biomaterial acts as the support system for cell growth and tissue regeneration. Various complex organs or tissues such as skin, cartilage, bone, heart, pancreas, blood vessel, and liver have been developed so far by tissue engineering processes (Khazaei et al., 2022).

Recent studies have demonstrated the enhanced viability as well as insulin secretion of stem cells differentiated ILCs and isolated islets by culturing them on 3D scaffolds rather than on 2D surfaces. Many TE scaffolds have been used for this purpose composed of natural or synthetic material such as gelatine, alginate, chitosan, polycaprolactone, PLA, PGA, PVA, etc that give mechanical support and also maintain the spherical morphology of transplanted islet or stem cell-derived insulin-producing cells (Hadavi, 2018) (Gomes et al., 2017). To increase the viability and insulin secretion of islets or ILCs, the presence of extracellular matrix components such as collagen IV, laminin, fibronectin, vitronectin, etc are quite vital in the preparation of scaffolds (Alosious and Nair 2014) (Anitha et al., 2020). These molecules bind to integrins on the islet cell or ILCs surface which regulate cell

migration, proliferation, viability, insulin secretion, etc. as per reports, a combination of collagen 1 and collagen IV is found to increase insulin secretion. In yet another study, islets cultured on scaffolds with collagen IV and laminin were shown to increase glucose-stimulated insulin (S et al., 2011).

To achieve successful islet transplantation for T1DM, encapsulation of transplanted pancreatic construct in a protective polymeric membrane is necessary to create a barrier between the transplanted construct and the autoantibodies of the recipient's immune system and serve as an optimal cell encapsulation device that is biocompatible, non-biodegradable and is stable. It should facilitate the mass transfer to maintain the viability and functionality of transplanted cells and also allow the transfer of insulin and glucose to maintain normoglycemia. Apart from this, it needs to have a well-controlled pore size to exclude the penetration of immune cells, autoantibodies, and pro-inflammatory cytokines (Zhang et al., 2022a). There have been numerous reports over the years regarding the macro and microencapsulation devices for islet transplantation with varying degrees of success.

Previously, Polymer-based encapsulation devices such as those made of polycaprolactone (PCL) based nanoporous encapsulation were used as long-term immunoprotection devices. However, the small pores size and biodegradability of PCL make it less efficient for long-term clinical applications. Similarly, a nanofiber-integrated cell encapsulation device (NICE device) was reported to prevent cell escape and reported to maintain normoglycemia over a longer period of time but

failed to obtain controlled nanopores are the critical defects to be used in clinical islet transplantation studies (Desai and Shea, 2017). There are reports

### **1.5 Hypothesis**

It was hypothesized that extracellular matrix protein conjugated 3D biomimetic scaffolds could enhance stem cell differentiation to islet-like clusters and maintain its survival and functionality when transplanted *in vivo* within 3D-printed nanoporous immunoprotection device.

## **6. Objectives**

- I. Selection and fabrication of scaffold for islet tissue engineering
  - a. Fabrication and protein conjugation of three-dimensional wet electrospun PCL scaffold.
  - b. Fabrication and protein conjugation of Dextran dialdehyde-gelatin scaffold.
- II. Isolation and characterization of adipose-derived mesenchymal stem cells (ADMSCs) and pancreatic islets from rats and differentiation of mesenchymal stem cells into Islet-like clusters (ILC) on 2D and on 3D polymeric scaffolds and its comparison.
- III. Fabrication and characterization of 3D printed immunoprotection device for transplantation studies.
- IV. *In vivo* assessment of the tissue-engineered pancreatic construct for the reversal of the hyperglycaemic condition.

## ***1.7 Significance***

Enhancing insulin secretion of stem cell derived islet like clusters and its safe delivery to the diabetic patient is a big challenge in the field of islet tissue engineering. Therefore fabricating a macro encapsulation system to increase the insulin secretion of islet-like clusters and to protect the transplanted cells from host immune system is necessary. In the present study, we fabricated two different scaffold systems conjugated with extracellular matrix protein for the generation of islet-like clusters from adipose-derived stem cells. Here, we have adopted a combinatorial approach in which ADMSCs were differentiated into ILCs on a 3D scaffold to increase the insulin secretion and viability and encapsulation of this construct in a nanoporous membrane to protect the transplanted cells from host immune response and to prevent the undifferentiated stem cell escape during transplantation. Hence, we fabricated an immuno-protective pancreatic transplantation device (IPTD) by encapsulating tissue-engineered pancreatic construct with ADMSC-derived ILCs on a protein-conjugated 3D porous scaffold encapsulated within a 3D printed nanoporous immunoprotective device. This device will ensure the safe and functional delivery of ILCs or islets during transplantation.

## **2 - LITERATURE REVIEW**

### ***2.1 History of diabetes mellitus***

Diabetes mellitus is a chronic metabolic disease that occurs either when the body does not produce enough insulin or the produced insulin cannot be utilized by the body. Both of these situations lead to prolonged hyperglycemia causing microvascular and macrovascular complications such as diabetic retinopathy, neuropathy, nephropathy, stroke, cardiovascular diseases, diabetic foot ulcer, etc. (Sapra and Bhandari, 2022).

The term “diabetes” was coined by Aratus of Cappodocia (81-133AD) meaning “go through” indicating polyuria and described it as a polyuric wasting disease. Later on, in 1675 Thomas Willis added the term “mellitus” meaning “sweet” after discovering the sweetness of the urine of diabetic patients. Nearly 200 years later (1776), Dobson proved that an excess of sugar in the urine and blood was the cause of the sweet taste of urine. In 1869, Paul Langerhans described the anatomy and histology of pancreatic cells, and these cells were named after Langerhans as islets of Langerhans. To fully understand the pathophysiology of diabetes mellitus, another 100 years were required. In 1889, Minkowski and von Mering discovered that pancreatectomized dogs exhibited indications of diabetes, establishing the first known association between the disease and a particular organ. In 1910, Sharpey-Schafer proposed that people with diabetes may be lacking in "insulin," a compound produced in the pancreatic islets (Ahmed, 2002).

There have been tremendous advances in our understanding of the mechanisms causing hyperglycemia throughout the past century. Early in the 1920s, Banting, Best, Collin, and Macleod successfully lowered blood glucose levels and glycosuria in a patient treated with a material extracted from bovine pancreata, demonstrating the important role of insulin in the regulation of glucose metabolism. A new era in diabetes treatment was started after the discovery of insulin. Later, in the middle of the 1930s, clinical observations raised the possibility of a differentiation between diabetes that is "insulin-sensitive" and diabetes that is "insulin-insensitive." These clinical observations could only be translated into pathophysiological and biochemical distinctions in the 1950s when a reliable indicator of circulating insulin became available, and the terms "insulin-dependent" and "non-insulin-dependent" were first coined. The first biosynthetic insulin was introduced in 1970 followed by the introduction of NovoPe, the first insulin pen delivery system by Novo Nordisk in 1985. In 1996 genetically engineered, FDA-approved insulin (lispro) was introduced. Naturally, this insulin is synthesized by pancreatic islets (Lakhtakia, 2013) (Karamanou et al., 2016).

## ***2.2 Islet of Langerhans***

The islets of Langerhans, named after their discoverer Paul Langerhans, are islands of endocrine cells that play a crucial role in energy homeostasis and nutrition metabolism. In humans, 30% of the islet volume is composed of glucagon producing  $\alpha$ -cells, 60% volume is insulin producing  $\beta$ -cells and the

remaining 10% is made of somatostatin producing  $\delta$ -cells, pancreatic polypeptide producing pp or  $\gamma$ - cells and ghrelin producing  $\epsilon$ -cells and these cells are distributed randomly (Fig. 1). Rodents have different islet architecture with  $\beta$ -cell core encircled by other endocrine cell types (Da Silva Xavier, 2018).

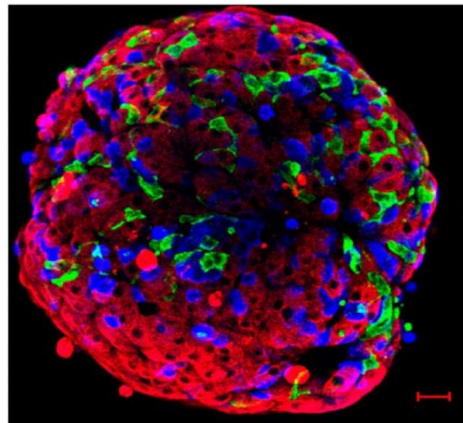


Figure 2.1: Islet architecture: Immunofluorescence analysis of mouse islet for insulin (red), glucagon (blue), and somatostatin (green), scale 20 $\mu$ m.

### ***2.3 Insulin hormone***

Insulin is a 51-residue anabolic protein synthesized by beta cells of pancreatic islets. With 51 amino acids and a molecular weight of 6000 Da, insulin is present in almost all animals, including humans. The two polypeptide chains, one A chain and one B chain, each with 21 and 30 amino acid residues, constitute the human insulin. Two disulfide connection between these two chains (CysA7-CysB7 and CysA20-CysA19), and a third disulfide bond joins CysA6 and CysA11 in chain A and various non-covalent interactions connect the insulin

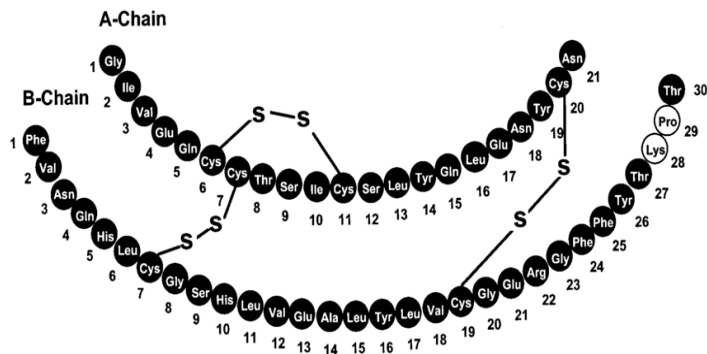


Figure 2.2: Structure of insulin

molecule (Figure 2). The main actions of insulin include: (i) promoting the oxidation and storage of glucose in the liver, as well as converting glucose into triglycerides and protein synthesis; (ii) promoting glucose uptake into cells in muscle tissue and storage of glucose as glycogen; and (iii) promoting glucose uptake into cells in fat tissue and storage of glucose as triglycerides. Any deviation from the functions of insulin leads to diabetes mellitus (Weiss et al., 2000).

## ***2.4 Current approaches for the treatment of diabetes mellitus***

The conventional treatment strategy for DM is antidiabetics and insulin therapy. But it has undesired side effects for patients. This paved the way for the emergence of other treatment modalities such as pancreas or islet transplantation, gene therapies, therapy targeting stem cell differentiation into beta cells, enhancing self-replication of beta cells, etc. (Krentz and Bailey, 2005).

### **2.4.1 Oral antidiabetics**

Different categories of antidiabetic drugs used for DM are listed in table 2.1

Table 2.1 Types of anti-diabetic drugs

S/ N	Drug class	Example of drug	Adverse effect
1	Insulin and analogues	Regular insulin	Hypoglycemia, Weight gain, Insulin allergy, Lypodystrophy at injection sites
2	Sulphonylureas	Glibenclamide	Hypoglycemia, Weight gain, Cardiovascular risk. Rash,Cholestatic jaundice, Bone marrow damage, Photosensitivity
3	Meglitinides	Repaglinide	Hypoglycemia, Gastro intestinal effect, Sensitivity reactions, Lactic acidosis
4	Biguanides	Metformin	
5	GLP-1 agonist	Exenatide	Gastrointestinal effect, Pancreatitis, Risk for cancer and cardiovascular events
6	DPP-1 agonist	saxagliptin	Pancreatitis, risk for cancer, acute hepatitis and kidney impairment
7	Thiazolidinedions	Pioglitazone	Hepatitis, Cardio vascular disease, Bladder cancer Water retention and weight gain
8	Dual PPARagonist	Saroglitazar	Gastritis, asthenia and pyrexia
9	Alpha glucosidase inhibitor	Acarbose	Gastro intestinal effect, Hepatitis
10	Amylin analogues	Pramlintide	Hypoglycemia, Allergy, Glycosuria, Cardiovascular concern
11	SGLT 2 inhibitor	Canagliflozin	

#### 2.4.2 Insulin therapy

Insulin injections continue to be the primary treatment for T1DM during insulin deficiency. When oral hypoglycemic medications fail to stabilize glucose and HbA1c levels in T2DM, insulin may be used as a therapy or in conjunction with other oral hypoglycemic medications. Types of insulin available are listed below (table 2.2) (Silver et al., 2018). Subcutaneous injections are the most common route of insulin administration. There are many devices for subcutaneous insulin delivery such as vials, syringes, pens, insulin pumps etc. there are some limiting factors for insulin

injections such as needle phobia leads to poor compliances and inadequate glycaemic control, and lipodystrophy (Swinnen et al., 2009).

Table 2.2 Mechanism and action of different types of insulin

<b>Insulin Types</b>	<b>Insulin details</b>	<b>Onset</b>	<b>Peak</b>	<b>duration</b>
Rapid-actin insulin	Human insulin analogues 1) Insulin lispro (Humalog) 2) Insulin aspart (Novorapid) 3) Insulin glulisine (Apidra)	15-30 min 12-18 min 12-30 min	0.5-2.5 h 1-3 h 1.5-3 h	2-4 h 3-5 h 3-4 h
Short-acting insulin	Recombinant human regular insulin: 1) Humulin R 2) Actrapid	30-60 min	2-4 h	6-8 h
Intermediate-acting insulin	NPH (Humulin N or insulatard)	1-4 h	8-12 h	12-20 h
Long-acting insulin	Insulin glargine (lantus) Insulin detemir (Levemir)	1-4 h 1-4 h	Peak less Peak less	24 h 18-24 h
Premixed insulin	1) Biphasic (Mixed 30 or Humulin 70/30): premixed 30% regular insulin + 70% intermediate-acting insulin 2) Biphasic (Mixed 50 or humulin 50/50): premixed 50% regular insulin + 50% intermediate-acting insulin 3) Biphasic insulin analogue • (Novomix 30%): premixed 30% insulin aspart + 70% protaminated insulin aspart • (Humalog Mix 25/75): premixed 25% insulin lispro + 75% protaminated insulin lipro	30-60 min 30-60 min 10-20 min 10-20 min	2-8 h 2-8 h 1-3 h 1-3 h	24 h 24 h 24 h 24 h

### **2.4.3 Pancreas transplantation**

Pancreas transplantation is the known therapeutic treatment for DM. In beta-cell penic diabetic patients, pancreas transplantation (PTx) is used to reestablish an endogenous source of servoregulated insulin production. Although at the cost of severe surgical morbidity and lifelong immunosuppression, restoration of beta-cell mass is consistently and reproducibly expected to produce insulin independence in technically successful PTx. Candidates for pancreatic transplantation can be divided into three groups based on renal function: uremic patients, post-uremic patients, and non-uremic individuals (Bahar and Devulapally, 2022). The optimum treatment for uremic individuals is a combined kidney and pancreas transplant. Patients with post-uremic disease may receive a pancreas following a kidney transplant. Patients who are non-uremic and whose diabetes is not well controlled enough to prevent hypoglycemia unawareness or who have developing chronic diabetes complications may be candidates for a pancreas transplant alone (Kochar and Jain, 2021).

The first clinical pancreas transplantation was attempted in 1966 to achieve insulin independence of type 1 DM patient by transplanting duct-ligated pancreatic segments along with kidney transplants at the University of Minnesota and over 30,000 pancreas transplants have been carried out globally since 1966. Although transplanting a portion of a pancreas donated by a living donor is conceivable and available at a few centers, the majority of pancreatic transplants come from deceased donors. In order to prevent graft rejection after a whole organ pancreas transplant, ongoing immunosuppression is necessary (Casanova and en nombre de

Grupo Español de Trasplante de Páncreas, 2017)

A laparotomy, significant vascular exposure, and anastomosis are required for a whole-organ pancreas transplant. Pancreatic exocrine secretions are often managed through a duodenal enterostomy or bladder drainage. Up to 5% to 7% of pancreatic grafts lose their function early due to surgical complications including graft thrombosis, while immunosuppression is the predominant cause of pancreas transplant-related (Casanova and en nombre de Grupo Español, 2017). In comparison to the total number of diabetic patients, only a small number of pancreas transplants are performed due to the limited availability of the human pancreas and the requirement for immunosuppression. The majority of diabetic patients probably won't be able to have a whole organ pancreas transplant regardless of the advancements in surgical technique or immunotherapy.

#### **2.4.4 Islet transplantation**

Islet transplantation is technically simpler and recovers more quickly than full pancreas transplantation for reducing hyperglycemia. The following three severe obstacles prevented the implementation of islet transplantation as a human diabetes treatment during the 1980s: Lack of an effective nontoxic immunosuppressive regimen capable of preventing alloimmune and autoimmune damage to the islet graft, lack of a donor source of human pancreas, inability to reliably extract a sufficient number of the viable islet from the human pancreas. Only half or fewer of the roughly 1 million islets in an adult human pancreas are consistently successfully

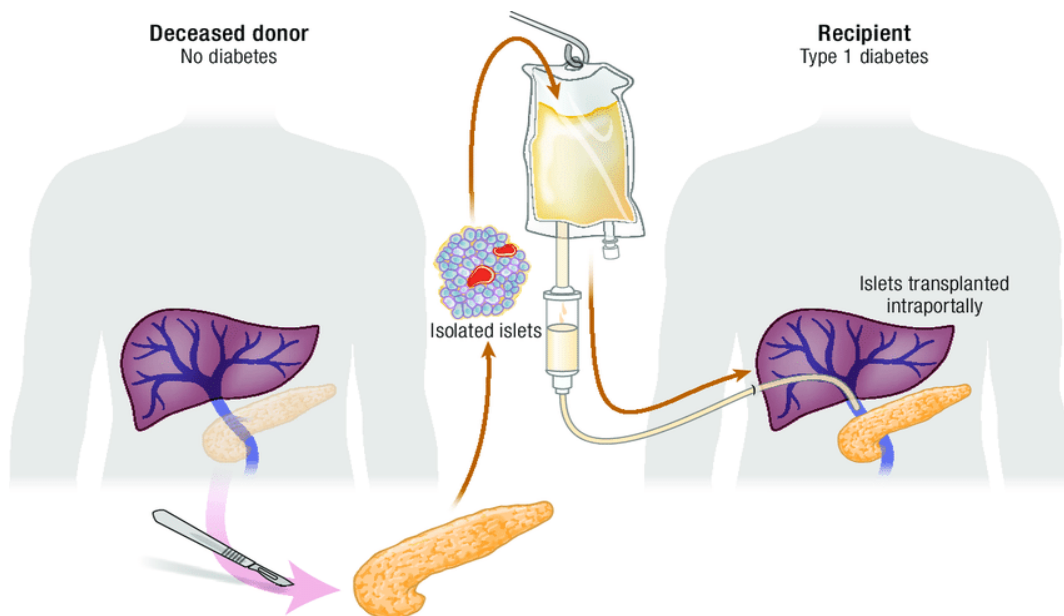


Figure 2.3: Schematic representation of islet transplantation

isolated. As a result, to provide enough isolated islets to achieve insulin independence, clinical islet transplantation frequently needs the donation of two or more donor pancreases (Shapiro et al., 2017).

New attempts at clinical islet transplantation for diabetes were made in the late 1980s and 1990s as a result of significant advancements in the field of islet transplantation, including the development of the collagenase perfusion followed by digestion in Ricordi chamber, dithizone staining, improvements in viability testing, and improved quantification of islet isolation outcomes. Despite the fact that the first attempts at islet transplantation in humans were made in the 1970s, islet transplant numbers increased as a result of advances in islet isolation. There had been 270 islet transplants for people with type 1 diabetes as of December 31, 1995, with a 10% overall insulin independence rate. Fourteen of the 270 patients with insulin dependence who got islet transplants achieved insulin independence for at least a

year. A steroid-free immunosuppressive protocol was created by Shapiro et al. For human islet transplantation. Additionally, a clinical experiment that may make use of multiple pancreas donors was created in recognition of the fact that almost all clinical islet transplant recipients showed partial function. Following islet transplantation, in 2000 Shapiro et al. presented a series of 7 type 1 diabetic patients who were insulin-independent. The steroid-free immunosuppressive treatment employed in these patients is known as the "Edmonton protocol". It included daclizumab (an IL-2 receptor antagonist), sirolimus, and low-dose tacrolimus. The use of numerous donors (up to three donors) to give a significant islet mass and the steroid-free immunosuppressive regimen appeared to be related to the success of this protocol.

As a result of the Edmonton group's success, established islet transplant programs have stepped up their efforts, and new islet transplant facilities have been established. 36 people with type 1 diabetes underwent islet transplantation using the Edmonton procedure as part of an international multicenter trial. 21 people (58%) achieved insulin independence at some time, and 5 of them did so after two years. The outcomes confirmed the Edmonton procedure and constituted a significant advancement in the area of islet transplantation, although it was evident that there were still certain obstacles that needed to be overcome. The majority of recipients' function decreased or was lost over time, insulin independence was not always reached, and infusion of an islet mass bigger than predicted was necessary (Gruessner, 2022).

Currently, the liver is the location of choice for islet transplantation since it requires minimal invasiveness, is easy to access, and has a low risk of bleeding and thrombosis. Through portal circulation, the liver can also oxygenate the transplanted islets until revascularization. This method also enables the delivery of insulin to the liver and intestine (Matsumoto and Shimoda, 2020). The quick establishment of blood flow for nutrient delivery, oxygen supply, and immune regulation is a crucial factor in improving islet graft survival after transplantation. Due to an immediate blood-mediated inflammatory reaction (IBMIR) and an initial immunological response, it is thought that 50% of transplanted islets survive in the first few days. As a result of the lack of vascularization for oxygen and food supply, fewer transplanted islets survive afterward. Apart from the liver, researchers are now focused on the establishment of new transplantation sites for better revascularization and graft survival like an omental pouch, intramuscular, spleen, subcutaneous space, etc (Witkowski et al., 2022).

### ***2.5 Cell sources for islet transplantation***

Supply of donor islet is a limiting factor for islet transplantation, as it is for the majority of organ transplants. Using pigs as an alternate supply of islet cells for transplant is possible due to the improvements in genetic engineering technologies. The presence of several dormant porcine endogenous retroviruses (PERVs), which could harm recipients, is a problem with the use of pigs as islet donors. In order to address this safety problem for the clinical use of porcine-to-human xenotransplantation, all 62 copies of the PERV pol gene were successfully

inactivated using CRISPR-Cas9. This resulted in a >1,000-fold reduction in PERV transmission to human cells (Moore et al., 2015).

It is possible to create pigs with complementary human organs that can be harvested for transplant by combining gene knockouts in important developmental genes with interspecies chimeras as an alternative to employing customized porcine organs. Nakauchi et al., first developed mice with rat pancreatic, and then rats with mice pancreas, as proof of concept for chimera complementation (Triolo and Bellin, 2021). These amazing achievements were made possible by infusing mouse pluripotent stem cells into early-stage rat embryos lacking the Pdx1 gene or rat pluripotent stem cells into early-stage mouse embryos. Furthermore, in recipient mice without chronic immunosuppression, islets obtained from rats with mouse pancreas were able to successfully treat diabetes for more than a year. The therapeutic potential of stem cell-derived islets produced via blastocyst complementation in a xenogeneic host is strongly supported by these studies (Gamble et al., 2018).

Since the demand for endocrine replacement therapy for T1D patients has increased, there has been a lot of interest in the differentiation of stem cells into pancreatic islets and/or insulin-producing beta cells. Studies examining the mechanisms of islet development have influenced efforts to differentiate pluripotent stem cells, whether embryonic stem (ES) cells or induced pluripotent stem (iPS) cells, and adult stem cells into insulin-producing beta cells. To achieve progressive differentiation of the cells through typical developmental pathways, it has taken a lot

of work to optimise the culture conditions, specifically the concentrations of medium ingredients and timing of the activation or inhibition of important signaling pathways (Sim et al., 2021).

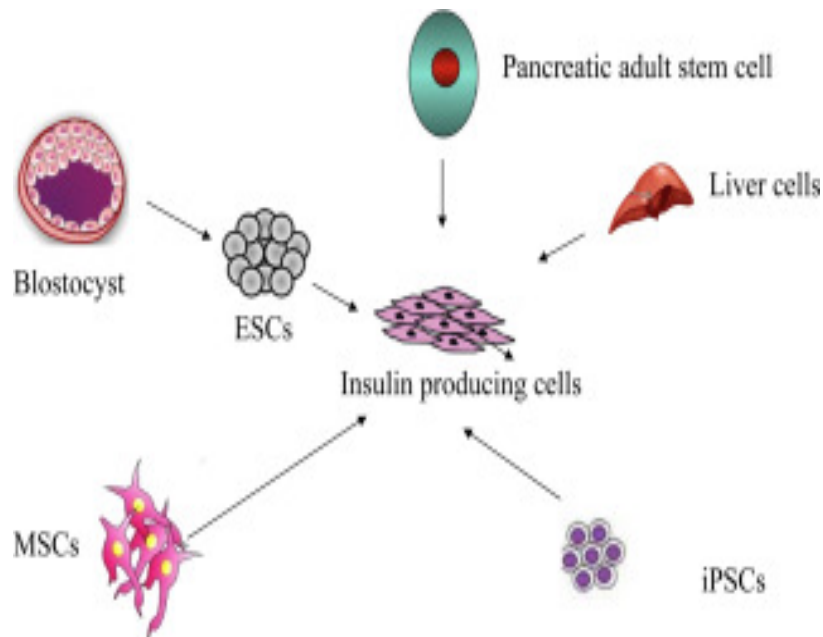


Figure 2.4: Cell source for the generation of insulin-producing cells

### 2.5.1 Embryonic stem cells

The most remarkable feature of embryonic stem cells (ESCs) is their ability to differentiate into every type of adult cell. Human ESCs were differentiated into definitive endoderm, gut-tube endoderm, pancreatic, and eventually islet cells using a stepwise method in which culture conditions were combined with the gradual addition of growth and differentiation agents. In vitro cell generation was capable of producing islet cell-like traits but immature cells (Raikwar and Zavazava, 2009). TGF-family molecules, retinoic acid, and fibroblast growth factors (FGFs), which play important roles in directed differentiation, are used in identical amounts in

protocols from various labs. The expression of stage-specific proteins serves to identify and validate each step, and the ultimate culture of  $\beta$ -cell activity is evaluated by insulin synthesis and secretion in response to glucose. While the pathways targeted by different labs' differentiation methods are similar, some protocols are distinct in terms of the exact chemicals and cell culture setups employed to create glucose-responsive cells. In order to reduce the culture time and increase the effectiveness of  $\beta$ -cell differentiation, various modifications have been made to the stepwise protocol. These changes are frequently made to the protein supplement, its concentration, or both. The differentiated beta cells' inadequate maturity is a significant limiting factor. The islets of Langerhans include  $\beta$ -cells that develop postnatally. As a result, most of the knowledge on beta cell maturation is from animal models (Dang Le et al., 2022) (Jiang et al., 2007).

Even though the molecular mechanisms underlying the functional development are still being studied, the differences between immature and mature  $\beta$ -cells have been identified by comparisons of fetal and adult islets, while mature cells have more insulin secretory granules and are more active at metabolizing glucose than immature cells. Upon maturation,  $\beta$ -cells also express MafA, Ucn3, and Err in addition to the  $\beta$ -cell markers Pdx1, Nkx6.1, and Isl1. Nair et al., obtained about 90% efficiency of  $\beta$ -cells by using cell cluster dissociation, sorting, and aggregation processes. These extra stages sought to replicate the environment in which  $\beta$ -cells mature in accordance with the clustering of islet cells during  $\beta$ -cell maturation during development. In order to effectively differentiate ESCs into beta-cells for islet

cell replacement treatment, differentiation techniques have been modified to mimic the signals the cells experience in vivo. Although there has been significant advancement in these scientific areas, there are still moral concerns about the harvesting of human embryos (Wei et al., 2013).

### **2.5.2 Induced-pluripotent stem cells**

The creation of induced pluripotent stem cells (iPSCs) from adult cells provides a renewable source of pluripotent cells. Adult somatic cells can have developed into ESC-like properties by being treated with Yamanaka factors like OCT4, KLF4, SOX2, and MYC in ESC-like culture conditions. iPSCs can develop into cells from all three lineages and share with PSCs similar morphological and transcriptome properties (Yamanaka, 2006). As a result, these cells carry the same risk of teratoma development as ESCs, but the use of iPSCs avoids ethical dilemmas because no embryos are destroyed. Similar methods to those developed for ESC differentiation can be used to differentiate iPSCs into beta-cells. However, a few studies have also asserted that iPSCs' varying epigenetic profiles and genetic instability have an impact on the requirements for and effectiveness of their differentiation (Maxwell and Millman, 2021).

By modulating the cytoskeleton, Högberg et al., improved the efficiency of  $\beta$ -cell differentiation using hiPSCs and hESCs. They used Latrunculin A to depolymerize the actin network in order to specify the endocrine system because they reasoned that actin polymerization has been proven to affect the specification of the endodermal lineage. In order to facilitate the development of  $\beta$ -cells that

demonstrated GSIS that was comparable to that of human islets and were able to maintain blood glucose levels in diabetic mice. The ability of stem cells to differentiate into beta-cells has improved, although this ability still falls short of native pancreatic islets in terms of responsiveness to glucose and expression of beta-cell-specific genes (Hogrebe et al., 2021).

### **2.5.3 Adult stem cells**

Due to their relative lack of ethical issues and limitless supply, adult stem cells are the most crucial source for cell therapy of numerous disease models. Numerous studies have shown that stem/progenitor cells found in bone marrow, adipose tissue, liver, gut, spleen, salivary glands, neural tissues, and umbilical cord blood can be used to generate insulin-producing cells (Pan et al., 2019).

#### **2.5.3.1 Pancreatic stem cells**

The pancreas is a source of stem cells like duct cells, acinar cells, and stem cells with the ability to differentiate and be reprogrammed to ensure the development of insulin-producing cells. The pancreas' adult stem cells have successfully differentiated into islet-like cells, despite initial disagreements regarding their makeup and even existence. In earlier studies, human pancreatic duct cells have been shown to multiply in vitro and develop into insulin-producing cells. In addition, it was discovered that after partial pancreatectomy in diabetic mice, ductal progenitors might develop into mature ductal epithelial cells. These findings indicate the existence of stem/progenitor cells in the pancreas, which may provide a prospective source of new islets (Silva et al., 2022).

Alpha cells exhibit reversible epigenetic suppression of  $\beta$ -cell genes and may serve as a reserve of pre- $\beta$ -cells in the adult. Partial  $\alpha$ -to- $\beta$  reprogramming is achieved by administering the methyltransferase inhibitor to human islets. Thorel et al., reported that following the loss of  $\beta$ -cells, genetically defined  $\alpha$ -cells immediately coexpress Nkx6.1, followed by insulin expression and the expression of the markers for an adult  $\beta$ -cells Pdx1, Nkx6.1, and Glut2, resulting in the formation of the majority of regenerated cells. According to Nouha et al., GABA promotes the expression of Arx to be downregulated, which causes cells to become  $\beta$ -like cells (Guo and Hebrok, 2009) (Muthyala et al., 2011).

### **2.5.3.2 Mesenchymal stem cells**

Multipotent mesenchymal stem cells (MSCs) are found in adult tissues and are distinguished by their capacity to self-renew and differentiate into cells of several lineages. MSCs can be extracted from bone marrow, the umbilical cord, and adipose tissue. MSCs can be expanded in vitro and, like iPSCs, have the benefit of reducing the chance of immunological rejection. Additionally, MSCs generate numerous growth factors that aid the growth and survival of neighbouring cells and have a low tendency to develop teratomas. Through the inhibition of IFN- $\gamma$  and TNF- $\alpha$  and the upregulation of IL-10, they have been proven to have immunomodulatory effects. Through the production and secretion of VEGF, HGF, IL-6, and TGF-1, MSCs also show pro-angiogenic properties (Rodprasert et al., 2021).

The most investigated sources of MSCs are adipose tissue and bone marrow. While extracting a sample from the bone marrow requires an intrusive, painful

process, liposuction aspiration is a common practice that produces a lot of material that shouldn't be discarded. The total amount of human marrow collected while under local anesthesia is no more than 40 ml. A harvest from adipose tissue, on the other hand, requires only 200 ccs of local anesthesia. Approximately 5000 adipose tissue mesenchymal stem cells can be obtained from 1 ml of adipose tissue aspirate, according to Strem et al., (AT-MSCs). About 600–1000 bone marrow mesenchymal stem cells are produced from the same volume of bone marrow aspirate (BM-MSCs). These findings show that adipose tissue is a superior source of MSCs to other sources. It has been reported that human ADSCs can differentiate into insulin-producing cells in vitro under specific medium conditions and that these cells express pancreatic developmental genes like Isl-1, Ipf-1, and Ngn-3 as well as the islet hormone genes glucagon and somatostatin. In a recent study, human adipose-derived MCs were differentiated to insulin-producing cells using growth factors like activin, FGF, and EGF, when implanted the patients' insulin requirements dropped by 30% to 50%, and their serum C-peptide levels increased by 4 to 26 fold, indicating that differentiated ADSC transplantation may be a useful therapeutic approach for the management of diabetes (Karnieli et al., 2007) (Kochar and Jain, 2021) (Aloysious and Nair, 2014) (Anitha et al., 2020).

## ***2.6 Tissue engineering of islet construct***

During pancreas organogenesis, tissues from several germ layers release and react to growth signals. Cells are grown as monolayers in 2D cultures during in vitro differentiation. As a result, there are no 3D interactions between cell types as they

take place during islet development in vivo. In addition, the islets experience cellular stress due to the degradation of the islet microenvironment and the loss of the supporting matrix that takes place during isolation, purification, and the pre-transplant culture period. Islet function and survival are compromised due to the poor microenvironment and lack of cell-cell contact. Tissue engineering, a process that combines the concepts of biology, engineering, and materials science to create biological substitutes for implantation into the body to either repair, replace, or restore tissue/organ function, has emerged as a means of overcoming the current limitations. The Edmonton technique has many drawbacks that a tissue engineering method has the ability to address, perhaps increasing the lifetime of islet transplantations. The three main elements of engineered tissues are called the tissue engineering triad: cells, scaffolds, and signaling cues. In tissue engineering, the idea of scaffolding is to at least partially mimic the functions of native ECM (Salg et al., 2019) (Giraldo et al., 2010).

### **2.6.1 Three-dimensional scaffolds**

The pancreatic islets lose all of their attachments to the extracellular matrix during the isolation process. The effect of ECM–islet interactions on islet survival and function has been highlighted in a number of studies. Scaffolds are used in tissue engineering procedures for islet transplantation as a temporary ECM that provides the islets with the necessary mechanical support during transplantation. A scaffold should be a three-dimensional, porous, and biocompatible matrix with a controlled

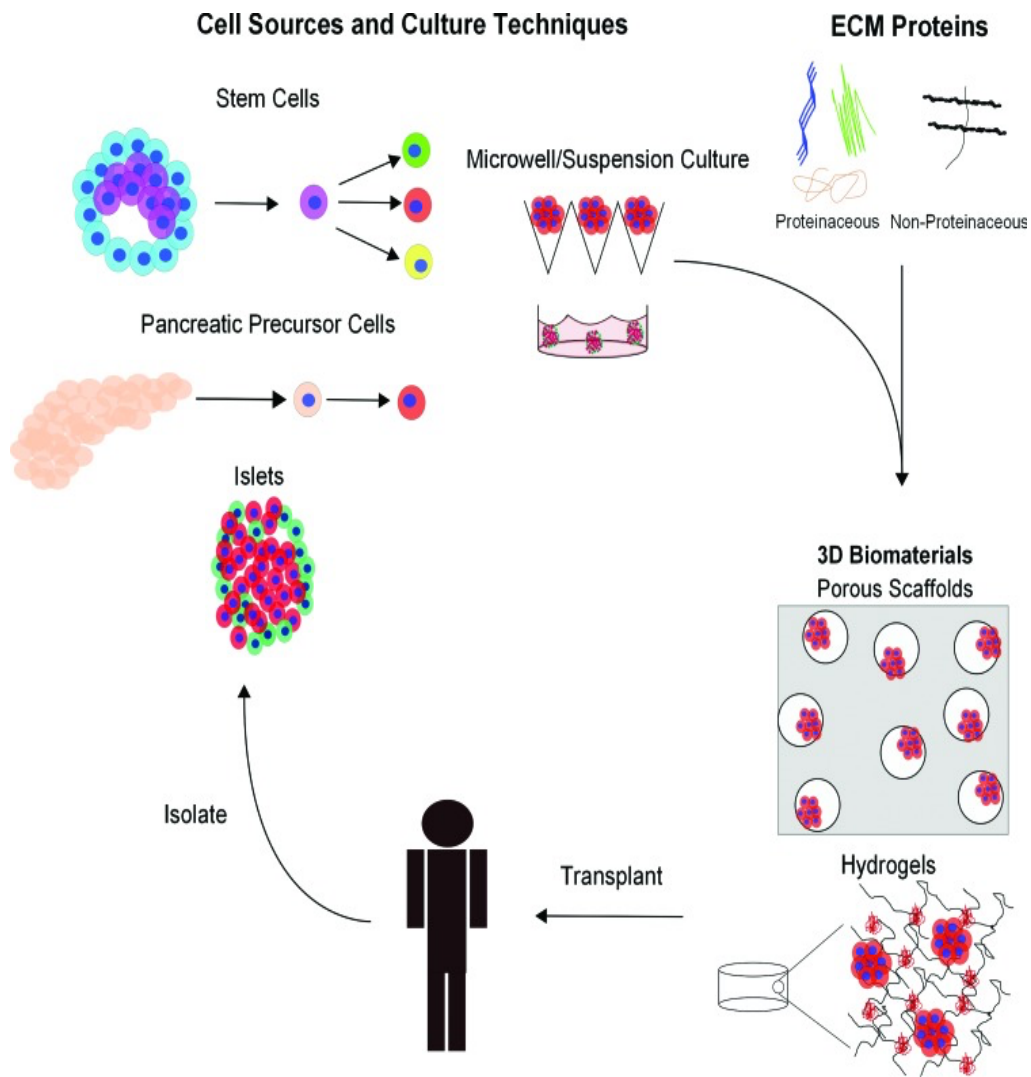


Figure 2.5: Image explaining the basic principles of islet tissue engineering.

rate of tissue creation that results in the degradation of the implanted material and its substitution by the newly created tissue (Li, 2017).

Scaffolds made of both synthetic and natural materials in islet transplantation have been extensively studied. Some of the synthetic polymers that are most frequently utilized in islet transplantation methods are polylactic acid (PLA), polyglycolic acid (PGA), polylactic-co-glycolic acid (PLGA), polyethylene glycol

(PEG), and polydimethylsiloxane (PDMS). These polymers allow for the large-scale fabrication of 3D, biodegradable, and nonimmunogenic structures with repeatable mechanical and physical properties. However, the hydrophobic nature of these materials limits their biocompatibility, and the generation of proinflammatory acidic byproducts during their decomposition limits their use (Kumar et al., 2017). In various *in vitro* and *in vivo* islet and islet-like transplantation procedures in animals, primarily at extrahepatic locations, synthetic scaffolds have been used alone as micro and macro encapsulating devices. The majority of these studies found that the immune response was reduced and that islet engraftment had improved. Furthermore, the combination of these scaffolds and islets with insulinotropic stimuli, such as glucagon-like peptide-1 (GLP-1), exendin-4 (Ex-4), or insulin-like growth factor-1 (IGF-1), as well as proangiogenic factors and cells, such as VEGF, platelet-derived growth factor (PDGF), and endothelial cells (ECs), has shown notable improvements in insulin secretion, islet survival, and engraftment. Furthermore, bioactive compounds that increase the hydrophilicity have been combined with these synthetic scaffolds in order to "functionalize" them, or increase their biocompatibility. Thus, in preclinical islet transplantation procedures, synthetic polymers coupled with various biological materials or with ECM proteins have been used successfully (Salg et al., 2019). Either pancreatic islet or stem cell derived insulin producing cells were cultured in selected biomaterial scaffold *in vitro* and transplanted to the diabetic patient.

Natural polymers have a higher biocompatibility than synthetic scaffolds because they don't release acidic byproducts after decomposition, which prevents an unfavourable inflammatory response. Polysaccharides and polypeptides are the two main kinds of natural polymers used in islet transplantation. The polysaccharides most frequently utilised as scaffolds include agarose, chitosan, and alginate. There are reports suggesting the *in vitro* and *in vivo* islet transplantation experiments, chitosan has been used as a scaffold, either alone or in combination with other materials like collagen or gelatin, to protect against the immune response and to promote islet survival and function. Another polysaccharide that has occasionally been used successfully in islet transplantation is cellulose (Smink et al., 2018).

The use of ECM-derived proteins as a scaffold in these methods is an appropriate modification considering the effect of ECM on islet survival and function. Similarly, scaffolds for islet transplantation have been made of polypeptides, ECM-derived proteins, or polymerizable proteins like fibrin or silk has been reported. One of the primary structural proteins of the ECM, collagen is the most abundant protein in mammals, when employed alone or in combination with growth factors it has increased islet survival and function both *in vitro* and *in vivo*. Fibrin hydrogels are frequently employed in tissue engineering, and 3D fibrin scaffolds function as a temporary ECM, supporting long-term islet survival and function. Although fibrin can help with islet graft vascularization, it is often combined with proangiogenic growth factors, especially when islets are implanted extra hepatic sites (Abadpour et al., 2021). Generation of insulin

producing islet like-clusters (ILCs) on 3D biomaterial scaffold has been reported. The formed islets on the 3D scaffold system showed increased viability and insulin secretion than ILCS formed on 2D surfaces (Aloysious and Nair, 2014) (Anitha et al., 2020).

### 2.6.2 Role of extracellular matrix on islet survival and function

Alternatives to pancreas transplantation include islet transplantation however, islet transplants have a low chance of engraftment. The isolation process, which separates islets from their natural habitat, is probably at least partially responsible for this. Isolation significantly disrupts the interactions between islet cells and macromolecules of the extracellular matrix, as well as the internal vascularisation and innervation of islets. It is known that signalling interactions between islet cells and the ECM control a number of islet physiological processes, such as survival, proliferation,

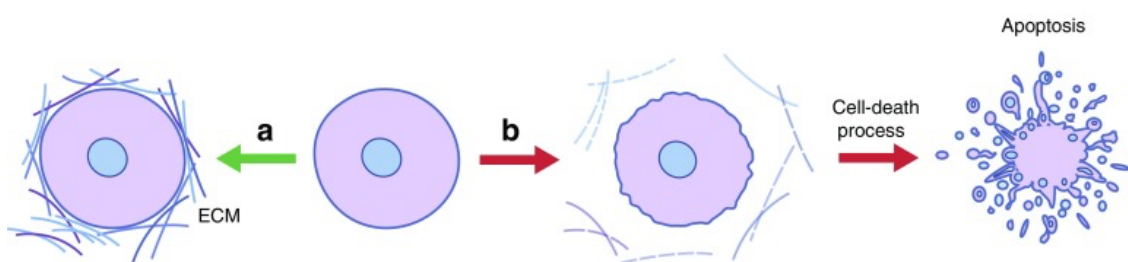


Figure 2.5: Image showing the loss of extracellular matrix leads to cell death.

and insulin secretions. The use of cells, matrix, and growth factors in tissue engineering hold the potential of overcoming the limitations of islet transplantation by creating functional tissue substitute. The benefits of spatiotemporal and matrix

interaction in three dimensions allow for the differentiation of cells to produce islet-like clusters with spherical architecture, maturation, enhanced function, and survival (Smink and de Vos, 2018) (Townsend and Gannon, 2019).

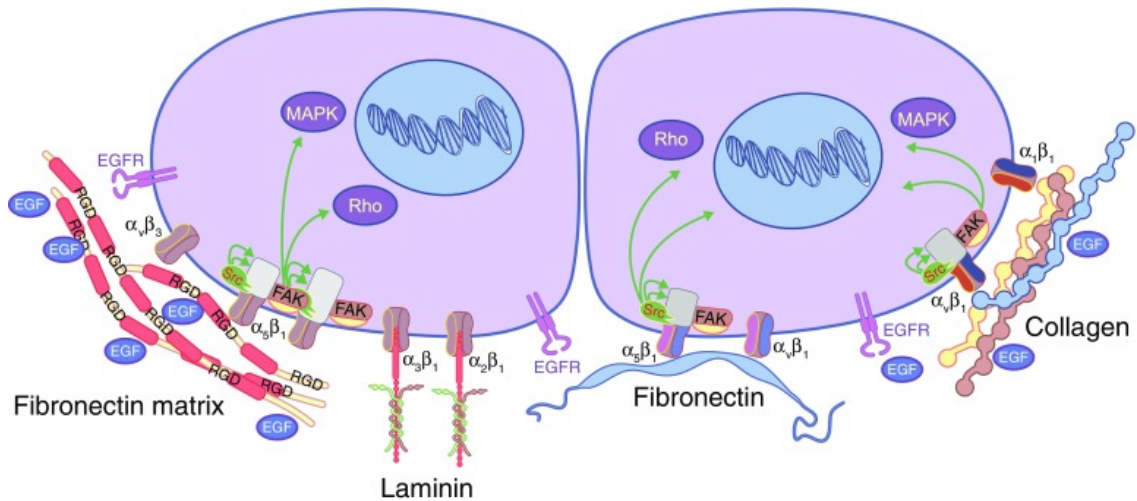


Figure 2.6: Attachment of pancreatic beta cells to extracellular matrix components.

Interactions with ECM or synthetic matrix materials of mature intact islets have been demonstrated to control survival, insulin secretion, and proliferation as well as help to maintain and restore spherical islet morphology (Wieland et al., 2021). ECM-based materials have also been demonstrated to control insulin production, proliferation, and survival in pure  $\beta$ -cell cultures. Most convincingly, it has been demonstrated that incompletely isolated islets that retain some of their natural ECM have much lower apoptosis rates and significantly better insulin response function in vitro than completely isolated and purified islets. The role of interactions between  $\beta$ -cells and the ECM in the activation of NF- $\kappa$ B signaling and the ensuing production of cytokines has been reported. In this report, moderate NF- $\kappa$ B

activation was activated by the interactions between the  $\beta$ -cell and the ECM and was demonstrated to be crucial for proper glucose-stimulated insulin secretion but had no impact on cell survival. The fibroblast growth factor receptor-1 (FGFR1), which regulates pathways involved in  $\beta$ -cell survival, function, and insulin expression, was shown in other research to modify  $\beta$ -cell expression. This receptor also mediates the role of  $\beta$ -cells in vascular endothelial cell remodeling (Llacua et al., 2016).

Adult human islets are generally surrounded by a capsule made up of a single layer of fibroblasts and the collagen fibers they secrete. The peninsular basement membrane (BM), a group of additional matrix proteins, is closely linked to this capsule. It is made up of separate layers of laminin (LM) and nonfibrillar collagen (Coll), which are connected by particular interactions with nidogen/entactin. BM is a specific form of ECM connected to epithelium and endothelium. Most frequently, LM and Coll-IV have been found to make up the peripheral ECM of adult human islets, however, fibronectin (FN), Coll-I, Coll-II, Coll-V, and Coll-VI have also been found. In a recent quantitative analysis of the peripheral matrix composition of human islets, Hughes et al. reported that Coll-VI was abundant (Cheng et al., 2011).

Vitronectin (VN), Fibronectin, and Coll-IV have been found in early precursor tissue emerging from pancreatic ducts, whereas Coll-IV and LM have been found in developing islets, with very little, FN and VN. These findings suggest that the distribution of matrix proteins in developing human islet tissue is different. Data show that VN receptor expression and motility on VN substrates are much higher in fetal  $\beta$ -cells than in their adult counterparts. These results seem to be in accordance

with research on other types of BM, where it has been discovered that VN is typically present throughout development but lacking in mature tissues (Daoud et al., 2010) (Stendahl et al., 2009).

### **2.6.3 Immunoisolation**

To achieve successful islet transplantation for T1DM, encapsulation of transplanted pancreatic construct in a protective polymeric membrane is necessary to create a barrier between the transplanted construct and the autoantibodies of the recipient's immune system and serve as an optimal cell encapsulation device that is biocompatible, non-biodegradable and is stable. It should facilitate the mass transfer to maintain the viability and functionality of transplanted cells and also allow the transfer of insulin and glucose to maintain normoglycemia. Apart from this, it needs to have a well-controlled pore size to exclude the penetration of immune cells, autoantibodies, and pro-inflammatory cytokines (Hu and de Vos, 2019). Generally, encapsulation strategies have been divided into two groups based on the size of the encapsulating structure: micro- and macroencapsulation. These broad categories share several considerations, such as choosing an acceptable tissue donor, preventing graft function loss due to a severe immune response, and providing proper mass transfer (O'Sullivan et al., 2011).

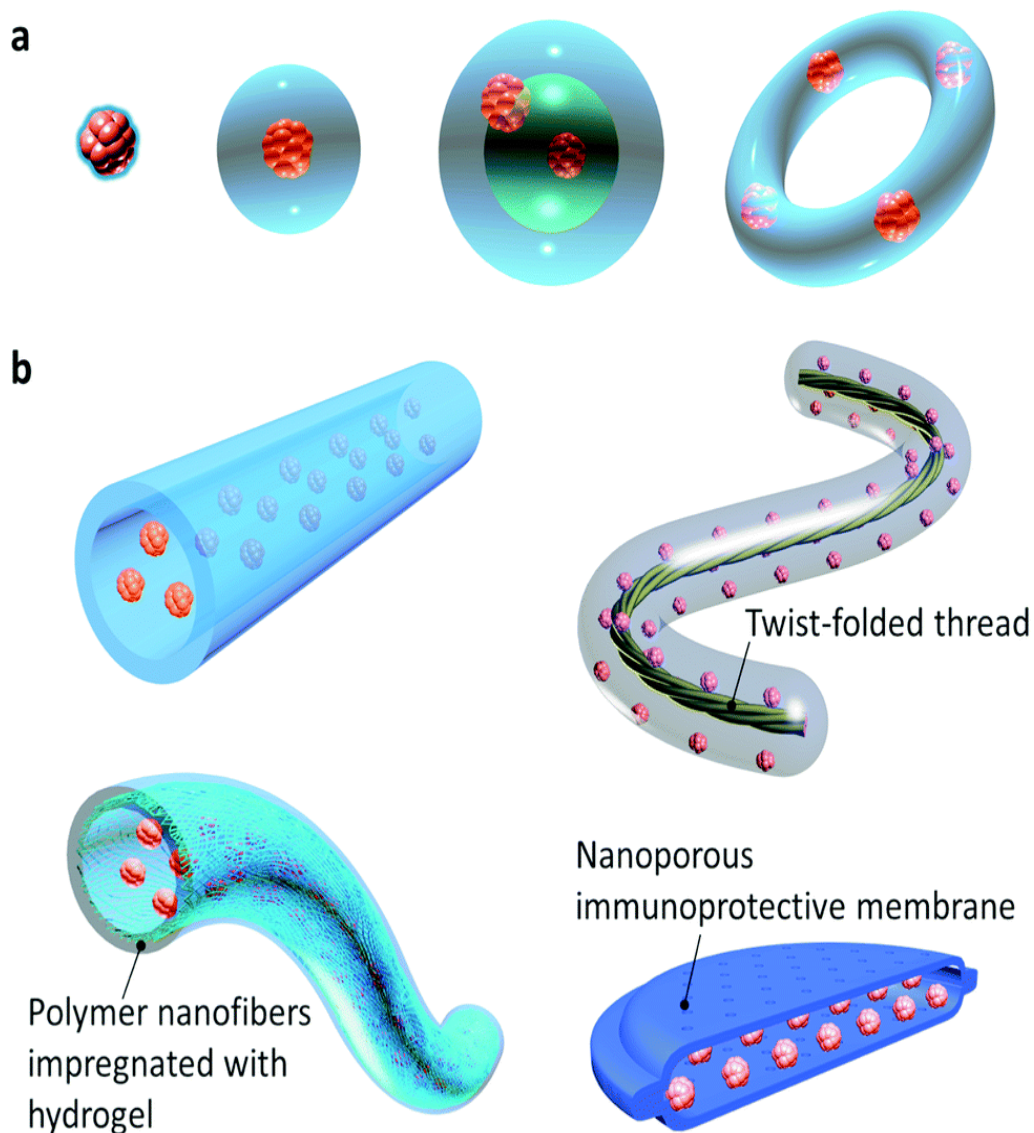


Figure 7: Microencapsulation (a) and macro encapsulation (b) strategies of islets.

One of the earliest examples of islet encapsulation for the treatment of diabetes was the xenotransplantation of human insulinoma tissue into rats in 1933 using membranous bags. However, immune-isolated islet transplantation did not become established until a series of studies in the early 1950s evaluated the survival rates of allo-transplanted tissue into an extravascular zone with and without a cell-impermeable encapsulating membrane. These studies showed that, although

receiving fewer nutrients, the non-vascularized transplanted tissue survived longer when an encapsulating membrane was used because it prevented immune cell interaction and the activation of the direct antigen presentation pathway (Kuwabara et al., 2022).

In 1980, Lim and Sun performed the first experiment on islet encapsulation in alginate microspheres for  $\beta$ -cell replacement therapy. In an effort to reduce nutrient diffusion distance and graft empty space, conformal islet coatings have since become a viable alternative to microcapsules. The enhanced surface area to volume ratio, which is helpful for mass transfer, and ease of implantation of microencapsulation are advantages, while total graft removal and monitoring are inherent disadvantages compared to larger devices (Elnashar et al.,).

The advantages of macro encapsulation over microencapsulation include better graft monitoring and often guaranteed complete cellular retrieval upon device removal. On the other hand, it is more challenging to obtain enough mass transfer and ease of implantation for these constructions. Over the past few decades, a wide range of islet-encapsulating devices have been created. These devices comprise cylindrical, planar, and hollow-fiber constructions. In recent years, improvements in 3D printing and microfabrication technology have also aided in the creation of increasingly complex shapes (Pathak et al., 2019).

There have been numerous reports over the years regarding the macro and microencapsulation devices for islet transplantation with varying degrees of success. Previously, Polymer-based encapsulation devices such as those made of

polycaprolactone (PCL) based nanoporous encapsulation was used as long-term immunoprotection devices. However, the small pores size and biodegradability of PCL make it less efficient for long-term clinical applications. Similarly, a nanofiber-integrated cell encapsulation device (NICE device) was reported to prevent cell escape and reported to maintain normoglycemia over a longer period of time but failed to obtain controlled nanopores are the critical defects to be used in clinical islet transplantation studies (Zhang et al., 2022).

## CHAPTER 3 - MATERIALS AND METHODS

### *3.1 Fabrication and characterisation of scaffolds*

#### **3.1.1 Fabrication of wet electrospun scaffold**

Polycaprolactone of molecular weight 70000-80000 (10%, Sigma Aldrich) was dissolved in 7:3 ratio of chloroform:methanol solvent system and stirred overnight. After dissolving, the solution was loaded into syringe (BD Bioscience, India, 10 ml, 21G) and the wet electro spinning was carried out using a customised flow pump and in which the needle is vertically placed pointing towards the collector. Unlike the conventional electro spinning which used stationary or rotating mandrel, in wet electrospinning fibers were collected over a coagulation bath. Here ethanol is used as the coagulation bath. Distance between needle to the collector was set as 6 cm and humidity was 70%. The flow of wet spinning was optimised at 1ml/hr and the applied voltage is 13 kV. The scaffold from ethanol bath was allowed to air dry in room temperature for 24 hrs and was washed in distilled water and air dried.

##### **3.1.1.1 Aminolysis and collagen conjugation on wet electrospun scaffold**

To aminolyse the PCL, it was immersed in 10% (W/V) of 1,6 hexadecylamine (Sigma Aldrich) / 2-propanol solution (Sigma Aldrich) for a given time at 37 °C. After aminolysis, scaffold was washed thoroughly with distilled water for 24 hrs at room temperature to remove unreacted 1,6-hexadecylamine and in air dried.

For collagen conjugation, aminolysed PCL scaffold was immersed in EDC-NHS solution (4:1 molar concentration) prepared in 10 mM MES buffer for 30

minute. After that, collagen (1mg/ml) dissolved in PBS was added and incubated for 16 hrs at room temperature. After the incubation period, scaffolds were washed and sterilised before cell culture use and aminolysed wet electrospun scaffold is designated as APCL, collagen coated scaffold as CPCL and unmodified scaffold as PCL.

### **3.1.1.2 Ninhydrin assay to quantify amino group**

Ninhydrin assay was carried out to quantify the amino group engraftment on PCL scaffold aminolysis (Yuan et al., 2012). 0.16% (W/V) stannous chloride and 200 mM citric acid was dissolved in 10 ml distilled water and 4% ninhydrin was also dissolved in ethylene glycol monoethyl ether and the two solutions were combined. pH of the solution was adjusted to 5.5 using 1M NaOH and stirred in the dark for 45 minutes. 3 mg of sample was weighed and 1 ml of ninhydrin was added. The reaction mixture was incubated at 100 °C for 20-30 min until the appearance of a purple colour. The formed purple colour was stabilised by adding 200 µl of 50% isopropanol and the formed rhesus's purple colour was recorded at 570nm.

### **3.1.1.3 Fourier Transform Infrared (FTIR) analysis**

To conform the amino group engraftment and collagen conjugation Fourier Transform Infrared (FTIR) spectroscopy was taken using Alpha Bruker spectrometer with diamond ATR accessory. The spectra were taken in the frequency range of 4000-400  $\text{cm}^{-1}$  with 50 scans and resolution of 4 in reflectance mode. The spectra were read using OPUS software and further analysed.

#### **3.1.1.4 Atomic force microscopy (AFM) analysis**

Changes in surface topography after aminolysis and collagen conjugation was studied by Atomic force microscopy. The topography of the surface treated PCL was studied by the change in the texture of the surface by profilometric analysis using Mountains SPIP software from the contact mode AFM images obtained (SPM 5500, Agilent, USA). Abbott firestone plot was derived from AFM images for further texture analysis.

#### **3.1.1.5 Fiber architecture and porosity measurement**

The microstructure of the scaffold was studied using scanning electron microscopy. PCL, APCL and CPCL scaffolds were sputter coated with gold and examined using SEM (JEOL JSM 6390LV, Japan). For calculating the fiber diameter and porosity from SEM images, Image J (NIH, USA) software was used. For calculating the fiber diameter, 30 random fibers from SEM images were analyzed and for evaluating the pore size was also calculated from 3 different SEM images using the above mentioned software.

#### **3.1.1.6 Contact angle measurement**

Hydrophilicity of the modified scaffold was characterized with sessile drop water contact angle (Data physics contact angle OCA Germany) measurement. For contact angle measurement, PCL films were casted on glass slides and aminolysis and collagen coating was carried out. Samples were pasted on a glass slide and 3  $\mu$ l of distilled water was placed over the samples using a motor driven Hamilton

syringe. The image was analysed using OCA 15 contact angle analyser and the contact angle of droplet was calculated using SCA 20 software.

### **3.1.2 Fabrication of ECM protein conjugated C-DEXGEL scaffold**

Dextran dialdehyde-gelatin (DEXGEL) scaffold was fabricated according to our previously reported protocol (Aloysious & Nair 2016). Briefly, 10g of dextran (Sigma Aldrich, MW 35000-45000) was dissolved in distilled water was reacted with 6.6 g of sodium metaperiodate (Sigma Aldrich) for 6 hrs. in dark. The solution is then dialyzed (Sigma, USA, dialysis tubing, Mw cut off 8303) against distilled water for 3 days at room temperature and lyophilized for 48 hrs.

Gelatin type A (Bloom 175, Sigma Aldrich) was dissolved in 1M sodium borate buffer (pH 9.4) at 45 °C and after dissolving, the solution was stirred at 2500 rpm for 20 minutes. There after equal part of dextran dialdehyde dissolved in sodium borate buffer (pH 9.4) was added and continued stirring for another 20 minutes. The solution was then poured in to vials and cross linked at room temperature for 24 hrs. The aldehyde group of dextran dialdehyde will form Schiff's linkage with secondary amino group of lysine and hydroxylysine of gelatin. After cross linking, the scaffold is cut into desired shaped and washed with distilled water and again dried by lyophilisation. ETO sterilization was carried out before cell culture use.

After the scaffold synthesis, two extra cellular matrix (ECM) proteins laminin and collagen IV were conjugated into the carboxylic acid group of gelatin on the DEXGEL scaffold via EDC (1-ethyl-3-(3-dimethyl aminopropylcarbodiimide) and NHS (N-hydroxysuccinimide) conjugation chemistry. Briefly, the DEXGEL

scaffolds were treated with 4 mM EDC and 2 mM NHS in 2-(N-morpholino)-ethanesulfonic acid buffer (MES buffer) with pH 5.5 for 30 minutes. After 30 minutes, 1mg/mL of collagen IV and 500µg/mL of laminin were added and incubated for 24 hrs. at room temperature. After the conjugation, scaffolds were washed thoroughly in distilled water to remove unreacted materials. The protein-conjugated scaffold was designated as C-DEXGEL and unconjugated as DEXGEL.

#### **3.1.2.1 ECM protein conjugation on DEXGEL scaffold**

To conform the collagen and laminin conjugation, immunohistochemical analysis was carried out. For that scaffolds were processed and paraffin embedded. 4 µm thickness sections were taken for further staining. For immunostaining, sections were deparaffinised by dipping in xylene and graded alcohol and immunohistochemistry was carried out using kit (Biogenex).

#### **3.1.2.2 Contact angle measurement**

For contact angle measurement, DEXGEL was casted over glass slides and protein conjugation was carried out as mentioned in section 3.1.2. After washing and drying, contact angle was taken to study the change in hydrophilic after protein conjugation as mentioned in section 3.1.1.6.

#### **3.1.2.3 Pore architecture and porosity analysis**

After conjugation, scaffolds were washed, lyophilized and sputter coated with gold and analyzed using scanning electron microscopy (JEOL JSM 6390LV, Japan) to study the pore morphology and microarchitecture of the scaffold as mentioned in section 3.2.1.5.

#### **3.1.2.4 FTIR analysis**

To study the change in structural analysis after protein conjugation, FTIR was carried out as mentioned in section 3.1.1.3

#### **3.1.2.5 Swelling test**

To study the change in swelling properties before and after protein conjugation, samples of known weight were immersed in PBS with pH 7.4 for known intervals of time. The swollen samples were taken out and excess PBS was blot dried followed by immediate weighing. The weight of the scaffolds was taken at intervals until the weight reached equilibrium with time. The swelling percentage was calculated using the formula

$$\text{Swelling ratio} = [(W_f - W_i) / W_i]$$

Where,  $W_i$ - initial weight of dry scaffold

$W_f$ - weight of swollen scaffold

#### **3.1.2.6 Degradation study**

Change in degradation profile before and after protein conjugation of scaffolds was studied by immersing the pre-weighed sample in 60 $\mu$ g/mL of collagenase solution at 37 $^{\circ}$ C and monitoring the weight loss over a period of 30 days. At 5 day intervals, the solution was removed, samples were washed and dry weight was taken after lyophilization and the percentage of degradation was calculated using the formula,

$$\text{Weight loss (\%)} = [(Initial\ weight - Final\ weight) / Initial\ weight] \times 100$$

### 3.1.2.7 *In vitro* cytotoxicity evaluation

Further, *In vitro* cytotoxicity of the protein conjugated and unconjugated scaffolds were carried out by direct contact, MTT assays, and live dead assay. For direct contact assay (ISO-10993-5) briefly, a scaffold (4 mm diameter and 3 mm thickness) was placed over a confluent monolayer of L929 mouse fibroblast cells and incubated for 24 hrs at 37 °C and 5% CO<sub>2</sub>. After the incubation period, culture plates were examined under a phase contrast microscope to study the morphological changes. The morphological changes of the cells in contact with the scaffold is compared with negative non-cytotoxic high-density polyethylene and positive cytotoxic polyvinyl chloride controls.

For the MTT assay, extracts of DEXGEL and C-DEXGEL scaffolds (4mm diameter and 3mm width/mL medium) were collected at different time points such as day 1, 7, and 14. L929 cells were grown on 96 well plates till semi confluence and culture media was replaced with 100% extract prepared in cell culture media and incubated for 24 hrs. Cell cultured in normal cell culture media is used as blank control. After the treatment period, 5 mg/mL of MTT prepared in PBS was added and incubated for 3 hrs. at 37 °C. MTT solution was then removed and formazan crystals were solubilized by adding DMSO and incubated for 30 minutes. Optical density was recorded at 540 nm using ASYS UVM 340. Untreated cells are considered as controls. Data given are mean  $\pm$  standard deviation of three similar experiments with n = 6. The percentage cell viability was calculated using the formula,

Percentage cell viability= [(Absorbance of test extract treated cells / Absorbance of Control cells) ×100]

The viability of L929 cells cultured on the DEXGEL and C-DEXGEL scaffold was also measured studied by live/dead staining. For that L929 cells with density  $0.5 \times 10^6$  were seeded on the scaffold (4 mmX3 mm) and allowed to attach for 1 hrs. and complete media was added. The cells were allowed to grow on the scaffolds for 7 days and live/dead staining was carried out using LIVE/DEAD Viability/Cytotoxicity Kit for mammalian cells (Thermo Fischer, USA). Briefly, the culture media was removed and the construct was washed with PBS. Constructs were incubated with 1  $\mu$ l of calcein AM and 1  $\mu$ l of ethidium bromide in 1 ml PBS for 20 minutes at 37 °C. After PBS washing the construct were observed under confocal laser scanning microscope (Nikon A1Rsi, Japan).

### ***3.2 Isolation and characterization of Adipose Derived Mesenchymal stem cells (ADMSCs)***

Adipose-derived mesenchymal stem cells were isolated from the inguinal fat pad of a rat after obtaining consent from Institute Animal Ethics Committee and Institutional committee for stem cell research using our previously reported protocol (Aloysious and Nair 2014). For cell isolation wistar rat weighing 200-250 g were selected and after anaesthetizing the animal with CO<sub>2</sub>, inguinal fat pad was aseptically collected in PBS containing 10X antibiotic-antimycotic (Gibco-USA). Adipose tissue was washed, chopped and digested with 0.1% collagenase 1 for 1 hr at 37 °C. Media

with serum was added to stop the digestion and the digested solution were centrifuged at 1800 rpm for 10 min. The supernatant was removed and pellet was resuspended in growth medium containing dulbecco's modified eagle's medium-high glucose (DMEM HG) (Gibco USA), 10% foetal bovine serum (FBS) (Gibco USA) and 1X ABAM. The isolated cells were plated on a 25 cm<sup>2</sup> culture flask (Thermo scientific, nunc) and cultured in a humidified incubator with 5 % CO<sub>2</sub> and 37 °C. The culture media was changed every alternate day. The morphology of the cells was observed under phase contrast microscopy. After reaching confluence the cells were subcultured using 0.25% trypsin-EDTA (Gibco USA) and seeded at a density of 2 x 10<sup>4</sup> cells/ cm<sup>2</sup> for further expansion.

### **3.2.1 Cytoskeletal organisation**

Isolated mesenchymal stem cells were seeded on 6 well tissue culture plates at a density of 1 x 10<sup>4</sup> cells/ cm<sup>2</sup> for F-actin staining. After reaching 70% confluence, cells are fixed with 4% paraformaldehyde for 20 min at room temperature washed with PBS and cells were permeabilised with 50% chilled methanol for 5 min. F-actin was stained with phalloidin-fluorescein iso-thiocyanate 488 (Invitrogen, Alexa Fluor 488, USA). Cells were incubated with phalloidin Alexa flour 488 for 30 min in dark. The nuclei were counter stained with 4,6-diamidino-2-phenylindole (DAPI) (Gibco USA). The stained cells were imaged with fluorescent microscope (Olympus Microsystem BH2, Japan).

### **3.2.2 Expression of stem cell markers**

The isolated mesenchymal stem cell's immunophenotyping was analyzed by immunofluorescence staining and flow cytometry analysis for the expression of positive and negative markers specific for stem cells. For immunostaining, cells were grown in monolayer on a 12 well tissue culture plate and after reaching sub confluency culture media was removed and washed with PBS. Cells were then fixed with 4% paraformaldehyde for 20 mins. After PBS wash cells were locked with bovine serum albumin (10mg/ml) for 30 minutes. Cells were incubated with mesenchymal markers such CD73, CD90 and CD105, CD34/CD45 for 1 hr. For cellular antigen vimentin, cell was permeabilised with 50% chilled methanol and blocked. After that incubated with vimentin antibody for 1 hr. Cells were then washed with PBS and incubated with specific secondary antibodies for 1 hr in dark. Nuclei were counter stained with DAPI and the stained cells were imaged with fluorescent microscope (Olympus Microsystem BH2, Japan). For flow cytometry analysis, cells cultured on tissue culture flask was trypsinised using 0.25% trypsin-EDTA and stained with CD73, CD90 and CD 105, CD43/45 using the above mentioned protocol. After washing, the percentage of positive cells were counted using flow cytometry with corresponding isotype controls using BD FACS Aria cell sorter. A minimum of 10000 events were recorded for each sample and the data was analysed using flowjo software.

Table 3.1 Antibody for mesenchymal stem cell characterisation

Primary antibody	Secondary antibody
Vimentin (SC biotechnology)	Anti-mouse (SC biotechnology)
CD90 (Invitrogen)	Anti-rabbit (invitrogen)
CD73 (Invitrogen)	(Anti-mouse (SC biotechnology))
CD105 (SC biotechnology)	Anti-mouse (SC biotechnology)
CD34 (Biolegend)	Anti-rabbit (invitrogen)

### 3.2.3 Multilineage differentiation

To evaluate the multi lineage differentiation potential, adipogenic, chondrogenic and osteogenic differentiation potential was carried out using appropriate differentiation media listed in table. Cells were seeded at a density of  $2 \times 10^4$  cells/cm<sup>2</sup> with specific induction media and cells growth without any additional factor served as controls. After specific time periods, adipogenic differentiation was analysed by Oil Red O staining, osteogenic differentiation was

Table 3.2 Trilineage differentiation media composition.

Chondrogenic Medium	Osteogenic medium	Adipogenic medium
DMEM HG	DMEM HG	DMEM HG
FBS 10%	FBS 10%	FBS 10%
ABAM 1X	ABAM 1%	ABAM 1%
NEAA 1X	$\beta$ -glycerol phosphate (60 $\mu$ g/ml)	Dexamethazone ( $10^{-6}$ M)
L-Glutamine (0.2mM)	Ascorbic acid (50 $\mu$ g/ml)	IBMX (0.5mM)
Sodium pyruvate (0.1mM)	Dexamethazone ( $10^{-8}$ M)	Indomethacin (50 $\mu$ M)
Dexamethazone ( $10^{-7}$ M)		
Ascorbic acid (50 $\mu$ g/ml)		

confirmed by Alizarin Red staining and chondrogenesis was studied by toluidine blue staining.

### ***3.3 Rat adipose derived mesenchymal stem cells on scaffolds***

#### **3.3.1 Differentiation of ADMSCs on 2D culture plates**

Differentiation of adipose derived mesenchymal stem cells (ADMSCs) into islet-like clusters (ILCs) was carried out using a 3 step protocol. For the generation of ILCs, ADMSCs were seeded on the cell culture plated and after reaching confluence, culture media was removed cells were supplemented with three different induction medium over a period of 21 days as listed in the table.

The morphology change and cluster formation during differentiation was observed using phase contrast microscopy and size of the formed clusters was calculated using ImageJ software. The differentiation was confirmed by the insulin immunofluorescence staining at the end point of differentiation. For that formed islets were fixed with paraformaldehyde for 30 minutes and after PBS washing permeabilised with 0.1% tritonX from 5 minutes. PBS washing was given thereafter and blocked with BSA (10mg/ml in PBS) for 30 minutes. After blocking the ILCs were incubated with specific antibodies such as anti-insulin (Santa Cruz biotechnology), glucagon and somatostatin (Invitrogen USA) for overnight at 4 °C. ILCs were then washed and stained with corresponding secondary antibodies tagged with FITC of phycoerythrin (Invitrogen USA). The nucleus is counterstained with

DAPI (Gibco USA) and imaged with Nikon AIR laser scanning confocal microscope.

Table 3.3 Differentiation media for the generation of islet like clusters

Serum free media A (SFM A)	Serum free media B (SFM B)	Serum free media B (SFMC)
DMEM HG	DMEM HG	DMEM HG
1X ABAM	1X ABAM	1X ABAM
$\beta$ -mercaptoethanol (50 $\mu$ M)	NEAA (1X)	B27 supplement (1X)
Activin A (4nM)	L-Glutamine (2mM)	Activin A 10ng/ml
	B27 supplement (1X)	Nicotinamide (10mM)
	Basic FGF (20ng/ml)	
	EGF (20ng/ml)	

### 3.3.2 Differentiation of ADMSCs on wet electrospun PCL scaffold

The formation ILCs on the PCL and CPCL wet electrospun scaffolds were compared with ILCs on the conventional 2D electrospun sheet. For that ADMSCs were seeded at a density of  $1 \times 10^6$  cells/scaffold and differentiation was carried out as described in section 3.3.1.

#### 3.3.2.1 Morphology of ILCs on wet electrospun scaffold

The morphology of formed ILCs after differentiation on PCL, CPCL wet electrospun scaffolds and 2D electrospun sheet was analysed using scanning electron micrographs (SEM) (JEOL JSM 6390LV, Japan). Before SEM analysis, ILCs on scaffolds was fixed with 4% paraformaldehyde for overnight at 4 °C and washed

with PBS followed by distilled water and observed under environmental scanning electron microscope (Quanta FEI, Hillsboro, USA).

### **3.3.2.2 Viability assay**

The viability of differentiated ILCs on PCL & CPCL wet electrospun scaffold and 2D electrospun sheet was analyzed by live/staining after 30 days using LIVE/DEAD Viability/Cytotoxicity Kit for mammalian cells (Thermo Fischer, USA) as mentioned in section 3.1.2.8. The images were analyzed using laser scanning confocal microscope (Nikon A1R is USA). The size of the ILCs formed on scaffolds was calculated using ImageJ software (National Institute of health, USA).

### **3.3.2.3 Gene expression studies**

Quantitative real-time PCR (qRT-PCR) was used to study the gene expression islet-specific markers such as insulin, glucagon, somatostatin, Pdx1, Nkx6.1, and GLUT2 after differentiation. The gene expression of ILCs on CPCL wet electrospun scaffold was compared with ILCs formed of 2D electrospun sheets. For gene expression studies, total RNA was isolated from the ILCs on scaffolds using trizol reagent (Gibco USA) and the isolated RNA was quantified using nanodrop spectrophotometer. From the isolated RNA, cDNA was synthesized using a high capacity cDNA reverse transcription kit (Applied Biosystems) using thermocycler (Eppendorf Master cycler, USA). For qRT-PCR, Power up™ SYBR™ Green Master mix (Applied Biosystems) was used according to the manufacturer's protocol using the qtower RT PCT (Analytic jena). Primers used is listed below in the table.

The fold change of islet-specific genes relative to ADMSCs culturing without differentiation media were calculated using the  $2^{-\Delta\Delta C_t}$  formula after  $\beta$ -actin normalization for each set of experiments. A minimum of replicates were used for each samples.

#### **3.3.2.4 Immunofluorescence analysis**

The ILCs formed on CPCL scaffold, APCL scaffold and electrospun sheets were analyzed for the expression of islet specific insulin hormone by immunofluorescence staining. The protocol used was as mentioned in section 3.3.1.

#### **3.3.2.5 Glucose stimulated insulin secretion**

ILCs on CPCL scaffolds and 2D electrospun sheets were washed and pre incubated with Krebs ringer bicarbonate (KRBH) buffer for 2 hrs. to remove any residual insulin in ILCs. After that the constructs were washed and incubated with KRBH containing 5 mM and 25 mM glucose for 30 minutes respectively and the solutions were collected. The insulin released by the ILCs on the collected solutions were quantified using rat insulin ELISA (Merckodia, Sweden) according to the manufacturer's protocol. Briefly, 10  $\mu$ l of test samples, calibrators, and controls were added to the micro wells and incubated with 100  $\mu$ l of 1X enzyme conjugate followed by an incubation for 2 hrs. at room temperature. After that washing was given using wash buffer followed by incubation with 200  $\mu$ l of substrate TMB and

incubated for 20 min at room temperature. Stop solutions were added and the cooler formed was recorded at 450 nm and the results were calculated.

### **3.3.3 Differentiation of ADMSc on ECM coated C-DEXGEL scaffold**

For the generation of ILCs, ADMSCs were seeded on the DEXGEL and C-DEXGEL scaffold at a density of  $1 \times 10^6$  cells/scaffold (4 mm diameter and 3 mm height) and the differentiation was carried out using the protocol as mentioned in section 3.2.1 and observed under phase contrast microscope. The size of ILCs formed on DEXGEL and C-DEXGEL scaffold was calculated using Image J software.

#### **3.3.3.1 Morphology of islet during differentiation**

The morphology of mesenchymal stem cells and islet like clusters during differentiation on DEXGEL and C-DEXGEL scaffolds were analysed using scanning electron microscopy (JEOL JSM 6390LV, Japan) on day 1 and day 20. Construct were fixed in 4% paraformaldehyde at 4 °C overnight followed by PBS washing. Dehydration was given in graded alcohol (30%, 50%, 70%,90% and 100%) 15 minutes for each stem and 2 changes were given for each alcohol concentration followed by critical point drying and gold sputter coating. To visualize the change in cytoskeleton arrangement during differentiation, F-actin string was carried out using phalloidin tagged Alexaflour 488 dye (Invitrogen USA).

#### **3.3.3.2 Viability assay**

The viability of formed islets on DEXGEL and C-DEXGEL scaffolds were confirmed using live/dead staining using calceinAM/ethidium bromide (Thermo Fischer, USA). The media was removed the PBS with calcein AM and ethidium bromide were added followed by incubation for 20 minutes at 37 °C. After that the solution was removed and washed with PBS and observed under confocal laser scanning microscope (Nikon A1Rsi, Japan).

### **3.3.3.3 Insulin immunofluorescence analysis**

The expression of insulin hormone of ILCS in DEXGEL and C-DEXGEL scaffold was confirmed by immunofluorescence staining according to the protocol mentioned in section 3.3.1.

### **3.3.3.4 Glucose stimulated insulin secretion**

To quantify the insulin secretion of ILCs on both DEXGEL and C-DEXGEL scaffold, glucose challenged insulin secretion followed by rat insulin ELISA was carried out as reported in section 3.3.2.5

## ***3.4 Isolation, characterisation and culture of rat islets on ECM coated DEXGEL scaffold***

### **3.4.1 Isolation of islet from rat pancreas**

Islets were isolated from the rat pancreas after obtaining approval from the institute's animal ethics committee. The Pancreas tissue was collected aseptically in

sterile PBS with 10X ABAM and digested with 10 mg/ml concentration of collagenase V (Sigma Aldrich) 20 minutes with continuous shaking at 37 °C. Liberated islets were then purified by passing through a 40 µm cell strainer (HiMedia) and observed under phase contrast microscope (Olympus). The isolated clusters were cultured in DMEM HG with 10% FBS and 1X ABAM at 37 °C and 5 % CO<sub>2</sub>.

#### **3.4.2 Diphenylthiocarbazone (DTZ) staining of rat islets**

Dithizone (Sigma Aldrich) stock solution (39 mM) was prepared in dimethyl sulfoxide (Sigma Aldrich) and stored briefly at -20 °C. The working solution was prepared by mixing 100 µl from dithizone stock and 10 ml of KRBH buffer. The solution was filtered through a 0.2 µm filter. Islets were centrifuged down and washed with KRBH buffer and incubated with freshly prepared dithizone working solution and incubated for 20 minutes at 37 °C. The stained islets are then observed under phase contrast microscope (Olympus).

#### **3.4.3 Viability and Immunocytochemistry of rat islets**

The viability of isolated islet after 7 days of culture was observed using LIVE/DEAD Viability/Cytotoxicity Kit for mammalian cells (Thermo Fischer, USA) and imaged using fluorescence microscope. The endocrine portion of isolated rat islets were analyzed using immunofluorescence staining the expression of insulin hormone. The islets are washed in PBS and fixed in 4% paraformaldehyde followed by washing and permeabilisation using 1% triton X for 30 minutes. Islets were then

blocked with bovine serum (10 mg/ml) and incubated with anti-insulin antibody (Santa Cruz biotechnology) for 16 hrs. at 4 °C. Islets were then washed and stained with secondary antibody tagged with phycoerythrin (Invitrogen) for 2 hrs. The nucleus was counterstained with DAPI and image with fluorescence microscope.

#### **3.4.4 Islet culture on ECM coated C-DEXGEL scaffold**

After isolation, 300 mature islets were seeded on DEXGEL and C-DEXGEL scaffolds and allowed to attach for 1 hr. After that construct were supplemented DMEM HG with 10% FBS and 1X ABAM at 37 °C and 5 % CO<sub>2</sub>. Media change was given for every 2 days.

#### **3.4.5 Morphology of rat islet on scaffold**

Morphology of islets cultured on DEXGEL and C-DEXGEL scaffold was analyzed with scanning electron microscopy after 7 days in culture. The construct was prepared as mentioned in section 3.3.2.3. and observed under scanning electron microscope (Hitachi S 2400).

#### **3.4.6 Viability and insulin immunocytochemistry of rat islet on scaffold**

After 7 days of culture, the viability of islets on DEXGEL and C-DEXGEL scaffold was studied by live/dead calceinAM/ethidium homodimer stains (Invitrogen, USA) staining was carried out according to the manufacturer's protocol. The islets were then imaged using a confocal microscope (Leica). The viability of islets seeded

on constructs was also assessed by MTT assay. For that, the media was removed and MTT assay was carried out as mentioned in section 3.1.2.7.

Expression of islet specific hormone insulin in islets seeded on DEXGEL and C-DEXGEL scaffolds was analyzed by immunofluorescence staining as mentioned in section 3.3.2.4.

### **3.4.8 Glucose stimulated insulin secretion of islet on scaffold**

To quantify the insulin secretion of rat islets on both DEXGEL and C-DEXGEL scaffold, glucose challenged insulin secretion followed by rat insulin ELISA was carried out as reported in section 3.3.2.5

## ***3.5 Fabrication and characterization of immunoprotection membrane***

### **3.5.1 Synthesis of PU-PVP semi IPN**

For the fabrication of immunoprotective membranes, polyurethane- polyvinyl pyrrolidone semi-IPN was prepared as reported earlier (Nair, 1995; Nair et al., 1999). Briefly, 10g of polyurethane (Tecoflex EG 60D) supplied by Lubrizolcorp (USA) was dissolved in 90 ml of dimethylacetimide. 10 ml N-vnylpyrrolidone (NVP) was mixed with 1 wt % of initiator azoisobisbutyronitrile. 10 ml of n-vinylyrrolidone was added to the polyurethane solution and stirred at 200 rpm for 2 hrs followed by adding 1% of Ethylene glycol dimethacrylate (2%) to form semi interpenetrating network of polyurethane-polyvinyl pyrrolidone in the ration 90:10. After mixing, the solution was poured in to clean glass petri plate and cured for 2 hrs. at 80 °C

followed by post curing at 60 °C for 48 h. After this the PU-PVP semi IPN films were cut in to pieces and washed with 20% ethanol for 2 hrs and washing in distilled water for 2 days and dried in dust free atmosphere.

#### **3.5.1.1 Thermogravimetric analysis**

Heat stability of the synthesized PU-PVP semi IPN was studied by thermogravimetric analysis (TGA) using TGA analyzer (TA instruments, SDT 2920). For that 5-10 mg of PU, PVP and PU-PVP semi IPN was heated from room temperature to 700°C in nitrogen at a rate of 10 °C /min.

#### **3.5.1.2 Mechanical testing**

The tensile properties of the synthesised PU-PVP semi IPN was analyzed using universal testing machine (INSTRON 3345, UK) and compared with polyurethane. For mechanical testing PU-PVP and PU films strips with 12mm width, 60mm length and .05mm thickness were cut and the experiment was conducted at room temperature with crosshead speed of 5mm/min and a load cell of 10N.

#### **3.5.1.3 Cytotoxicity evaluation**

*In vitro* cytotoxicity of the material as evaluated by direct contact sassy, MTT assay, and live dead staining as mentioned in section 3.1.2.8.

### 3.5.2 Fabrication of immunoprotection membrane

#### 3.5.2.1 3D printing of PU-PVP semi IPN

After PU-PVP semi-IPN synthesis, immunoprotective membranes were fabricated by 3D printing using a 12% PU-PVP solution by dissolving in chloroform. To obtain nano pores, we have designed 3 patterns with different infill densities in a graded manner. The first four-layers base was printed with 10% infill density followed by 4 layers of 20% infill density and on top of that another 4 layers of 30% infill density was printed. The printing parameters are listed in table 3.4.

Table 3.4 3D printing parameters

Needle	27 gauge
First layer height	0.1mm
Layer height	0.1mm
Fill density	10%,20%,30%
Fill pattern	Grid
Speed for print moves	8mm/s
Speed for nonprint moves	130mm/s
Solution used	12% PU-PVP
Total layers	12

#### 3.5.2.2 Porosity analysis of 3D printed membrane

The porosity of the 3D printed membrane was analyzed by phase contrast microscopy and AFM images. To measure the porosity created by different infill densities, each layer was printed over a glass slide and observed under phase contrast

microscope. The micro pores created was calculate using Image J software. After the complete printing of the membranes, nanopores on the surface of the membrane were studied by atomic force microscopy (AFM, Agilent 5500).

### **3.5.2.3 Diffusion of molecule across the membrane**

To conduct the diffusion studies of insulin, glucose and immunoglobulin across the 3D printed membraned, 24 well cell insert (HiMedia, India) was modified by replacing the barrier of cell insert with the 3D printed nanoporous membrane. For the diffusion studies, 300 $\mu$ L of insulin, glucose, and IgG prepared in PBS were placed in the top compartment and 1mL of PBS was placed in the bottom compartment. Diffusion studies were carried out at 37 °C. Glucose and insulin diffusion was studied for 5-10 minutes and IgG diffusion was studied for 7 days. After the study period, solutions from the bottom compartment were taken and insulin diffusion was quantified using insulin ELISA (Merckodia), diffused glucose was quantified by glucose detection kit, and IgG using a BCA kit.

### **3.5.3 Fabrication of immunoprotective pancreatic transplantation device (IPTD)**

Immunoprotective pancreatic transplantation device (IPTD) was fabricated by encapsulating C-DEXGEL seeded with islets/ILCs in the 3D nanoporous membranes by heat sealing at the ends. The membrane of dimensions 4 mm length and 4 mm breadth was taken and a pouch is created by folding the membrane heat sealing at ends. Three C-DEXGEL scaffolds seeded with 300 islets each or ILCs were placed inside the pouch and closing the pouch by heat sealing created the IPTD.

### **3.5.3.1 Viability and insulin secretion of islet and ILCs on IPTD**

Viability of islets and ILCs encapsulated in IPTD was studied by live/dead staining and MTT assay as mentioned in section 3.1.2.8 and compared with the viability of islets or ILCs on C-DEXGEL scaffold and tissue culture plate.

## **3.6 *In vivo* studies**

### **3.6.1 Diabetic animal model**

Animal experiments were conducted after getting the approval from the institute's animal ethics committee, SCTIMST. Wistar rats (male) with weight in the range of 300g-350g were used for the study. All experimental animals were housed individually in ventilated cages under standard laboratory conditions with feed and water ad libitum.

Table 3.5 Test groups for in vivo experiment.

Group 1	Islet on C-DEXGEL scaffold
Group 2	Islet on IPTD
Group 3	ILCs on C-DEXGEL scaffold
Group 4	ILCs on IPTD

### **3.6.2 Diabetes induction and metabolic monitoring**

Diabetes was induced by streptozotocin administration. For that, animals were kept fasting for 4 hrs., and freshly prepared streptozotocin at a concentration of 30 mg/kg in sodium citrate buffer (pH4.5) was injected intraperitoneally. Drinking water was given immediately after injection and animals were kept on fasting for

another 4 hrs. After 72 hrs. diabetes was confirmed by measuring the blood glucose level using one touch glucometer. To measure the food intake and urine volume, animals were transferred to metabolic cages where food and water was given and urine was collected in a contained and urine volume was recorded.

### **3.6.3 Implantation of tissue engineered construct**

Eight days after STZ injection, animals with BGL>450 were selected for the studies. For transplantation studies, animals were categorized into the following test groups. A total of 3 C-DEXGEL scaffolds seeded with rat islets or stem cell derived ILCs were used for each groups. 350 islets were seeded on each scaffold and  $0.7 \times 10^6$  ADMSCs/scaffold were used for the generation of ILCs. The diabetic controls groups receive did not received any implants. The constructs were implanted in the intraperitoneal cavity of the rats. For that, animals were anaesthetized by intraperitoneal administration of ketamine and xylazine. The abdomen was shaved and prepared for implantation. A midline incision was made and the construct was implanted in the intraperitoneal cavity. The abdominal muscles and skin were sutured in two layers using a silk suture (mersilk, Johnson & Johnson, USA). Animals were maintained in individual cages and betadine was administered in the surgical wound for 7 days and tetracycline was given daily for 7 after the surgery. Water and food were given ad libitum and the animals were observed for 60 days' post transplantation. Fasting blood glucose levels and body weight of the animals were recorded every 7 days until the end of study period.

#### **3.6.4 Intra peritoneal glucose tolerance test and Serum collection (C-peptide assay)**

Thirty days after transplantation, intraperitoneal glucose tolerance test was performed. After overnight fasting, 2g/kg of D glucose (Invitrogen, USA) was administered intraperitoneally. Blood glucose were measured by tail vein bleeding before glucose administration and at fixed time intervals (15,30,60, and 120 minutes) after glucose injection.

Blood was collected by retro orbital vein bleeding and the blood samples were centrifuged at 4000 rpm for 10 minutes. The serum was transferred to a fresh vial and kept at -80 °C until the C-peptide analysis. The serum C-peptide concentration was measured using a rat c-peptide ELISA kit (Merckodia) according to the manufacturer's protocol.

#### **3.6.5 Histological analysis**

The implanted construct and pancreas was collected and fixed with 10% neutral buffered formalin (Sigma Aldrich) and kept in room temperature. After 1 weeks the formalin fixed samples were dehydrated, processed and embedded in wax using sample processor. Further, 4 µm thick sections were cut using microtome (Leica, Germany). The sections were stained with Harris hematoxylin and the nucleus were counter stained with eosin. Immunofluorescence staining of the construct were also carried out to analysed the expression of insulin hormone in

transplanted constructs. Trichrome staining was carried out on construct sections using a three step trichrome staining kit (Sigma).

## **CHAPTER 4: RESULTS OF THE STUDY**

In this chapter the results obtained for the current study are explained. This chapter is divided in to six subsections. The first subsection deals with the results of fabrication and characterization of two scaffold systems. Isolation and characterization of adipose derived mesenchymal stem cells (ADMSCs) are detailed in the second section. The role of scaffolds supporting the differentiation of ADMSCs into islet like clusters (ILCs) was detailed in the third section. The fourth section deals with the effect of extra cellular matrix (ECM) molecule on the viability and functionality of rat islets. The fifth section details the results of the fabrication and characterizations of 3D printed immunoisolation bags. Results of the sixth section are obtained from *in vivo* evaluation of the tissue-engineered construct in diabetic rat models.

### ***4.1 Fabrication and characterizations of scaffold systems***

The first objective of the study was to fabricate two scaffold systems suitable for islet tissue engineering. This section again divided in to two subsections in which first section deals with the fabrication of highly porous wet electrospun scaffold made of a synthetic polymer polycaprolactone (PCL) and in the second section, results regarding the fabrication and ECM conjugation of a natural polymer dextran dialdehyde-gelatin scaffold is detailed.

#### **4.1.1 Fabrication of wet electrospun scaffold**

Electrospinning is a versatile technique widely used for the production of extracellular matrix (ECM) mimicking fibrous matrices (Jun et al., 2018). However,

the major drawback of conventional electrospun scaffold is its small pore size and densely packed nanofibers that limits the cell infiltration and may lead to the formation of large ILCs, which has low viability and insulin secretion. Since porosity of the scaffold is the key factor in generation ILCs of desired sizes, it is important to fabricate highly porous 3D scaffolds with ECM mimicking architecture (Anitha et al., 2020). There have been numerous attempts to fabricate highly porous scaffolds through electrospinning such as wet electrospinning. In this study, we have used a commonly used synthetic polymer polycaprolactone (PCL), which has good mechanical properties and have bio-inertness and biocompatibility to fabricate the 3D scaffold. Instead of conventional electrospinning, here we adopted wet electro spinning to create 3D scaffolds with large pores that are ideal for ILC culture.

Figure 4.1 shows the schematic representation of wet electrospinning. In wet electrospinning, instead of solid collectors, nanofibers are collected in a stationary or rotating liquid bath to achieve three dimensional nanofibrous scaffolds with increased porosity. Figure. 4.2 show the wet electrospun scaffold in comparison with conventional electrospun sheets. PCL dissolved in chloroform was electrospun into an ethanol bath. The fiber diameter and porosity of conventional electrospun sheets are between  $1.5\pm 1\ \mu\text{m}$  and  $15\pm 4\ \mu\text{m}$ . The fiber diameter of wet electrospun scaffold is  $3\pm 2\ \mu\text{m}$  and the porosity was increased to  $70\pm 40\ \mu\text{m}$  after wet electrospinning which is favourable for the generation of islet like clusters with smaller sizes.

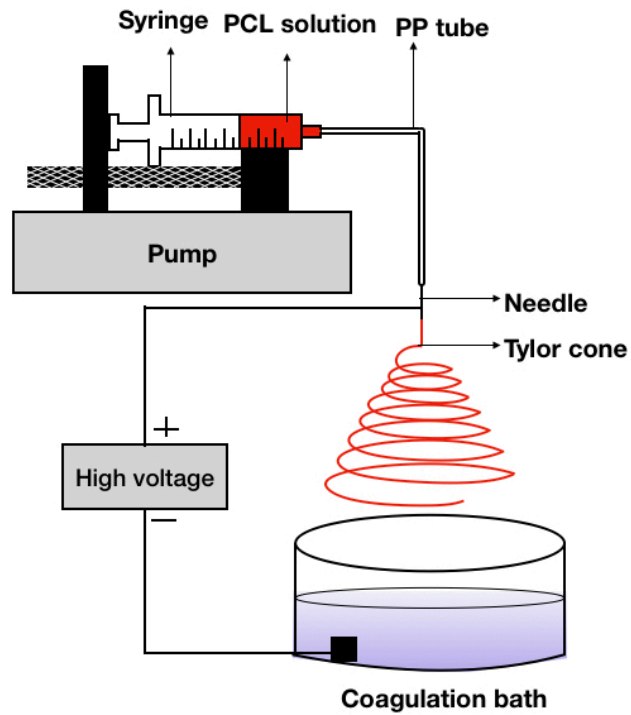


Figure 4.1 Schematic representation of wet electrospinning.

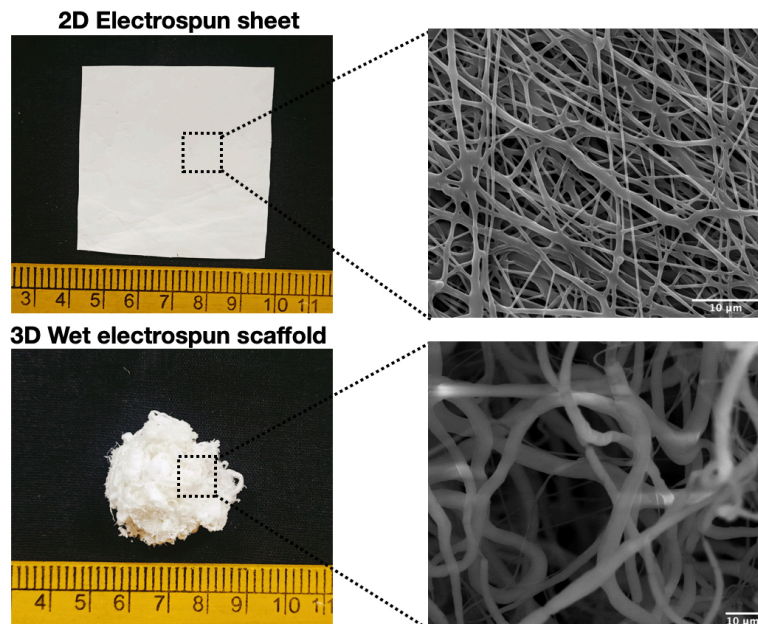


Figure 4.2 Comparison between conventional electrospun sheet and wet electrospun scaffold.

#### 4.1.2 Aminolysis and collagen conjugation

To increase the cell attachment and cell viability, we conjugated collagen I to the 3D PCL scaffold. For that amino group was incorporated to PCL by reacting with 1,6 hexadamine. In PCL molecules, ester groups (-COO-) are abundant. The amino groups can also be introduced to the polyester surface by a reaction with diamine, ensuring that one amino group forms a covalent connection, or -CONH-, with the -COO group while the other amino group remains unreacted and free. The introduced amino group on the surface of PCL was quantified by ninhydrin assay. The blue reaction product of ninhydrin with free amino group was dissolved in isopropanol and has absorbance at 540 nm. The quantity of amino group conjugated was increased with time. As shown in figure 4.4, the maximum NH<sub>2</sub> density yielded at 1.5 hrs is  $\sim 1.7 \times 10^{-8}$ /mg. After 2 hrs, the amino group density was decreased due to the further reaction with carboxyl of the free amino group on the terminal chain or by the degradation of surface layer by prolonged duration of aminolysis (Yuan et al., 2012).

Conjugation of free amino group on PCL membrane created the active site for biomolecule such proteins, polypeptides and polysaccharides to make the PCL scaffold more cell friendly. To achieve the conjugation of collagen I, the aminolysed PCL membrane was incubated with collagen solution in EDC-NHS (Fig.4.3). Conjugation of collagen I will is expected to make the scaffold more cytocompatible for the attachment and growth of cells.

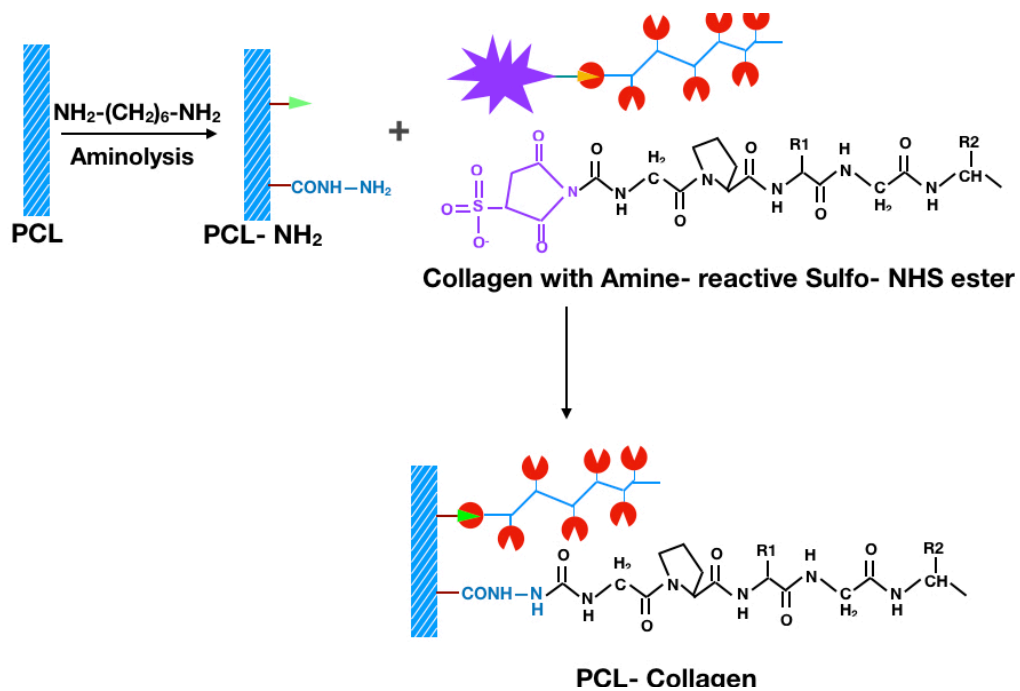


Figure 4.3 Schematic representation of aminolysis and collagen conjugation to PCL scaffold.

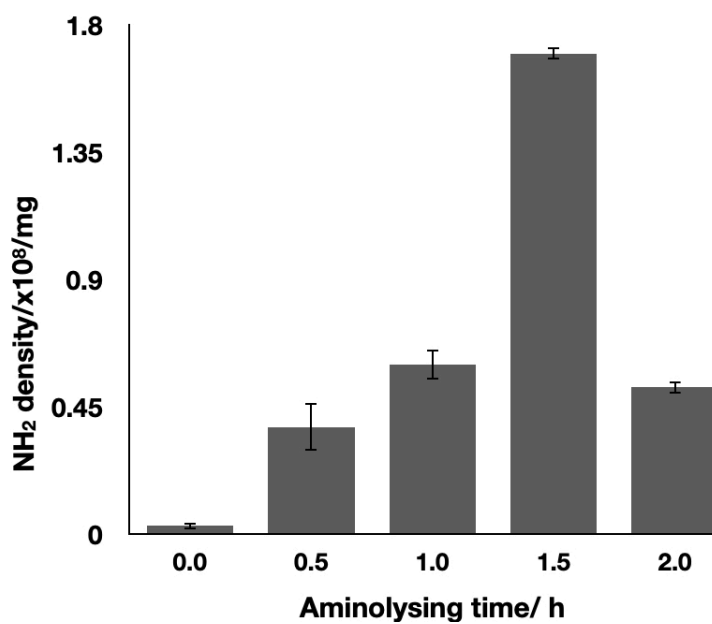


Figure 4.4 Ninhydrin assay showing concentration of amino group on PCL.

#### 4.1.1.2 Confirmation of collagen conjugation by FTIR analysis

Fourier transform infrared (FTIR) spectroscopy of unmodified polycaprolactone scaffold (PCL), aminolysed PCL scaffold (APCL), and collagen coated PCL scaffold (CPCL) was taken to confirm the collagen conjugation. For PCL, the distinct carbonyl peaks at 1722  $\text{cm}^{-1}$  and the aliphatic groups at 2939  $\text{cm}^{-1}$  and 2861  $\text{cm}^{-1}$  were detected. An additional peak, corresponding to  $\nu$ -NH of amide II, observed at 1558  $\text{cm}^{-1}$ , confirming the incorporation of the amino group. Collagen-I conjugation was confirmed by detection of three additional formed peaks at 1658  $\text{cm}^{-1}$ , 1558  $\text{cm}^{-1}$ , and a large peak at 3325  $\text{cm}^{-1}$  on the APCL scaffold (Fig 4.5).

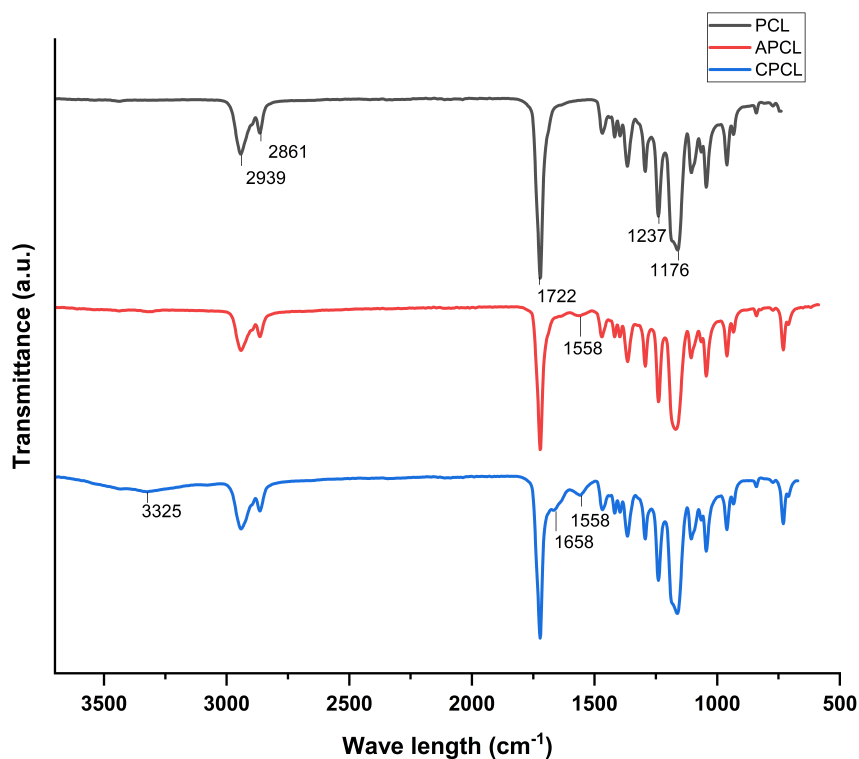


Figure 4.5 FTIR spectra of PCL, APCL and CPCL scaffolds.

#### 4.1.1.3 Hydrophilicity of the scaffold

Change in hydrophilicity of the material after aminolysis and collagen I conjugation was analysed by static air-water contact angle test. The aminolysis and collagen I conjugation of the PCL scaffold were further verified by the water contact angle measurement shown in Figure 4.6 and table 4.1. After aminolysis, the PCL membrane contact angle was reduced from  $78^{\circ}\pm 3$  to  $66^{\circ}\pm 4$ , indicating an increase in hydrophilicity. This shows that the free  $-NH_2$  group has grafted onto the PCL membrane. The contact angle further decreased to  $25^{\circ}\pm 4$  after collagen conjugation.

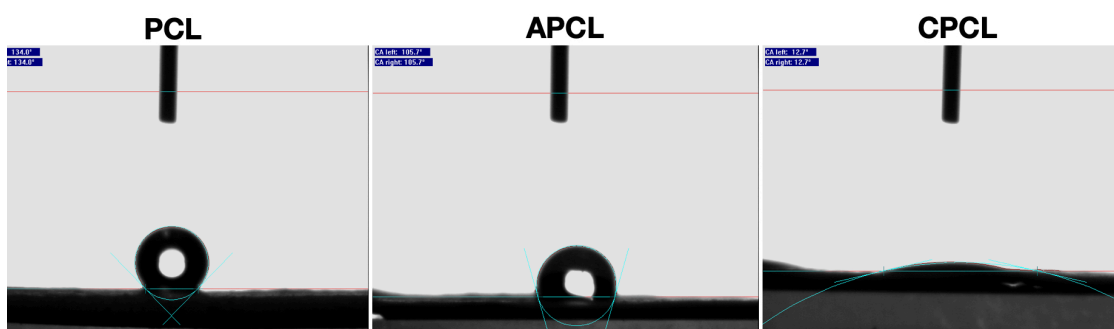


Figure 4.6 Water contact angle measurement of PCL, APCL and CPCL scaffolds

Table 4.1 showing contact angle measurements

Groups	Contact angle (°)
Control PCL	$78\pm 3$
Aminolysed PCL (APCL)	$66\pm 4$
Collagen coated PCL(CPCL)	$25\pm 4$

#### 4.1.1.4 Fiber architecture and porosity of the scaffold

Porosity and morphology of scaffolds were analysed by scanning electron microscopy. Fiber diameter of PCL scaffold was  $3\pm 2\mu\text{m}$ . No change in fibre diameter was observed after aminolysis and collagen conjugation. Wet electrospun scaffold was highly porous and due to the presence of liquid medium, which creates larger inter fibrillar distance and pore size. The porosity of the scaffold before modification was  $70\pm 40$ , which doesn't alter by aminolysis and collagen conjugation. The high porosity of the scaffold helps in the stem cell infiltration and generation of insulin like clusters (Fig 4.7).

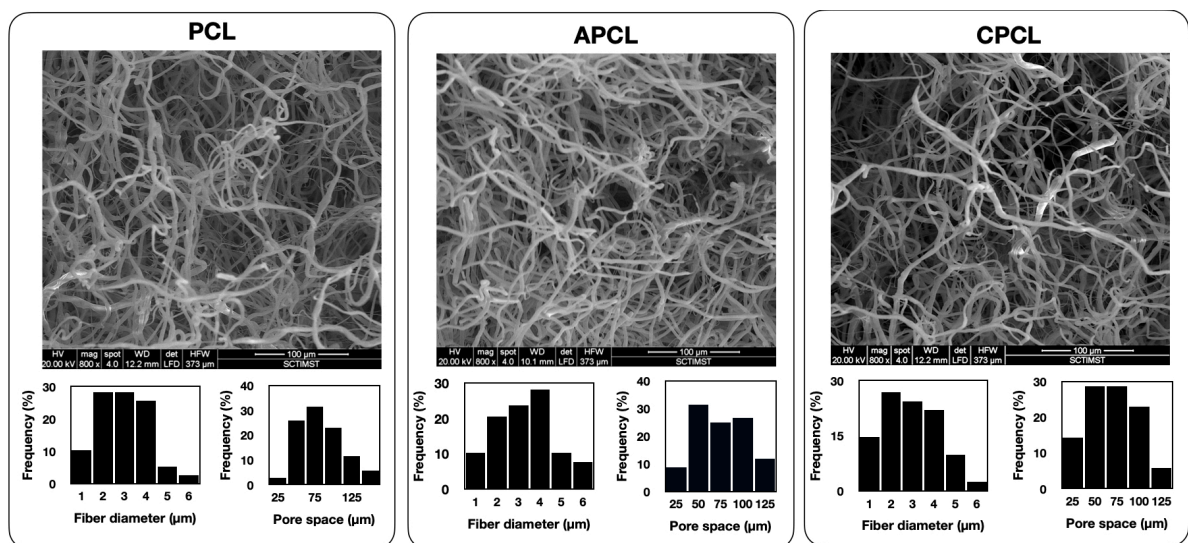


Figure 4.7 Showing SEM images of PCL, APCL and CPCL scaffolds.

#### 4.1.1.5 Surface topography by AFM

By profilometric analysis with Mountains SPIP programme from the obtained contact mode AFM images, the topography of the surface treated with PCL was verified by the change in surface texture (SPM 5500, Agilent, USA). From the abbot

firestone curve derived from AFM images, the surface of the PCL generated a textured surface with a maximum height increase from 50 to 70 nm and an isotropy of 16.95% after aminating this surface then shown a decrease in the textured height with an isotropy of 37.6% after final collagen conjugation. In line with the previous study results, this demonstrated that the collagen treatment had been carried out on the PCL surface (Fig.4.8).

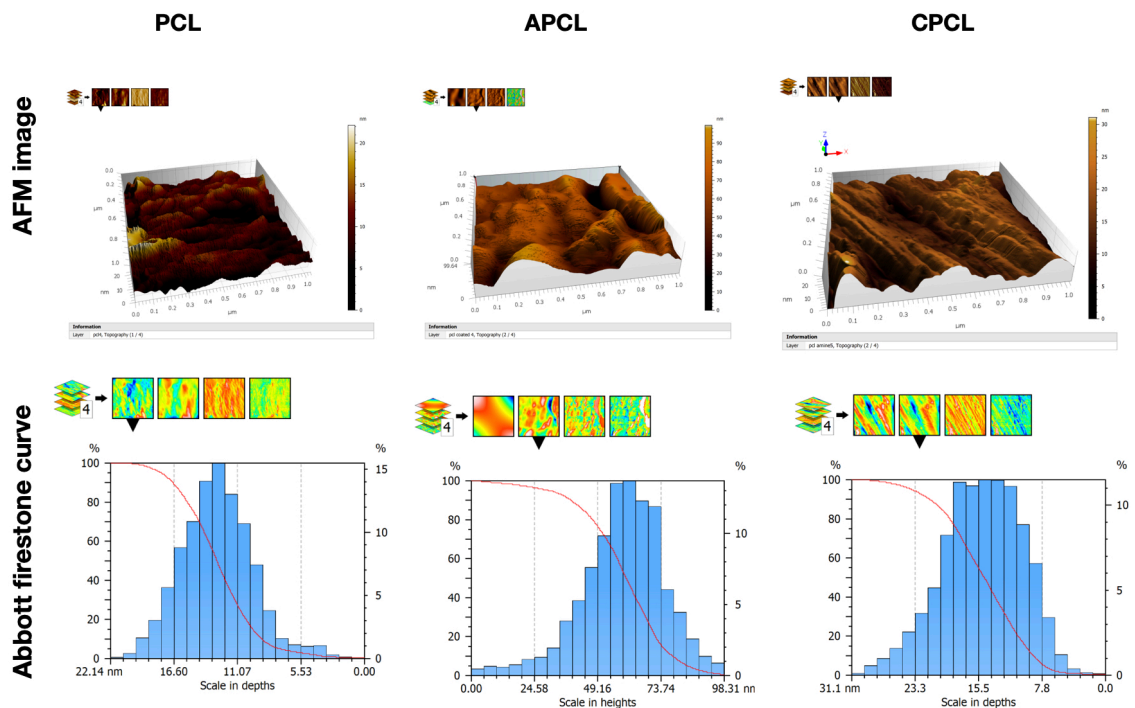


Figure 4.8 AFM analysis of surface topography of PCL, APCL and CPCL scaffolds.

#### 4.1.2 Fabrication and characterisation of C-DEXGEL scaffold

Dextran and gelatin are two natural polymers. Dextran dialdehyde (DDA) was prepared by oxidating the dextran with periodate, the hydroxyl groups in dextran was modified into aldehyde groups. A 10% (w/v) solution of DDA with a 50%

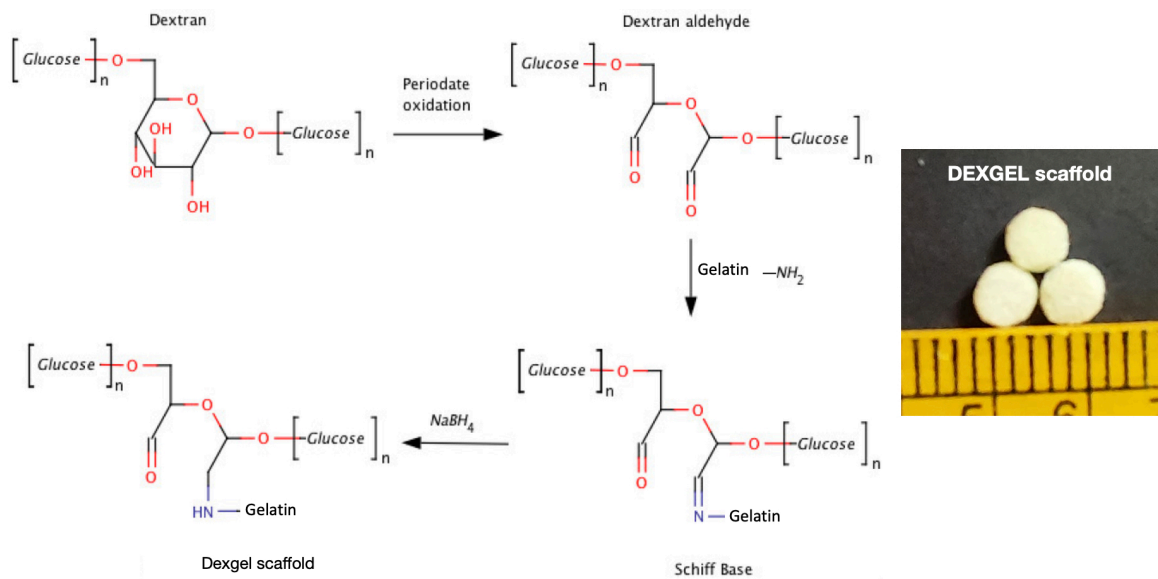


Figure 4.9 Schematic representation of DEXGEL scaffold fabrication. Image showing the formation of Schiff's linkage between dextran dialdehyde and gelatin and fabricated DEXGEL scaffold.

#### 4.1.2.1 ECM protein conjugation

To mimic the islet microenvironment, we conjugated two ECM protein collagen IV and laminin to the free carboxyl residue of gelatin on the scaffold by EDC-NHS mechanism. Figure 4.10 represents the conjugation of ECM molecule collagen IV and laminin to the fabricated DEXGEL scaffold and the ECM protein conjugated scaffold is named as C-DEXGEL scaffold.

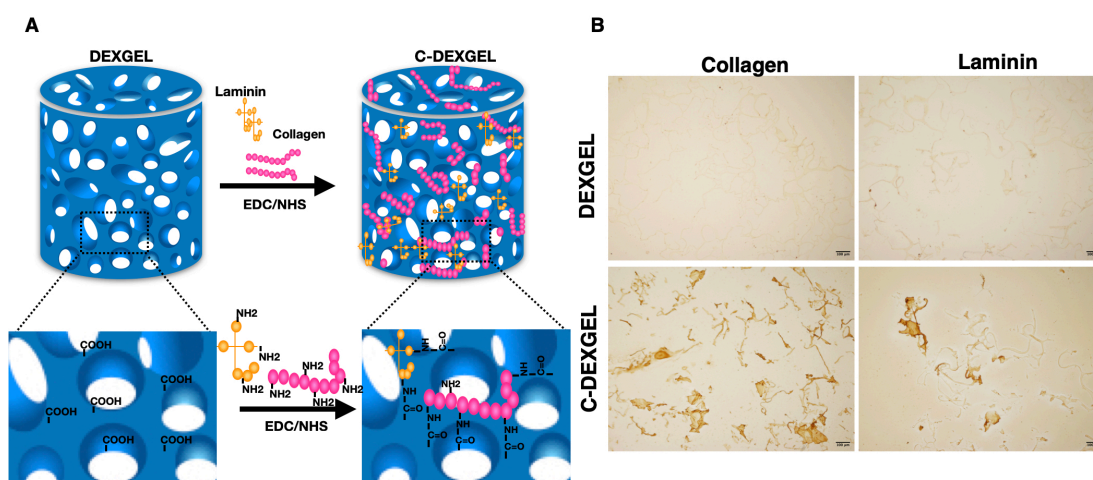


Figure 4.10 Showing the conjugation of ECM molecule to the DEXGEL scaffold. (A) Represents the conjugation of ECM molecule collagen IV and laminin to the fabricated DEXGEL scaffold. (B). Immunohistochemical staining confirming the conjugation of collagen IV and laminin to the scaffold.

#### 4.1.2.3 Change in hydrophilicity of the scaffold

A balance between hydrophilicity and hydrophobicity is necessary for cell attachment and growth. Contact angle is a measurement of hydrophobicity of a material. The contact angle of DEXGEL scaffolds was found to be  $62 \pm 3^\circ$  and after conjugation, no significant change in hydrophilicity was observed and the contact angle of C-DEXGEL scaffold is  $64 \pm 4^\circ$ . After protein conjugation, scaffold maintained a balance between hydrophilicity and hydrophobicity contributing to the better cell attachment (Fig 11)

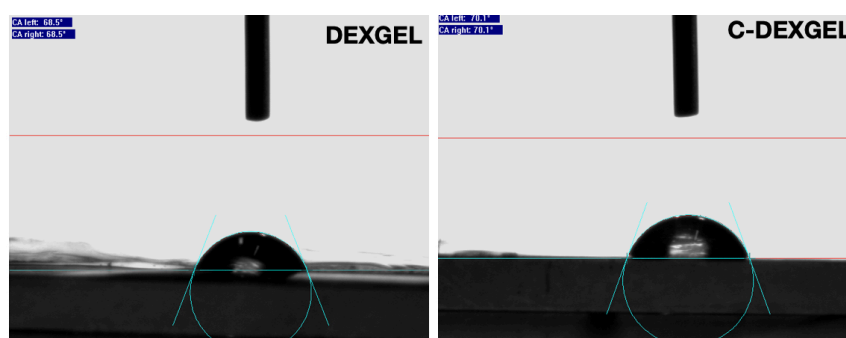


Figure 4.11 Contact measurement of DEXGEL and C-DEXGEL scaffolds.

#### **4.1.2.3 Change in porosity and pore architecture**

Scanning electron micrograph showed the porosity and microarchitecture of DEXGEL scaffold. The DEXGEL scaffold is highly porous and the porosity is in the range of 100-300  $\mu\text{m}$  diameter and. The high porosity of the scaffold is favorable for the attachment and maintenance of native islets and stem cell derived islet like clusters with porosity 100-200 $\mu\text{m}$ . After protein conjugation, no changes in the porosity and pore architecture was observed. Porosity of C-DEXGEL scaffold is same as that of DEXGEL scaffold.

#### **4.1.2.4 Swelling ratio**

During *in vitro* cultures, the scaffold swells and the pore size expands, making it easier for cells to attach, migrate inside, and proliferate in a three-dimensional manner. Additionally, the cells receive the scaffold's entire internal surface area. The swelling ratio of unconjugated DEXGEL scaffold is  $8.2 \pm 3$  as shown in the figure 4.14A slight decrease in the swelling ratio to  $7.3 \pm 0.5$  was observed after protein conjugation (Fig 4.14.A).

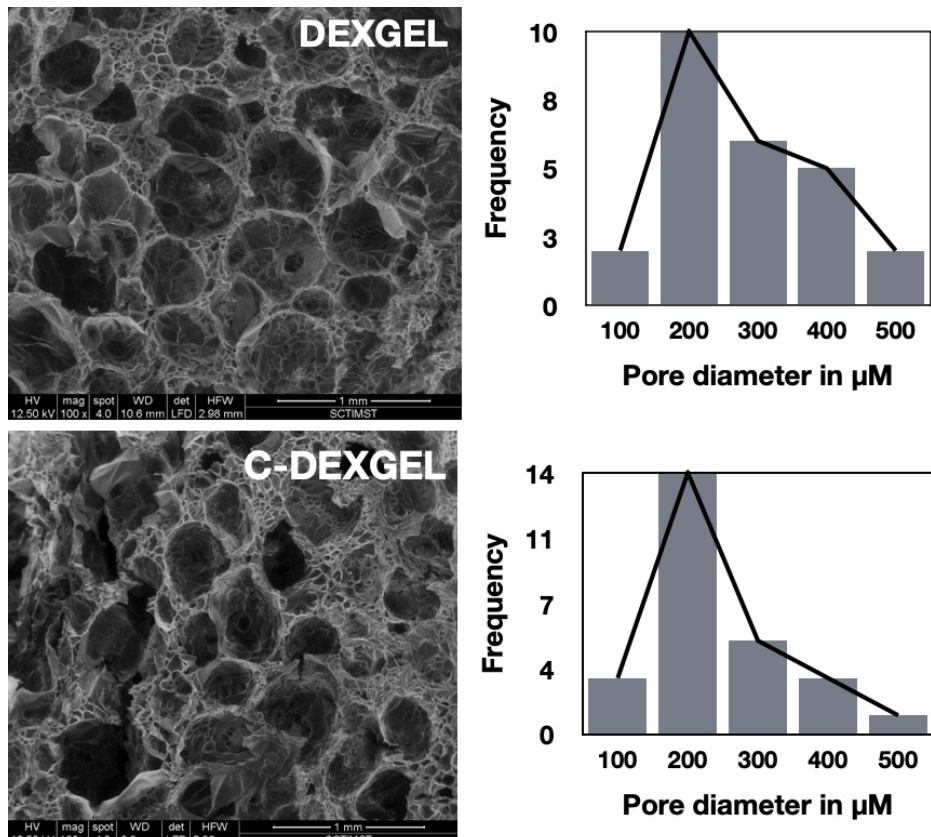


Figure 4.12 SEM images showing porosity and pore distribution of DEXGEL and C-DEXGEL scaffolds.

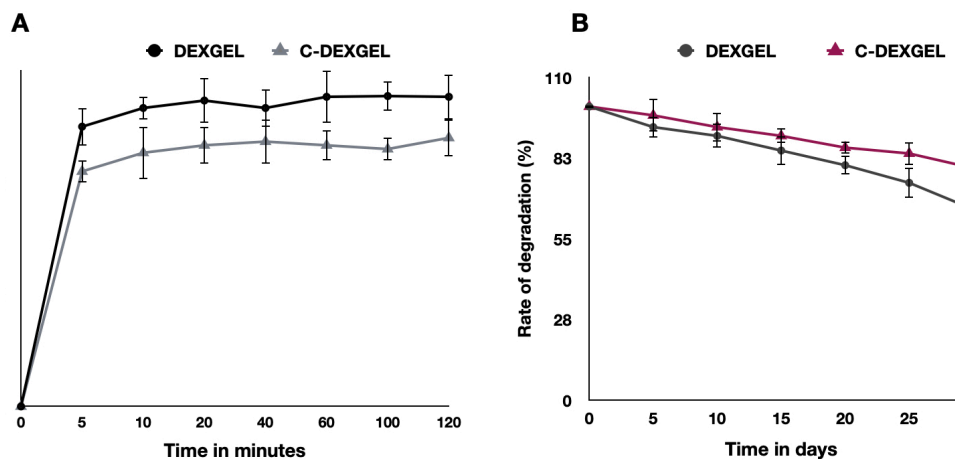


Figure 4.14 A&B Swelling and degradation of DEXGEL and C-DEXGEL scaffolds

#### **4.1.2.5 Degradation study**

Degradation of the scaffold was studied by measuring the weight loss of scaffold in PBS. The rate of degradation of the DEXGEL scaffold was slower, 25% of weight loss over a period of 21 days and it was comparable to the rate of ILC formation. The slow rate of degradation proves the effective crosslinking between gelatin and dextran dialdehyde. After ECM protein conjugation, the degradation was decreased to 18% (Fig 4.14 B) which further increased the stability of the scaffold.

#### **4.1.2.6 Evaluation of cytotoxicity**

Cytotoxicity of DEXGEL and C-DEXGEL scaffolds were evaluated by MTT assay, direct contact assay and live/dead staining. L929 cultured for 24 hrs with DEXGEL and C-DEXGEL scaffold showed no morphological changes compared to positive and negative control (Fig 4.15 A). The metabolic activity of L929 cell treated with the extract of DEXGEL and C-DEXGEL scaffold at various time points showed more than 85% viability compared to untreated control (Fig 4.15 B). Viability of the L929 cells seeded on scaffolds were studied by calcein-ethidium bromide staining in which the live cells stained with calcein appeared green and the dead cells stained with ethidium bromide appeared red. (Fig 4.15 C). L929 cells seeded on scaffolds showed negligible amount of dead cells after culturing for up to 4 days.

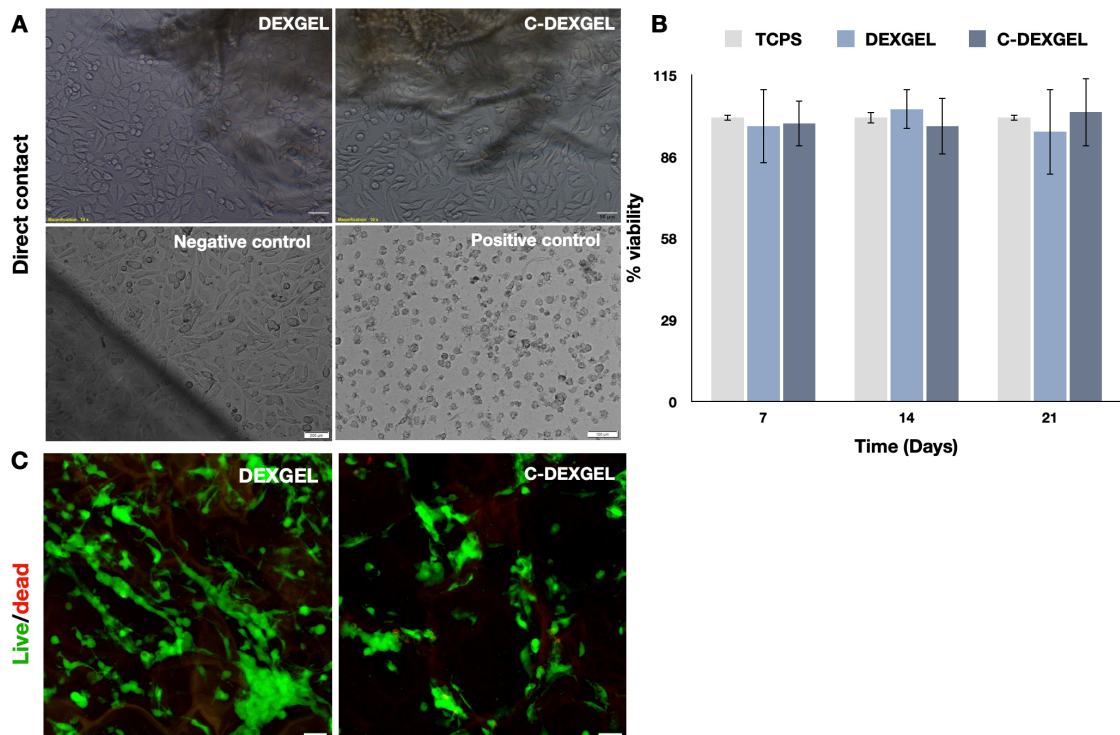


Figure 4.15 Cytotoxicity evaluation of the scaffolds showing A) Direct contact assay, B) MTT assay, C) Live/dead staining

#### ***4.2 Isolation and characterisation of Adipose Derived Mesenchymal stem cells (ADMSCs)***

The adipose tissue was obtained from the supra scapular region of rat was digested using 0.1% of collagenase II. The isolated cells obtained after digestion were directly plated into tissue culture flask supplemented with DMEM HG, 10% FBS, and 1% ABAM. Non adherent cells were removed during media change and the adherent cells showed fibroblast (Fig 4.16A) morphology and obtained confluency by day 7 and passaged further by trypsinization. Actin cytoskeletal

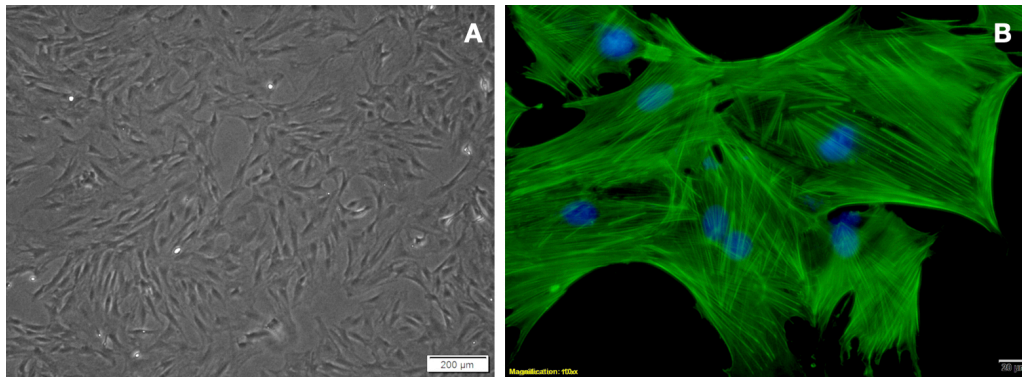


Figure 4.16 Phenotypic characteristics of isolated stem cells from rat adipose tissue. A) phase contrast image of rat adipose stem cells. (B) Cytoskeletal organization evident by actin stain showing fibroblast phenotype.

staining by phalloidin confirmed the fibroblastic morphology of the isolated stem cells cultured on tissue culture plate (Fig 4.16 B).

#### 4.2.1 Surface marker analysis

Immunofluorescence staining of cytoskeletal marker vimentin was positive for isolated cells confirmed that the cells were mesenchymal origin and negative for CD34/45 confirmed the absence of hematopoietic cells. Positive results for CD73, CD90, and CD105 indicated that the isolated cells are stem cells (Fig 4.19). Flow cytometry analysis also confirms the presence of positive stem cell marker CD73, CD90, and CD105 and negative marker CD34/45 (Fig 4.20).

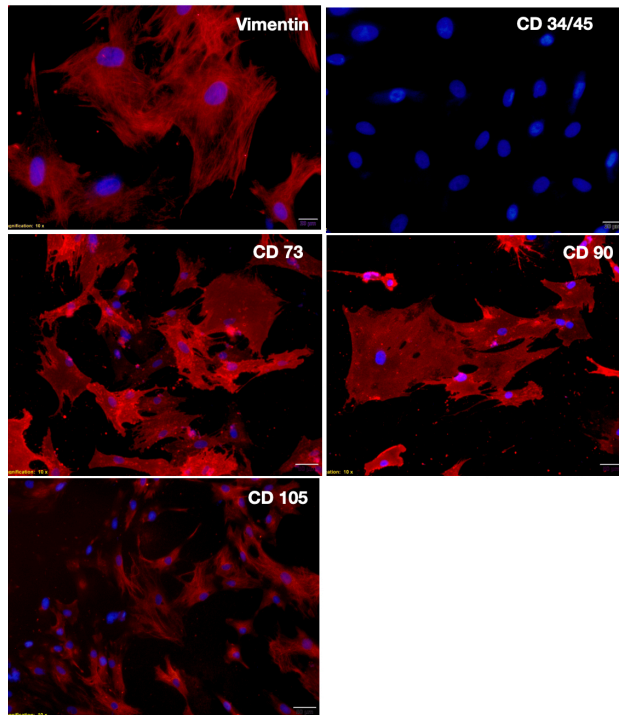


Figure 4.17 Immunophenotype characterization of rat adipose derived cells. The cells were positive for mesenchymal marker vimentin and Negative for hematopoietic marker CD45/CD34. The cells were also positive for stem cell markers D73, CD90 and CD105.

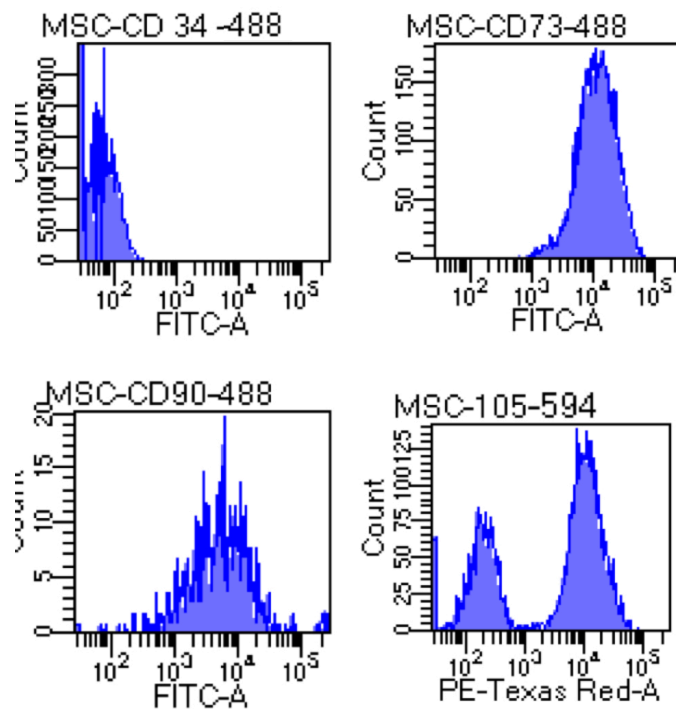


Figure 4.18 Flow cytometry analysis of rat adipose derived cells.

### 4.2.2 Multilineage differentiation

To confirm the stemness of isolated cells, trilineage differentiation was carried out. Differentiation to osteogenic lineage was confirmed by oil Red O staining of formed lipid droplets in the differentiated cells (Fig 4.19A). Chondrogenic differentiation was confirmed by toluidine blue staining of sulphated glycosaminoglycan deposition of differentiated cells (Fig 19 B). Alizarin red staining was performed to confirm the osteogenic lineage. Calcium deposited by the differentiated cells stained red collar by alizarin red (Fig 4.19 C).

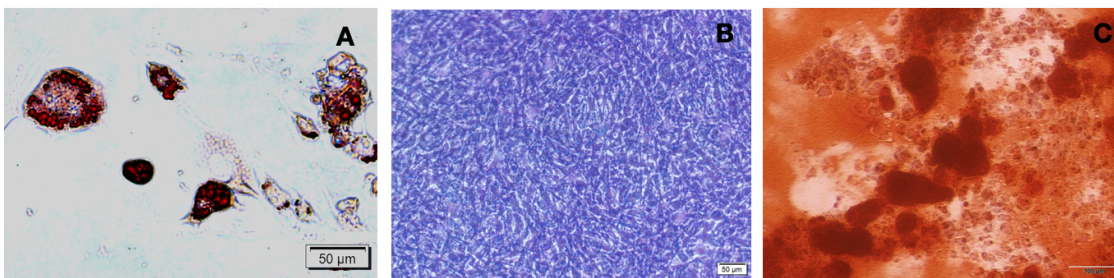


Figure 4.19 Multilineage differentiation of adipose stem cells showing A) lipid droplet stained by oil red O, B) toluidine blue staining for glycosaminoglycan, C) alizarin red staining for calcium deposition.

### 4.3 Differentiation of ADMSCs into ILCs

Rat adipose derived MSCs were differentiated into ILCs on tissue culture plates. 24 hours after seeding the cells were confluent and exhibited fibroblast morphology. On day 3 of differentiation, a change in morphology of the cells were observed. By day 10, clustering of cells were observed and at the end point of differentiation mature ILCs resembling islets were formed. The size of formed islets is  $< 300 \mu\text{m}$  diameter (Fig 4.20A). 2D differentiation created larger ILCs which are

less efficient in insulin secretion and less viable compared to smaller ILCs. Immunocytochemistry analysis revealed that the differentiated islets express insulin, glucagon and somatostatin hormones (Fig 4.20B).

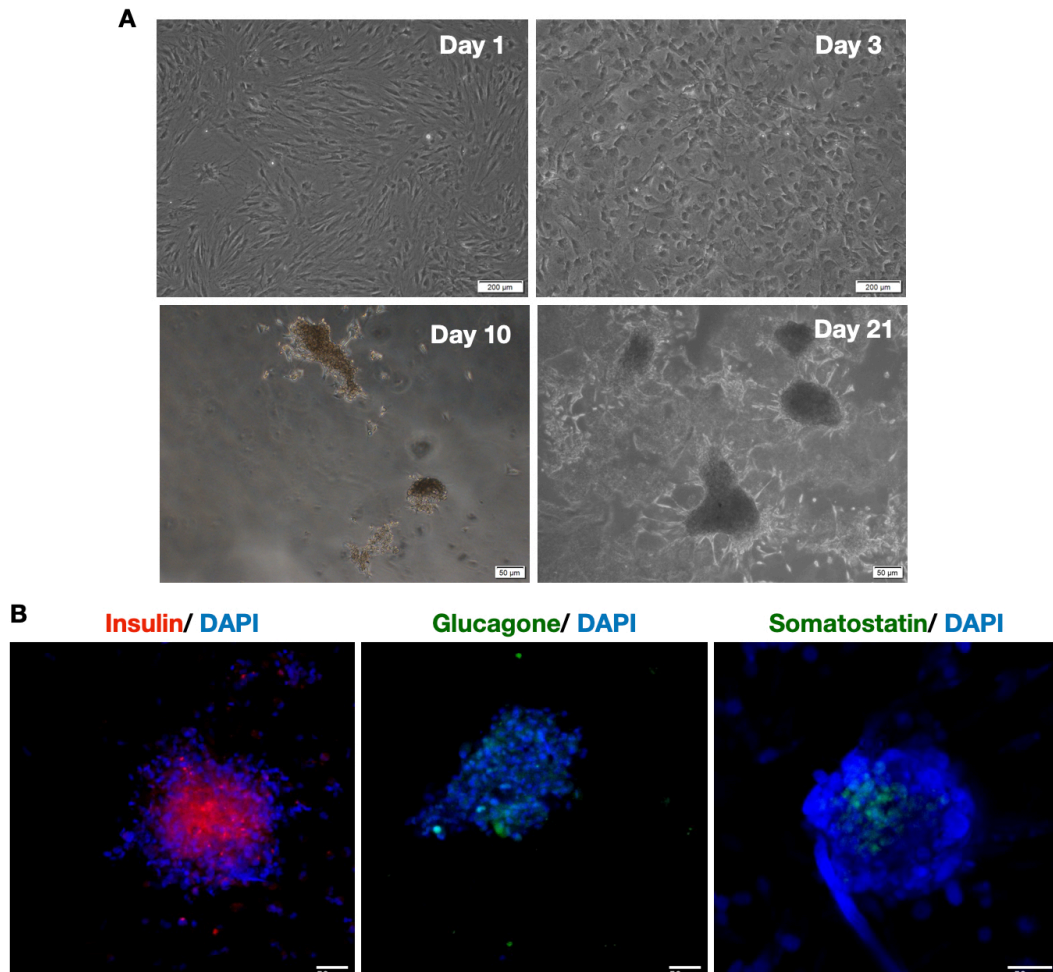


Figure 4. 20 Generation of ILCs on tissue culture plates. Change in morphology of stem cells during differentiation towards islet like clusters on tissue culture treated dish and immunocytochemistry A) Day 1, Day 3, Day10 and Day 21. The cells underwent clustering pattern and islet-like cluster morphology was observed on day 21. B) Immunofluorescence analysis of insulin, glucagon and somatostatin. Nucleus is counterstained with DAPI.

### 4.3.1 Rat ADMSCs on wet electrospun PCL scaffold

#### 4.3.1.1 Differentiation of MSCs on scaffold

Formation of ILCs on wet electrospun scaffold was compared with collagen coated conventional 2D electrospun sheets. ADMSCs were seeded on the scaffold and differentiated to ILCs. Collagen coated scaffolds supported the attachment and formation of ILCs. Porosity of the wet electrospun scaffold facilitate the migration

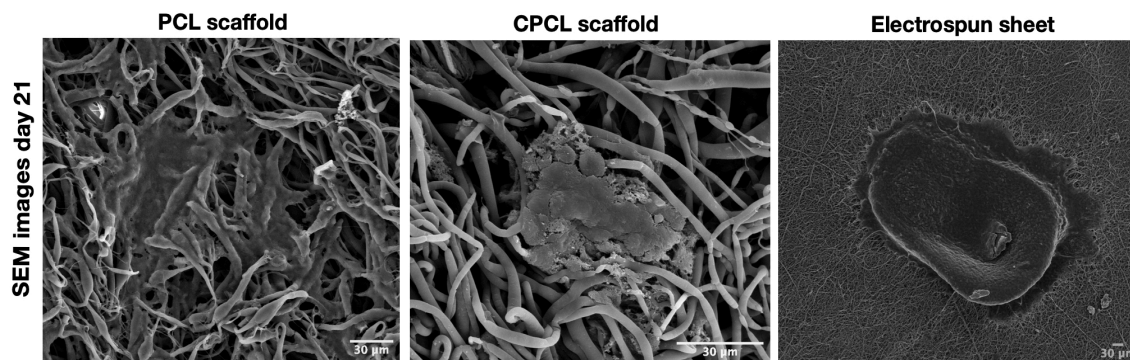


Figure 4.21 Morphology of islet like clusters differentiated from adipose derived stem cells on PCL and CPCL scaffold compared to electrospun sheet.

and clustering cells throughout the scaffold. Formed ILCs displayed spherical morphology like the native islets. Figure 4.21 shows the SEM images of differentiated ILCs on scaffold. CPCL scaffold supported the formation of ILCs of size  $70\pm 20$   $\mu\text{m}$  diameter. Due to the lack of cell attachment moieties, PCL scaffold does not support the long term culture of cells. Initially, cell clustering was observed on PCL scaffold but as time progressed, clusters were detached from CPCL scaffold. Furthermore, the traditional electrospun scaffolds' small pore size and high fiber density prevented cell penetration, which resulted in the formation of the large ILCs on their surface with diameter  $< 300$   $\mu\text{m}$ .

#### 4.3.1.2 Viability of ILCs on scaffold

Viability of the formed ILCs were studied by calcein/ethidium bromide staining. ILCs generated in electrospun sheet had a high percentage of dead cells and just a small percentage of live cells. Because of the large cluster size, there is a limited oxygen supply to the ILCs' centre, which causes necrosis in the cluster's central core region, and the live/dead staining of the wet electrospun and conventional electrospun sheet samples showed this to be quite obvious. The wet electrospun scaffold had very few dead cells, and it was observed that the ILC clusters were more stable in the collagen coated CPCL scaffold than the PCL scaffold. Even though there were hardly any dead cells in the PCL scaffold, the clusters were observed to be disintegrating (Fig 4.22).

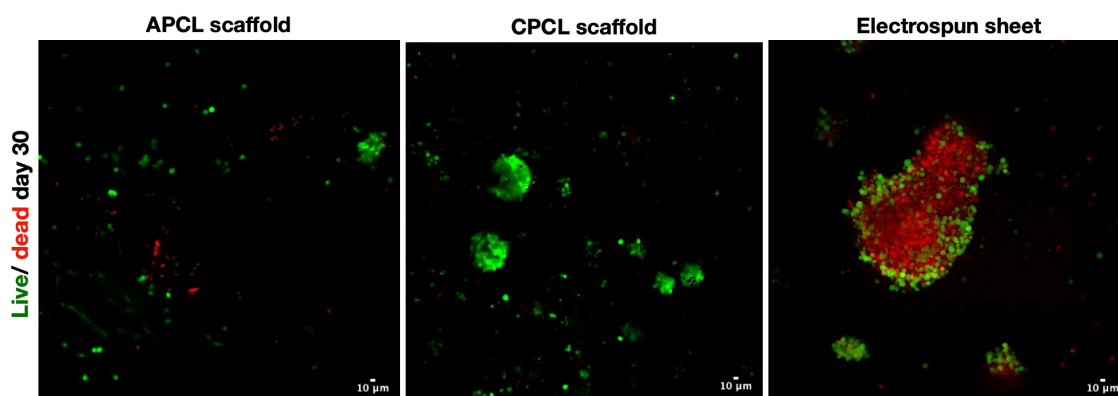


Figure 4. 22 Viability of ILCs formed on scaffold on 30<sup>th</sup> day of culture.

#### 4.3.1.3 Hormone expression and functionality of ILCs

Immunocytochemistry analysis of ILCs formed on PCL, CPCL and conventional electrospun sheet confirmed the presence of insulin hormone at the end point of differentiation (Fig 4.23). When challenged with 25 mM glucose, the

glucose challenge assay of ILCs differentiated on CPCL scaffold showed more insulin secretion than ILCs on electrospun sheet ( $P < 0.05$ ). This may be due to the cell loss due to necrosis in larger ILCs formed on electrospun sheet.

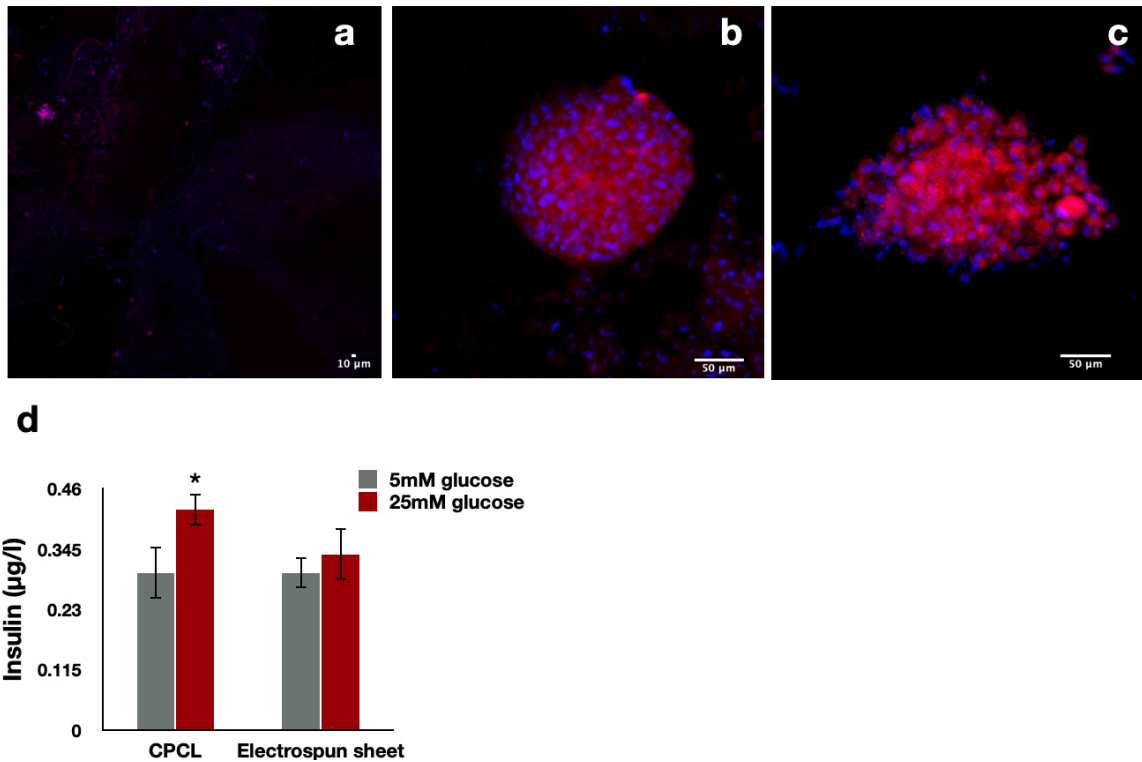


Figure 4.23 Immunophenotypic characterization of islet like clusters stained positive for insulin hormone on a) PCL scaffold b) CPCL scaffold and c) electrospun sheets e) glucose stimulated insulin secretion of ILCs on scaffold (one way ANOVA \* $p < 0.05$ ).

#### 4.3.1.4 Gene expression of ILCs

Expression of islet specific markers at the end point of differentiation was evaluated by RT-PCR. Key pancreatic endocrine markers including Pdx1 and Nkx6.1 were expressed by ILCs developed on the CPCL scaffold and electrospun sheet. The differentiation of ADMSCs to ILCs is confirmed by the co-expression of these two markers, which is only expressed in pancreatic beta cells. Compared to ILCs

generated in electrospun sheets, ILCs in CPCL scaffold showed a 68-fold increase in insulin gene expression. The higher insulin protein expression of the wet electrospun samples seen in the glucose challenge assay was further supported by the gene expression results. Despite glucagon and somatostatin expression being non-significant in the CPCL scaffold compared to the electrospun sheet scaffold, expression of Pdx1, Nkx6.1, and GLUT2 exhibited a significant increase (Fig 4.29).

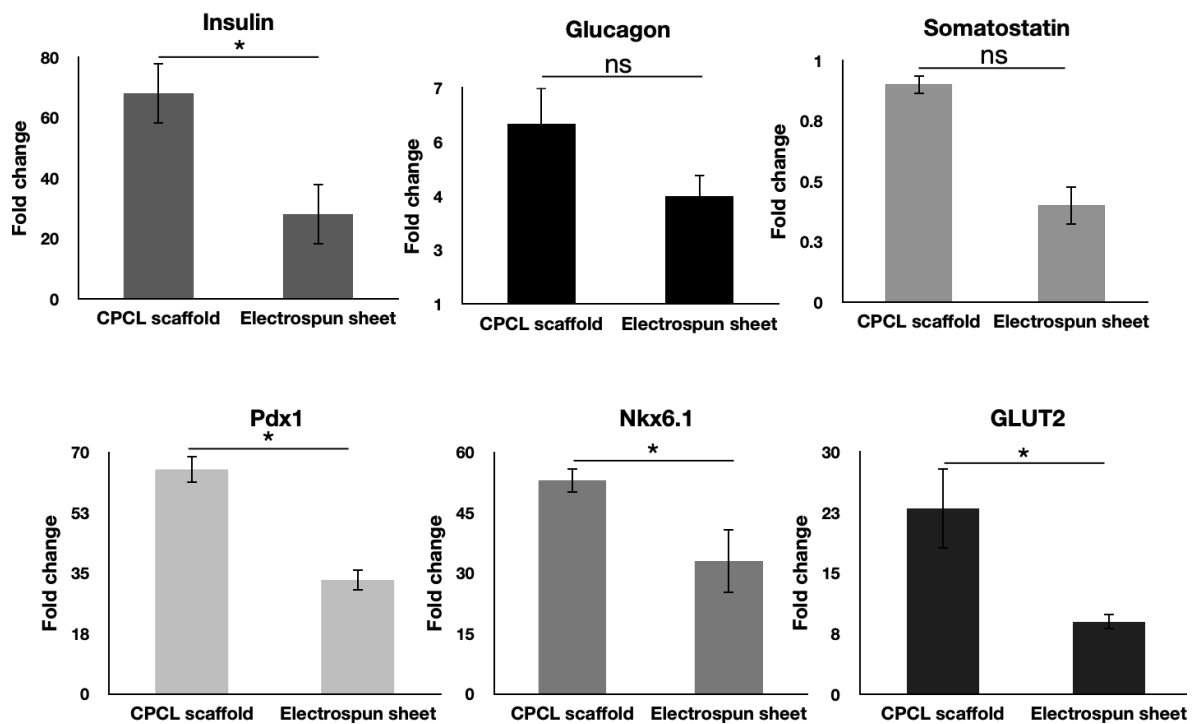


Figure 4. 24 Quantitative analysis of pancreatic islet specific genes on adipose stem cell differentiated islet like clusters (ILC) generated on CPCL scaffold and electrospun sheets using Real Time Polymerase Chain Reaction (unpaired t test \* $p < 0.05$ ).

#### 4.3.2 Differentiation of rat ADMSCs on C-DEXGEL scaffold

The differentiation stem cells into ILCs on protein conjugated C-DEXGEL scaffold was compared with DEXGEL scaffold. Figure 4.25 shows the phase contrast

image of generated islets at 21 day of differentiation. The size distribution of ILCs formed on both DEXGEL and DEXGEL are similar having 50-200  $\mu\text{m}$  diameter like the heterogeneous size distribution of islets in native pancreas.

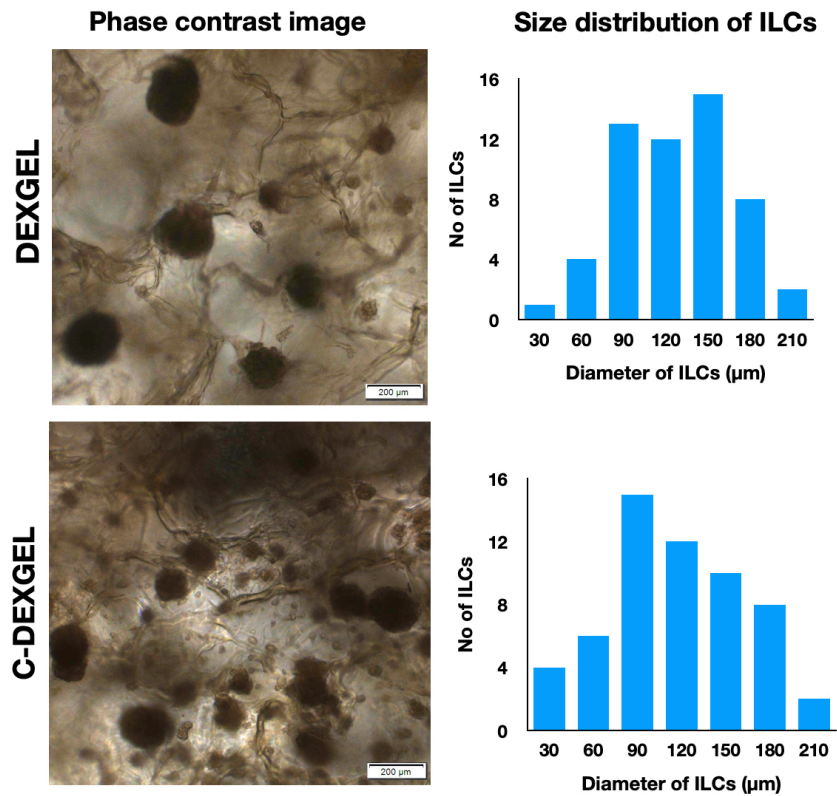


Figure 4.25 Phase contrast image of stem cell derived islet like clusters formed on DEXGEL and C-DEXGEL scaffolds at the end point of differentiation.

#### 4.3.2.1 Morphology and cytoskeleton organization of ILC

Figure 4.26 shows the cytoskeletal organization MSCs seeded on scaffold. Cells are attached and spread on the scaffold. MSCs on the scaffold showed fibroblast like morphology with long and thin actin filaments running to the orientation of cells.

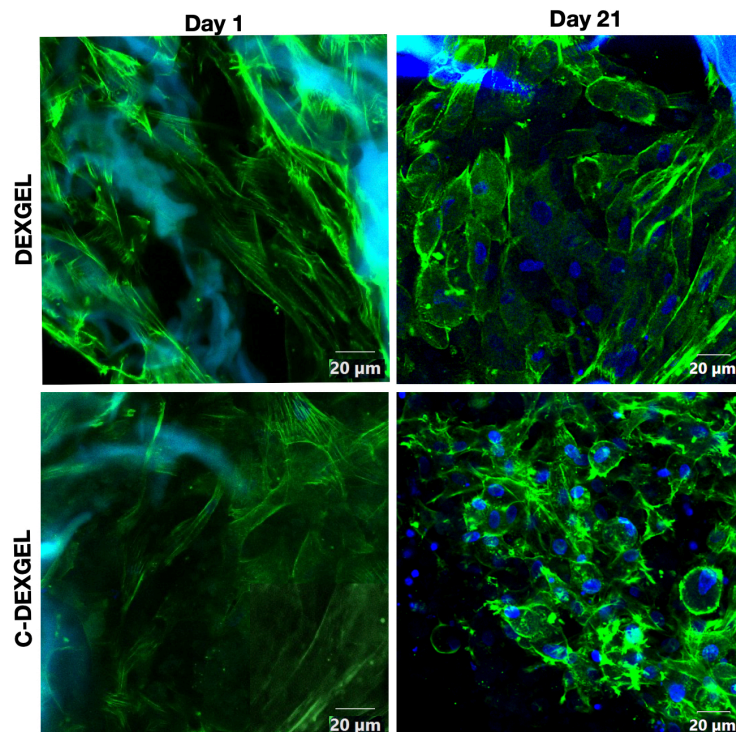


Figure 4.26 Cytoskeletal organization mesenchymal stem cells during differentiation on day 1 and day21 in DEXGEL and C-DEXGEL scaffold.

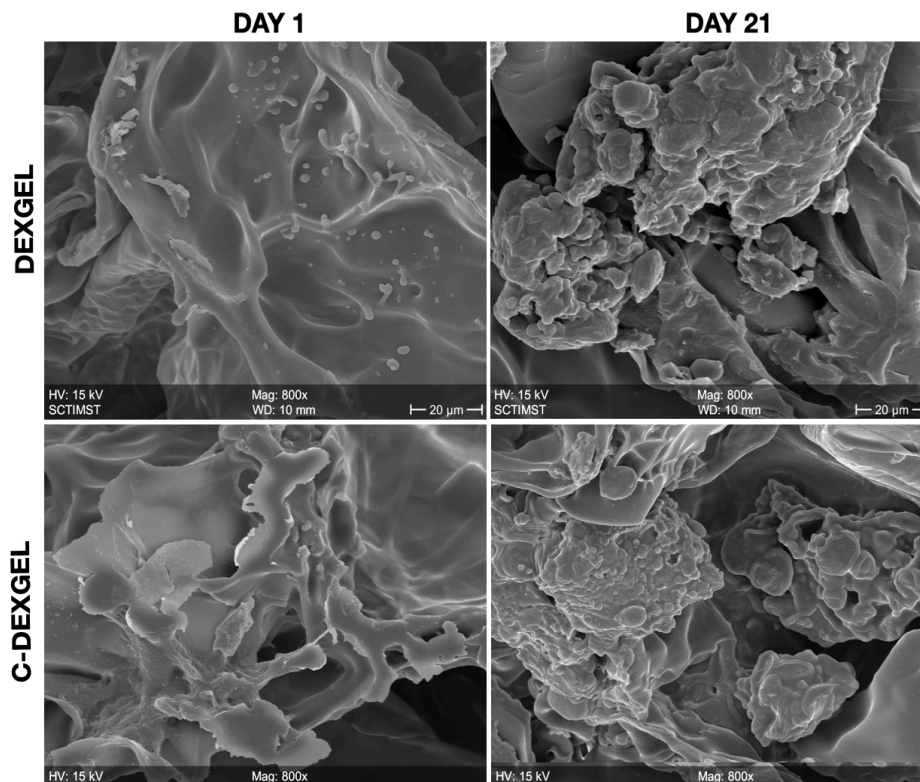


Figure 4.27 SEM image showing the Differentiation of rat adipose derived stem cells to islet like clusters on DEXGEL and C-DEXGEL scaffolds. Day 1-cells attached on the scaffold, Day 20-islet like cells observed attached onto scaffolds.

However, upon differentiation to ILCs the parallel fibers disappeared and more thick and condensed stress fibers were appeared (Fig 4.26). Electron micrograph images also confirmed the clustering of ADMSCs during differentiation. 24 hrs. after seeding, stem cells were spread over the scaffold and at the end of differentiation period fully formed clusters were visible on both DEXGEL and C-DEXGEL scaffold (Fig 4.27).

#### **4.3.2.2 Viability of ILCs**

Viability of cells seeded on the scaffolds were analysed by calcein/ethidium bromide staining. Both DEXGEL and C-DEXGEL scaffolds supported the attachment and growth of AMSCs. There were negligible dead cells were observed on both the scaffolds. After 24 hours of seeding, ADMSCs were attached and spread through the scaffold. At the endpoint of differentiation, mature viable ILCs with spherical morphology was observed and there were fewer to negligible number of dead cells observed (Fig 4.28).

#### **4.3.2.3 Hormone expression and functionality of ILCs**

Immunocytochemistry analysis of ILCs formed on DEXGEL and C-DEXGEL scaffolds confirms the presence of insulin hormone at the end point of differentiation (Fig 4.29 A). The insulin secreted by ILCs upon glucose challenge was quantified by ELISA. ILCs on both scaffold exhibited same pattern of insulin secretion when challenged with 5 mM glucose. At 25 mM concentration of glucose, ILCs on C-DEXGEL scaffold secreted 1.2 times significant amount of insulin than ILCs formed on DEXGEL scaffold (Fig 4.29 B).

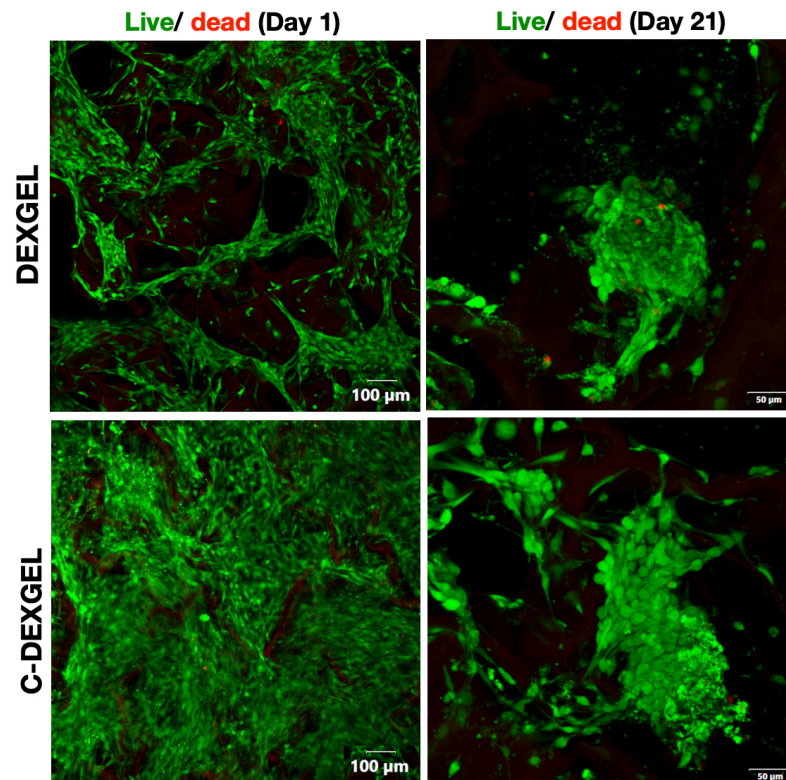


Figure 4.28 Viability of adipose stem cell differentiated islet like clusters (ILC) on DEXGEL and C-DEXGEL scaffold assessed by calcein-ethidium bromide staining. On day 1 and day 21.

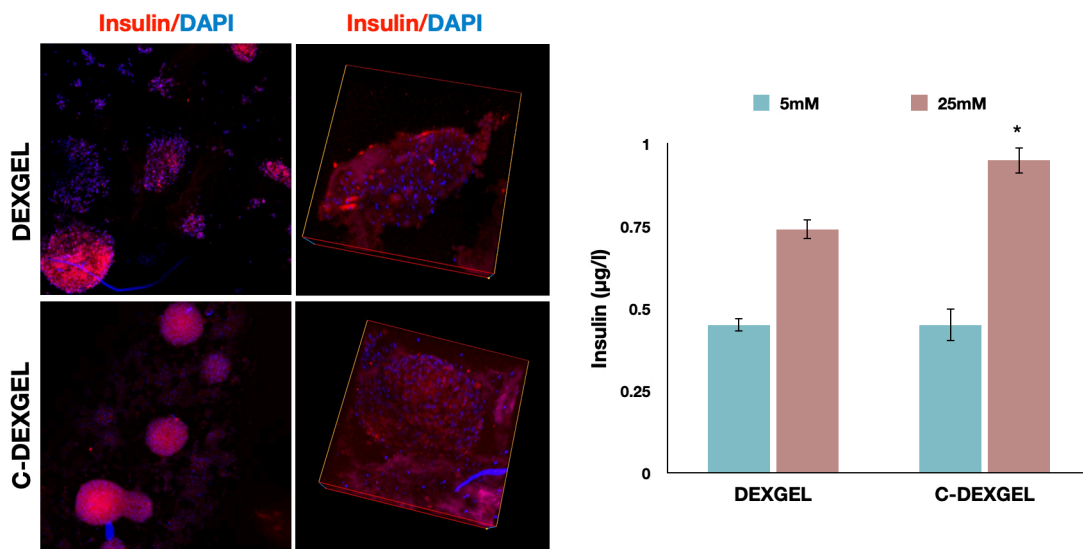


Figure 4.29 qualitative and quantitative analysis of insulin hormone in generated ILCS. A) Immunophenotypic characterization of islet like clusters stained positive for insulin hormone on DEXGEL and C-DEXGEL scaffolds B) Amount of insulin secreted by ILCs on scaffolds in response to various glucose concentrations (5 mM and 25 mM) quantified by ELIZA (One way ANOVA and two keys pos hoc analysis  $*p < 0.05$ ).

## ***4.4 Isolation and characterizations of rat islets on ECM coated C-DEXGEL scaffold***

### **4.4.1 Isolation and characterizations of rat islets**

Islet cells were isolated from the rat pancreas by collagenase V digestion. Under phase contrast microscope, the isolated islet exhibited cluster morphology of size ranging from 50-250 $\mu$ m diameter. In dithizone staining, islet appeared crimson red since it is a zinc chelating agent that binds to the zinc granules of islet beta cells. Live/dead assay confirms that the isolated islets are viable. Immunofluorescence staining of insulin confirms that the isolated cells are islet of langerhans (Fig 4.31).

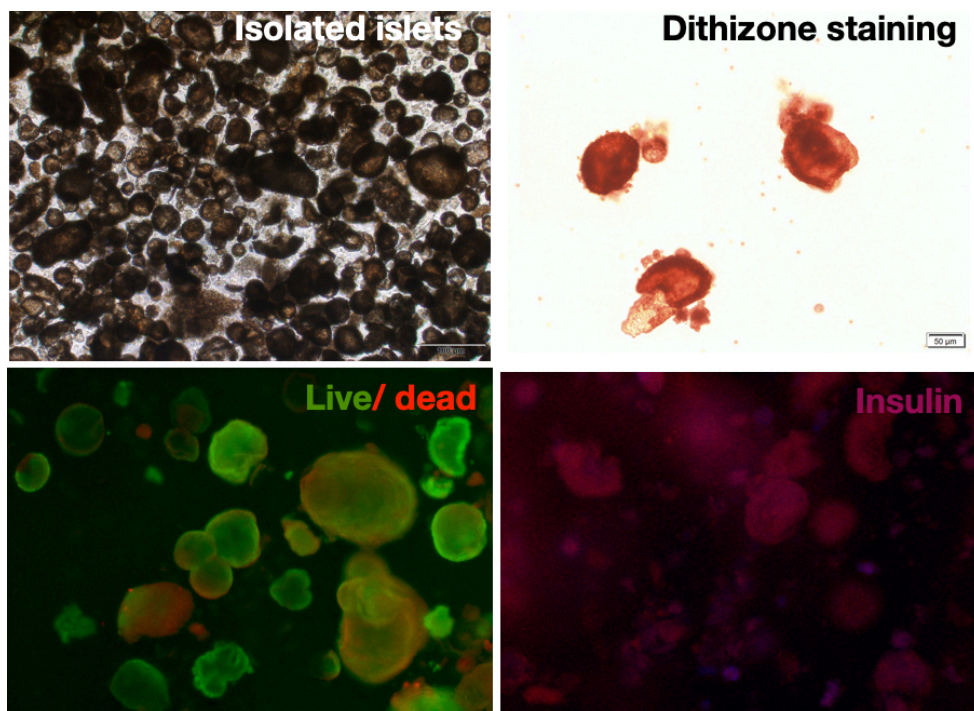


Figure 4.31 characterizations isolated rat islets showing phase contrast image of isolated islets by collagenase V digestion, dithizone stained islets appeared crimson red due to the presence of zinc granules, live/dead staining of islets and the immunocytochemistry of islets positive for insulin.

#### **4.4.2 Islet morphology in 3D culture**

To validate the effect of ECM proteins collagen IV and laminin, primary isolated rat islets were seeded on the DEXGEL and C-DEXGEL scaffolds to study the islet attachment, viability, and insulin secretion. Islets were seeded on each scaffold, and cultured for 7 days in a growth medium containing DMEM HG, 10% FBS and 1X ABAM. After 7 days of culture of islet on scaffolds, electron micrographic images were taken to study the morphology of islets in 3D culture. Both DEXGEL and C-DEXGEL scaffold provided favourable pore size and supported the growth of islets. Spherical morphology of islet was maintained in both scaffolds since the pore size is important to accommodate the heterogenous size distribution of islets (Fig 4.32).

#### **4.4.3 Viability of islets**

After 7 days of culture, viability of islets on the C-DEXGEL scaffold was compared with DEXGEL scaffold. Islets on both scaffolds exhibited less to negligible amount of dead cells compared to islet on 7 days of 2D culture. Number of attached islets were more in laminin and collagen coated scaffolds than in DEXGEL scaffold (Fig 4.33)

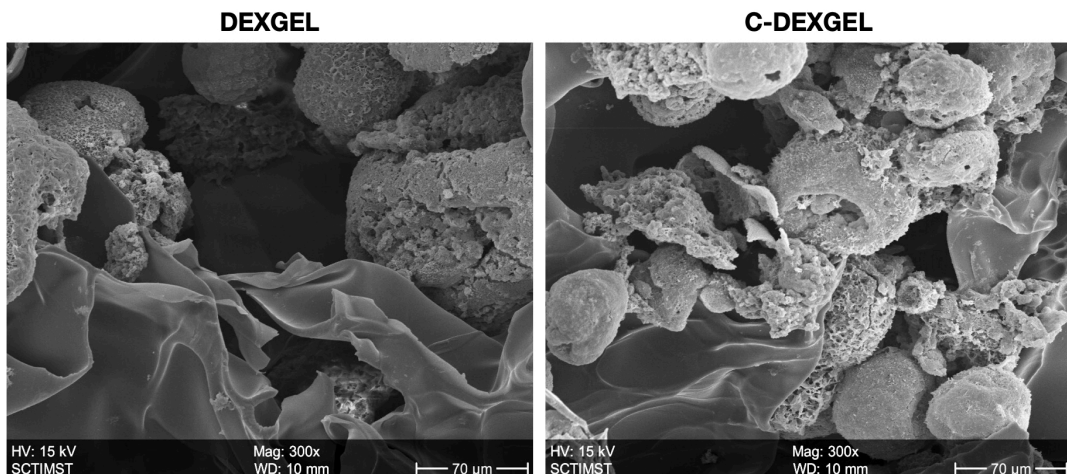


Figure 4. 32 Scanning electron micrograph showing the intact cluster morphology of islets maintained when cultured on DEXGEL and C-DEXGEL scaffolds.

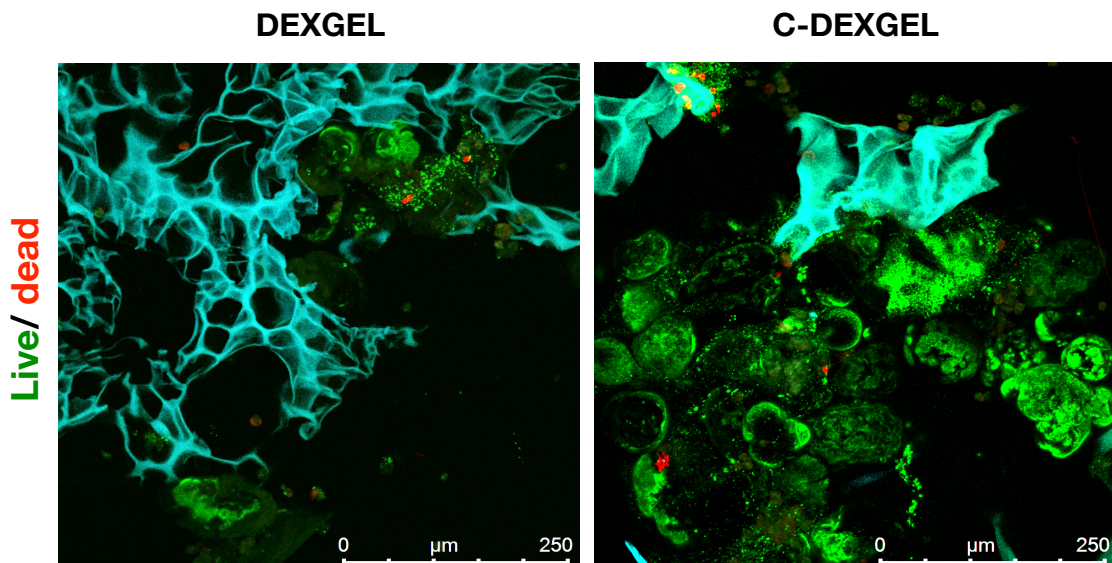


Figure 4.33 Viability of rat islets cultured on DEXGEL and C-DEXGEL scaffold by calcein-ethidium bromide staining.

#### 4.4.4 Expression of insulin hormone

Islets cultured on DEXGEL and C-DEXGEL scaffolds were stained for the expression of insulin hormone. Islets on both scaffolds were stained positive for

insulin and moreover the number of islets were higher in C-DEXGEL scaffold (Fig 4.34).

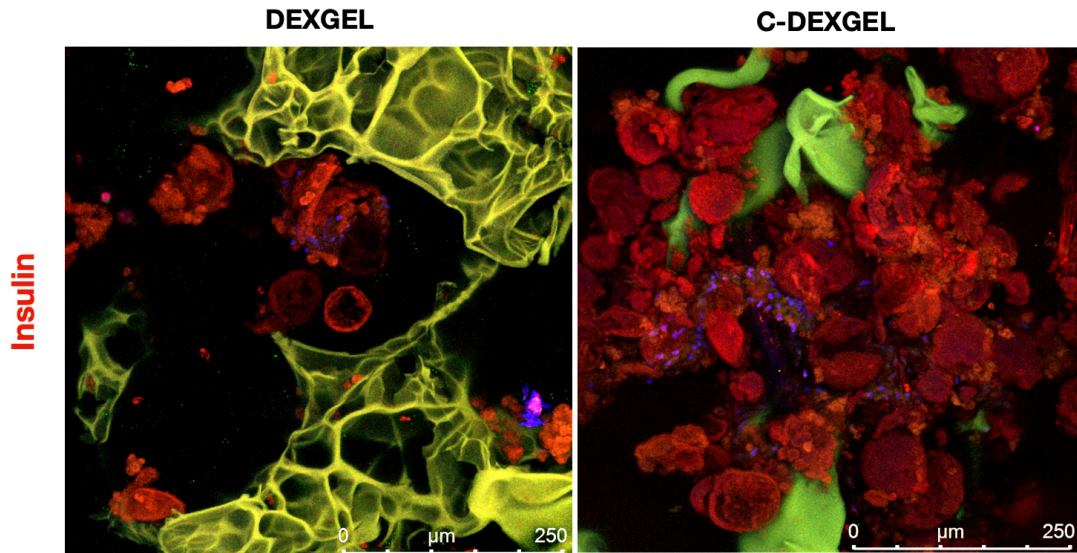


Figure 4.34 Immunofluorescence staining of rat islets on DEXGEL and C-DEXGEL scaffold. Islets in scaffold were positive for insulin hormone (green – scaffold, red-insulin).

#### 4.4.5 Islet function on the scaffold

To assess the functionality of the islets encapsulated in the scaffolds, the cells were challenged with low and high molar concentrations of glucose. Islets on the C-DEXGEL scaffolds secreted 1.5-fold higher insulin than on DEXGEL scaffold (Fig 4.35 A). The metabolic activity of islets on the scaffold was studied with MTT assay (Fig 4.35B). Over a period of 21 days, cells on C-DEXGEL scaffolds showed increased viability than on the DEXGEL scaffold which may be attributed to the increase in the islet cell attachment on the ECM coated scaffolds.

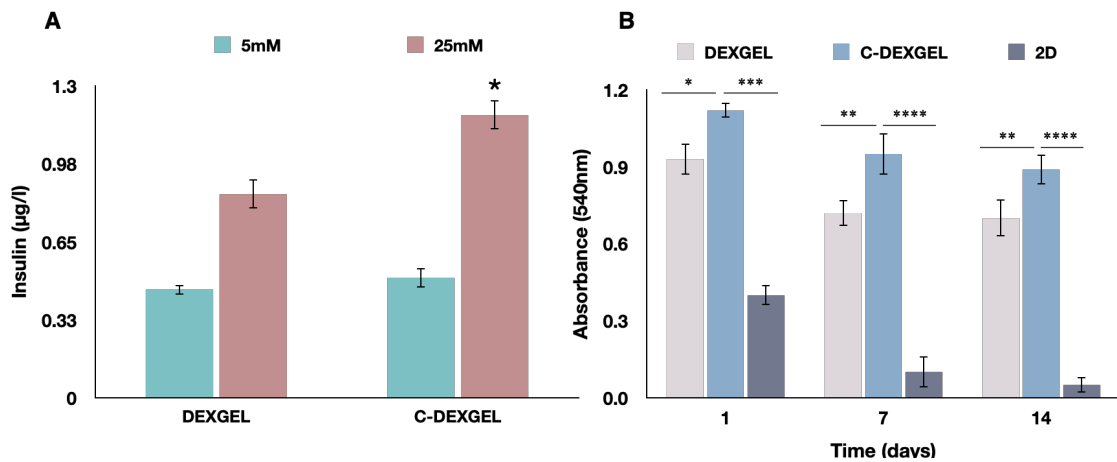


Figure 4.29 qualitative and quantitative analysis of insulin hormone in generated ILCs. A) Immunophenotypic characterization of islet like clusters stained positive for insulin hormone on DEXGEL and C-DEXGEL scaffolds B) Amount of insulin secreted by ILCs on scaffolds in response to various glucose concentrations (5 mM and 25 mM) quantified by ELIZA (One way ANOVA and two keys pos hoc analysis \* $p < 0.05$ )

#### 4.4.6 Gene expression studies

Figure 4.36 shows the fold expression of insulin, glucagon and Pdx1 gene of islets seeded on DEXGEL and C-DEXGEL scaffolds. The result of insulin secretion by glucose challenge also correlate with gene expression studies in which expression of insulin, glucagon, and Pdx1 were significantly higher ( $p < 0.05$ ) in ECM protein-coated C-DEXGEL scaffold than in uncoated DEXGEL scaffold.

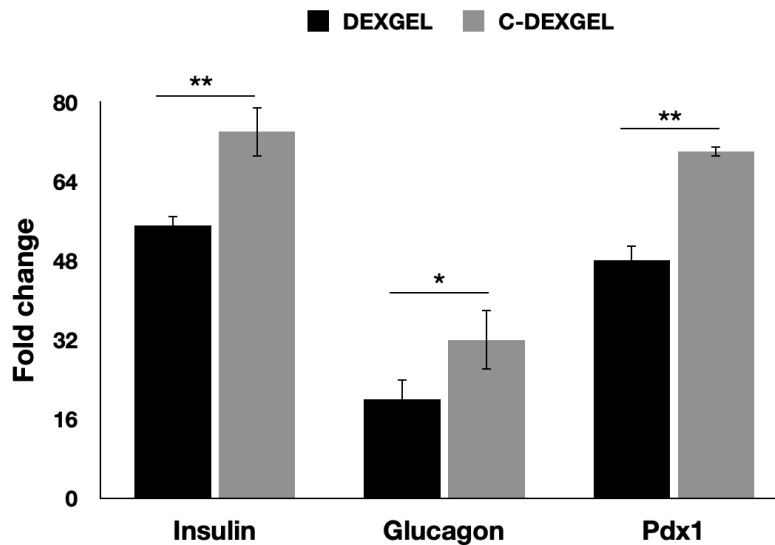


Figure 4.36 Quantitative analysis of pancreatic islet specific genes of islets cultures on DEXGEL and C-DEXGEL scaffolds using Real Time Polymerase Chain Reaction (One way ANOVA and two keys pos hoc analysis  $*p < 0.05$ ).

## ***4.5 Fabrication and characterization of immunoprotection membrane***

### **4.5.1 Synthesis of PU-PVP semi IPN**

PU-PVP with 10% PVP was synthesized according to our previously reported protocol. Semi IPNs were synthesized by incorporating polyurethane (PU) network in to polyvinylpyrrolidone (PVP). By swelling the PU (EG 60D) in N-vinylpyrrolidone with azobisisobutyronitrile as the initiator (Nair P D, 1995).

#### **4.5.1.2 Thermal stability of PU-PVP semi IPN**

Thermogravimetric analysis was carried out to study the thermal stability of synthesized semi IPN. PU started its degradation at 286 °C and that of PVP is 91 °C. But in 10% semi IPN, the starting of degradation was observed at 304 °C. In PU,

95% of degradation was observed at 445 °C and that of PVP and PU-PVP are 471 °C and 445 °C (Fig 4.37 A).

#### 4.5.1.3 Contact angle measurement

The static water contact angle measurement of PU was  $111\pm 5^\circ$  and that of PVP was  $62\pm 2^\circ$ . By the synthesis of semi IPNs of PU-PVP, a balance between hydrophilicity and hydrophobicity was observed which is  $71\pm 10^\circ$  (Fig 4.37 C).

#### 4.5.1.4 Mechanical properties of synthesized PU-PVP semi IPN

The mechanical properties of the synthesized PU-PVP were confirmed by mechanical testing using universal testing machine. The results showed that both PU and PU-PVP semi IPN is highly elastic in nature (Fig 4.37 B). No difference in elastic property was observed when PU formed semi IPN with PVP.

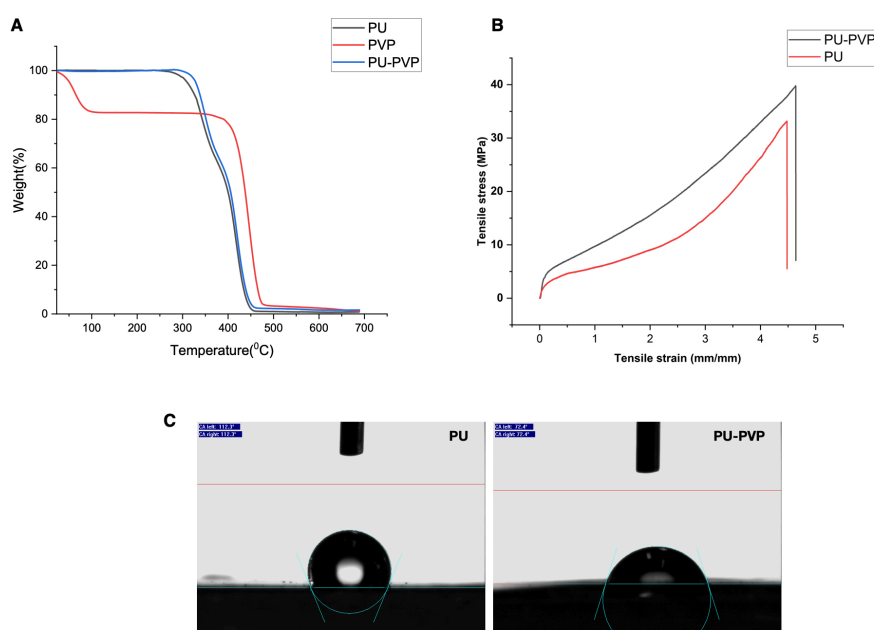


Figure 4.37 Showing physico-chemical characterization of synthesized PU-PVP semi IPN. A) Thermogravimetric analysis B) Mechanical property by UTM. C) Contact angle measurement and

#### 4.5.1.5 Cytotoxicity evaluation

Cytotoxicity of the material was evaluated by direct contact test, MTT assay and live dead staining. Figure 4.38 A shows the direct contact assay. Films of PU-PVP was placed over the L929 cells and incubated for 24 hrs. and no morphological changes were observed compared to negative and positive controls. MTT assay also showed comparable more than 80% of cell viability when L929 cells were incubated with 1,7 and 14-day extract of the material (Fig 4.38 B). Live dead staining of L929 cell culture over the PU-PVP films for 48 hrs. 90% viability with negligible dead cells (Fig 4.38C).

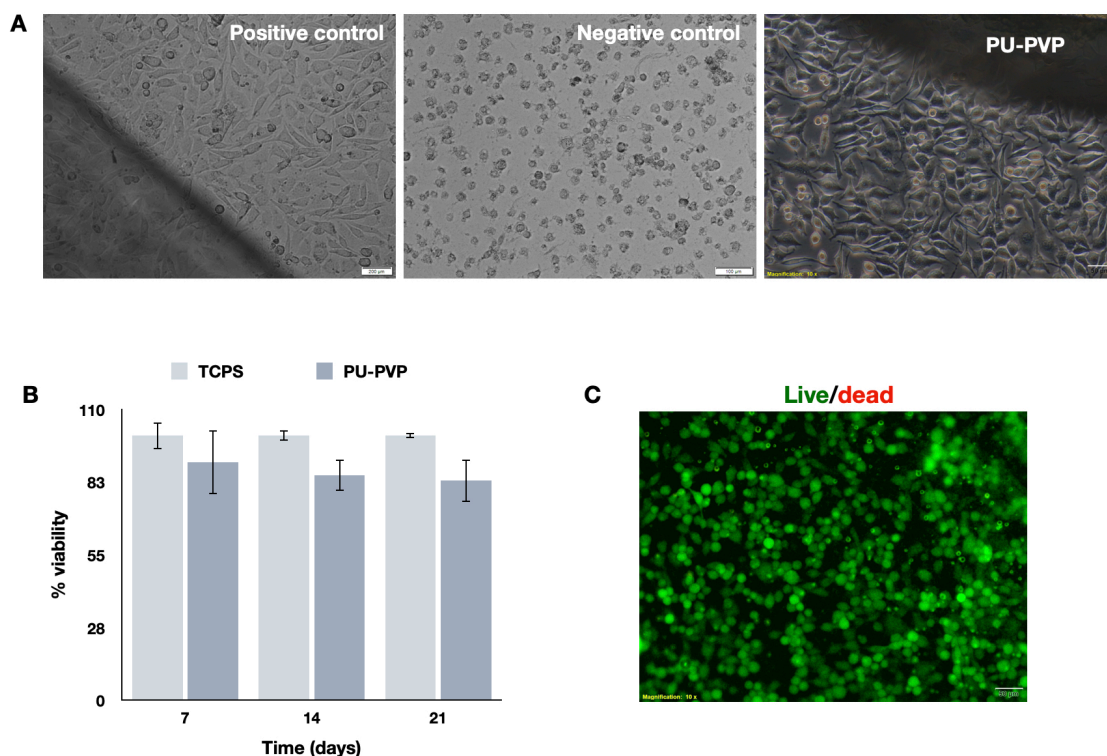


Figure 4.38 Cytotoxicity evaluation of PU-PVP semi IPN. A) Direct contact assay. No evident morphological change in cells cultured in the vicinity of PU-PVP semi IPN B) MTT assay showing cell viability with 100% scaffold extract compared to control group by indirect contact method C) Live dead assay showing live cells with negligible dead cells.

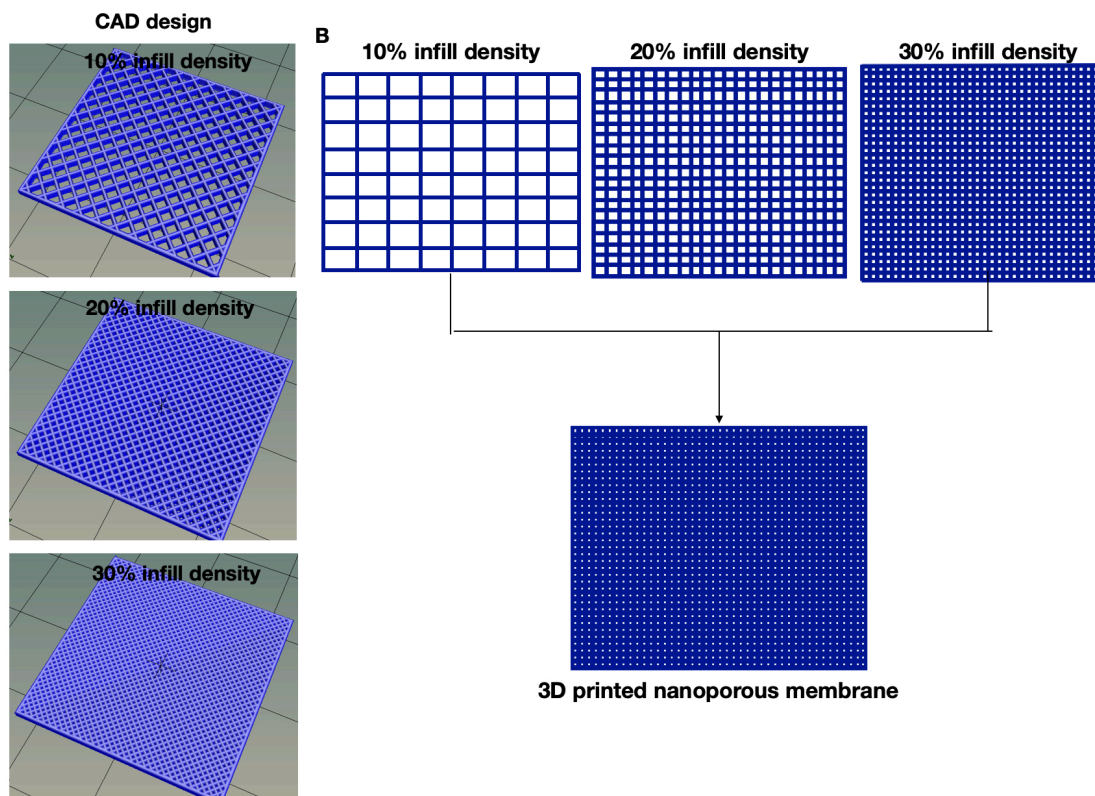


Figure 4.39 Design for the fabrication of Immunoisolation membranes. A) CAD image showing layers with different infill densities. B) diagrammatic representation of the top down approach for the creation of nanopores.

membrane was fabricated via a 3D printing technique. Nanoporous membrane was fabricated via 3D printing technique (Figure 4.39) in which 12% of PU-PVP solution prepared in chloroform was printed using a custom-made 3D printer. The membranes were composed of 12 layers. Nanopores were created by varying the infill density of printed layers. The first 4 layers are printed with 10% infill density creating a pore size of  $1.18 \pm 0.1 \text{ mm}^2$ . After that, another 4 layers with 20% infill density were printed which decreased the pore size to  $0.23 \pm 0.05 \text{ mm}^2$  (Fig 4.40 B). The final 4 layers were printed with 30% infill density leading to the closure of remaining

micropores and allowing the formation of nanopores (Fig 4.40 A, Fig 4.40 B). AFM analysis of the 3D printed membranes confirms the presence of nanopores with a diameter of  $200\pm 50$  nm (Fig 4.41) and the membrane thickness is 0.05 mm.

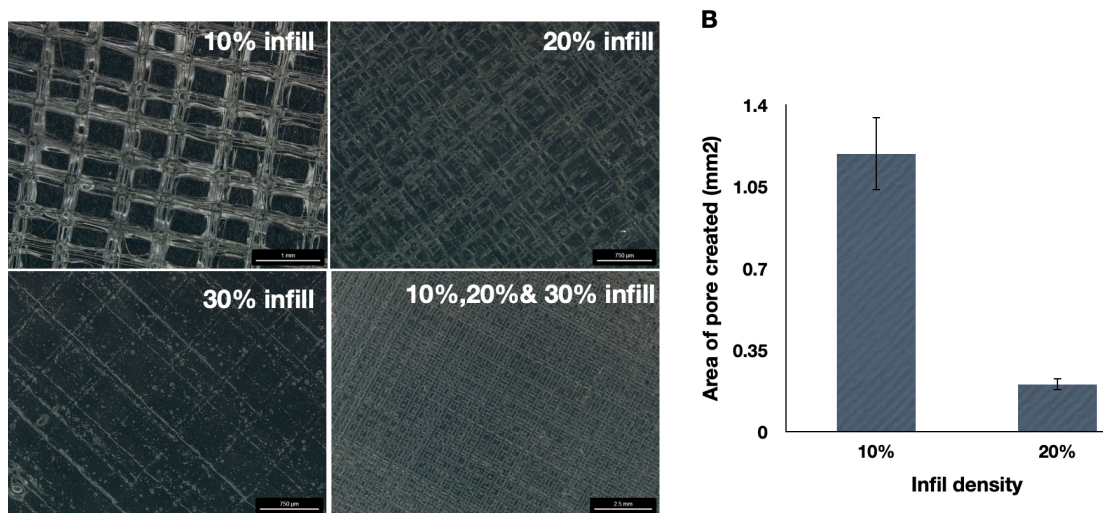


Figure 4. 40 Nanopore creation by 3D printing A) Stereo microscopic images showing the pores created by different infield density. B) Pore size created by printing layers with 10% and 20% infill density.

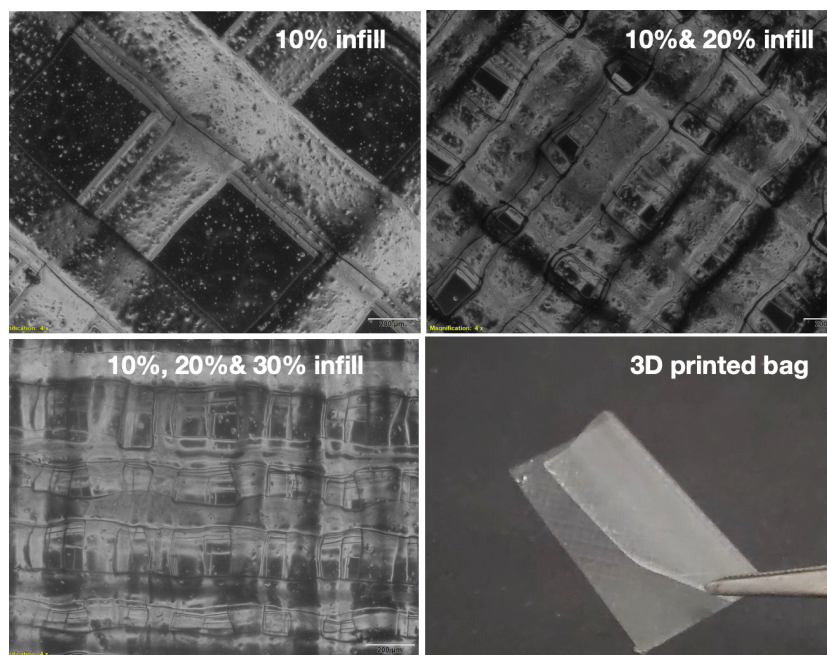


Figure 4.41 Showing phase contrast images of printed layers.

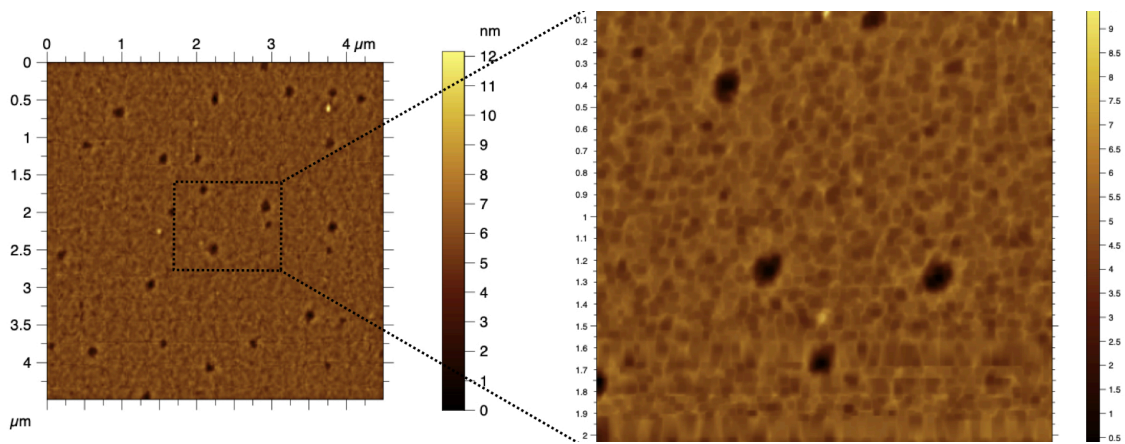


Figure 4.41 AFM image showing the nano pores created on the surface of 3D printed membranes.

#### 4.5.3.2 Diffusion of molecules across the membranes

Free diffusion of glucose and insulin is a key factor as it is important in maintaining the blood glucose level. For the diffusion studies of molecules, modified transwell was used (Fig 4.42A). Amount of glucose and insulin diffusion across the membranes over 10 minutes at 37°C was studied. (Fig 4.42B). More than 50% of glucose and insulin diffusion was observed over 10 minutes (Fig 4.42 C). The ability of the nanoporous membrane to block IgG diffusion was also studied for 7 days. The results indicate that the membrane was able to limit the IgG diffusion to <10% (Fig 4.42D). Overall, the diffusion studies suggest that 3D printed nanoporous membranes allowed the passage of smaller molecular weight species such as insulin and glucose and decreased the diffusion of larger molecules like immunoglobulins.

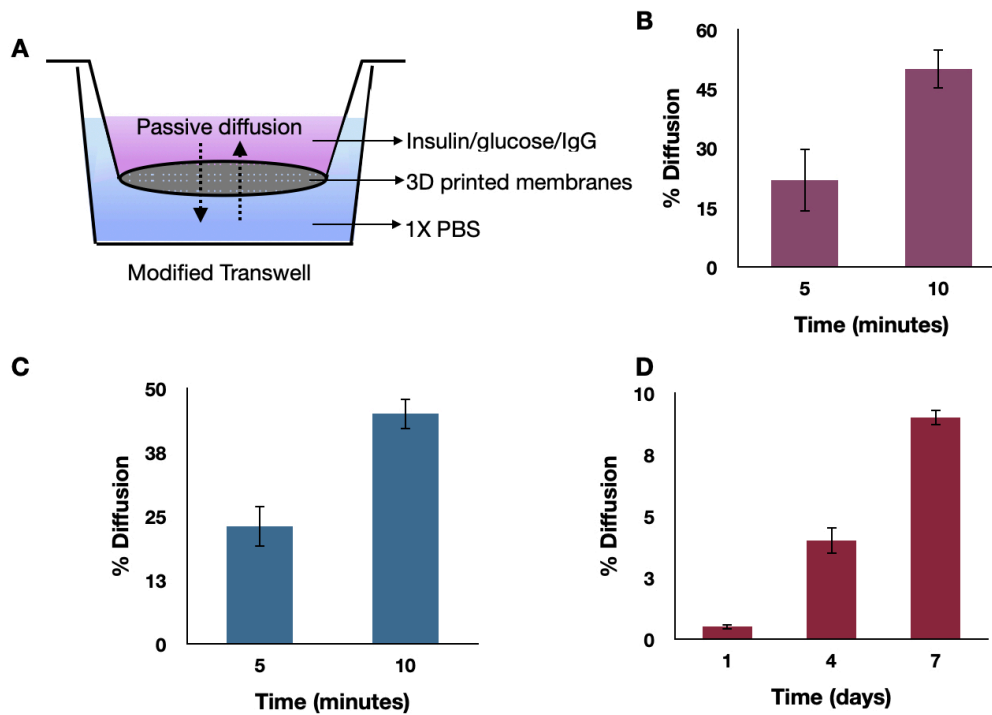


Figure 4.42 Diffusion of molecules across the 3D printed membranes. A) Schematic representation of diffusion assay, (B-D) diffusion of glucose, insulin and IgG across the membranes.

### 4.5.3 Fabrication of immunoprotective pancreatic transplantation device (IPTD)

After confirming the diffusions of molecules across the membranes, we tested the 3D-printed nanoporous membrane's capacity to maintain the viability and function of encapsulated islets and ILCs. For that, an islet or ILC-seeded C-DEXGEL scaffold was encapsulated in a 3D printed nanoporous membrane and heat sealed along the edges to form a bilaminar, flexible, and easy-to-handle nanoporous immunoprotection device named as immunoprotective pancreatic transplantation device (IPTD) (Fig 4.43).

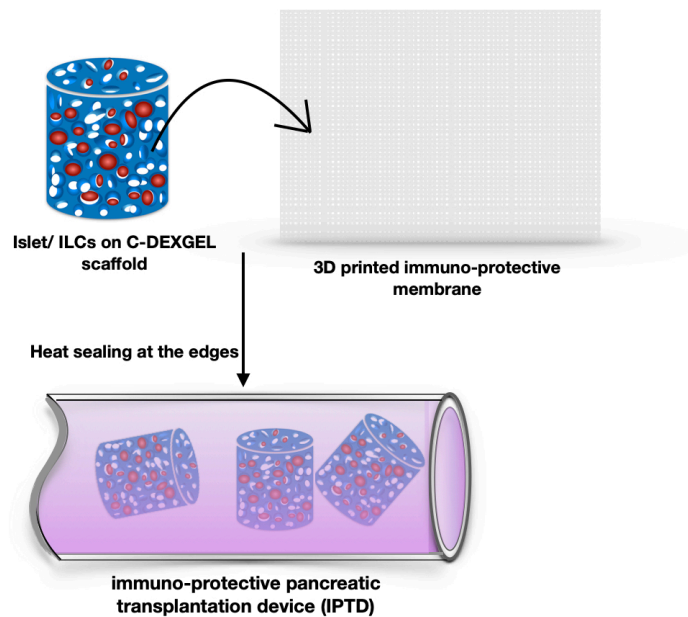


Figure 4.43 Showing schematic representation of the fabrication of immunoprotective pancreatic transplantation device (IPTD).

#### 4.5.3.1 Viability and insulin secretion of islet and ILCS on IPTD

After device fabrication, viability and insulin secretion of islet on IPTD was carried out and the results were compared with islet cultured on C-DEXGEL scaffold and on TCPS. After 7 days of culture, islets cultured on IPTD, C-DEXGEL scaffold and TCPS was challenged with low and high concentration of glucose. There was no significant decrease in insulin production between IPTD and C-DEXGEL scaffold. But islet on tissue culture plated showed less insulin secretion than other groups (Fig 4.44 A). The viability of islets on day 7, 14, and 21 of these groups were analysed by MTT assay. Islets were viable in IPTD and C-DEXGEL scaffold during the study period. Viability of isles on 2D culture plate was decreased as time progresses (Fig 4.44 B). Viability and functionality of differentiated ILCs on IPTD was compared with

ILCs on IPTD and tissue culture plated. The viability remains same over the study period between the groups. There was no difference in insulin secretion between ILCs on IPTD and ILCs on C-DEXGEL scaffold (Fig 4.G 44 C&D).

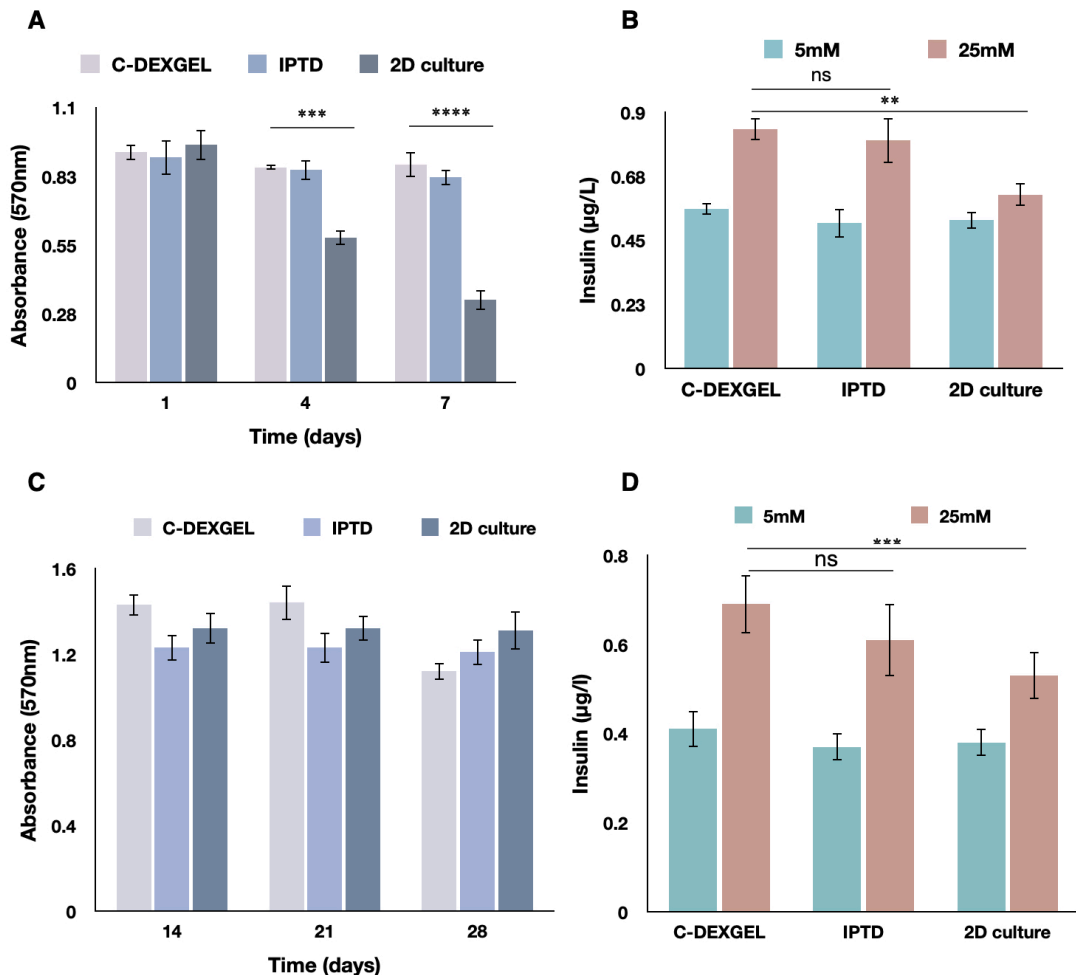


Figure 4.44 Viability and functionality of islet in immunoprotective transplantation device (IPTD) A&B) Viability and insulin secretion of islet on IPTD compared to islet on C-DEXGEL scaffold and tissue culture plate. C&D) Viability and insulin secretion of stem cell derived ILCs on IPTD (two way ANOVA \*\*\* $p < 0.001$ , \*\*\*\* $p < 0.0001$ )

#### ***4.6 In vivo assessment of the tissue engineered construct***

To investigate the function of IPTD in reversing diabetes, we encapsulated C-DEXGEL scaffold seeded with primary rat islets or ILCs in nanoporous membranes and fabricated the IPTD. The IPTD is implanted in the intraperitoneal cavity of diabetic wistar rats and compared the results with the group implanted without nanoporous membrane and diabetic and nondiabetic controls.

Table 4.1 Test groups for in vivo experiment.

Group 1	Islet on C-DEXGEL scaffold
Group 2	Islet on IPTD
Group 3	ILCs on C-DEXGEL scaffold
Group 4	ILCs on IPTD

##### **4.6.1 Blood glucose measurement**

After implantation, random blood glucose and body weight was monitored for every 7 days for two months. In animals transplanted with islet-IPTD (group 2), blood glucose concentration dropped from  $450\pm 30$ mg/dl to  $170\pm 50$  mg/dl within 14 days and remained normoglycemic till the end of the study. In animals transplanted with islets on the C-DEXGEL scaffold (Group 1), blood glucose was brought down to the  $200\pm 30$ mg/dl within 14 days of implantation. But after one month, animals became hyperglycemic. Whereas, in animals transplanted with ILCs encapsulated in IPTD, the BGL was brought down to  $250\pm 20$  mg/dl and maintained this range throughout the study period as comparable that of the previous reports. In animals

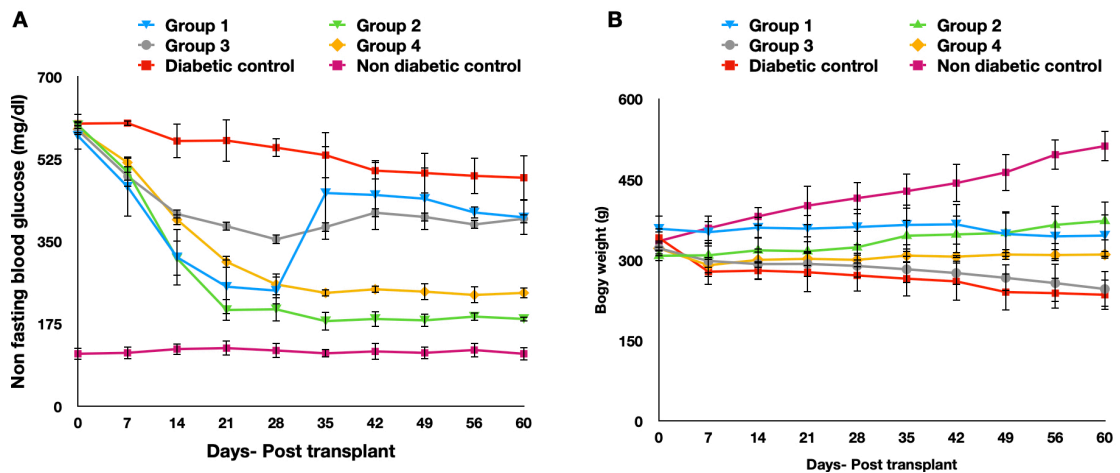


Figure 4.45 Blood glucose and body weight of diabetic rats transplanted with tissue engineered constructs in comparison with diabetic and nondiabetic rats as controls. A) Random blood glucose measurement. B) Body weight of animals.

with ILCS without any immunoprotection bag, the BGL was  $380 \pm 40$  mg/dl (Fig 4.45 A). The body weight of diabetic animals was decreased from  $320 \pm 30$ g to  $210 \pm 40$ g. In case of IPTD transplanted animals, after transplantation increase in body weight was observed. In healthy animals, increase of body weight from  $335 \pm 20$  to  $520 \pm 25$  was observed (Fig 4.45B).

#### 4.6.2 Response to glucose challenge

On day 30 of implantation, an intraperitoneal glucose tolerance test (IPGTT) was conducted to assess the metabolic regulation of blood glucose. Compared to healthy mice, engrafted animals had a higher peak value of blood glucose after stimulation. However, group 1 and group 2 animals reached basal level within 120 minutes after glucose bolus like the healthy rats. Group 4 also reached normal level within two hours but their responses are not as effective as animals transplanted with mature islets. In group 3 (ILCs on C-DEXGEL scaffold), the blood glucose was only

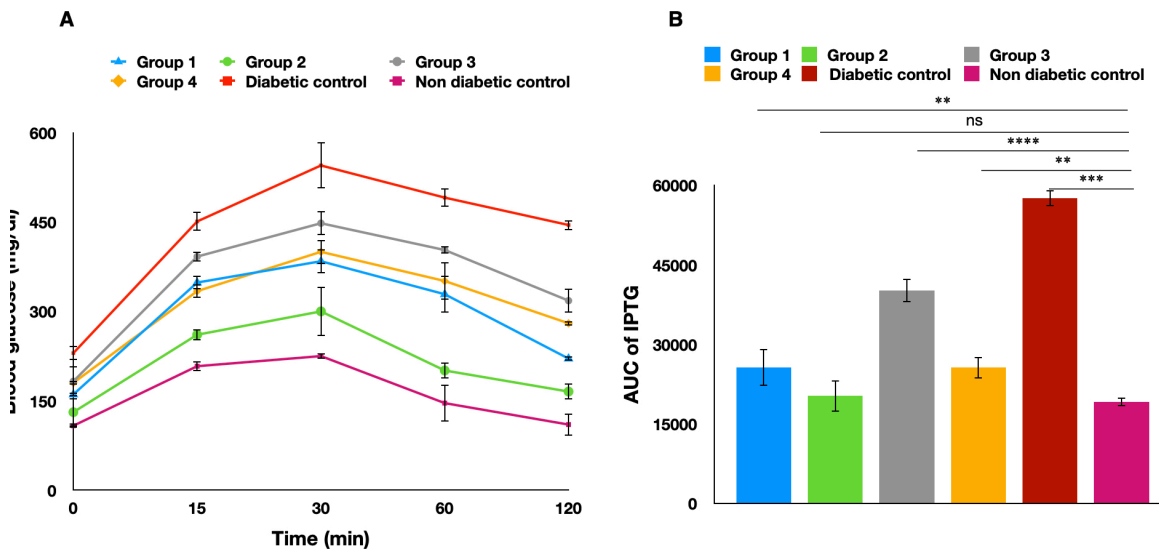


Figure 4.46 Intra peritoneal glucose tolerance test (IPGT) showing A) Blood glucose measurement. B) Area under the curve of IPGT (one way ANOVA  $**p < 0.01$ ,  $***p < 0.001$ ).

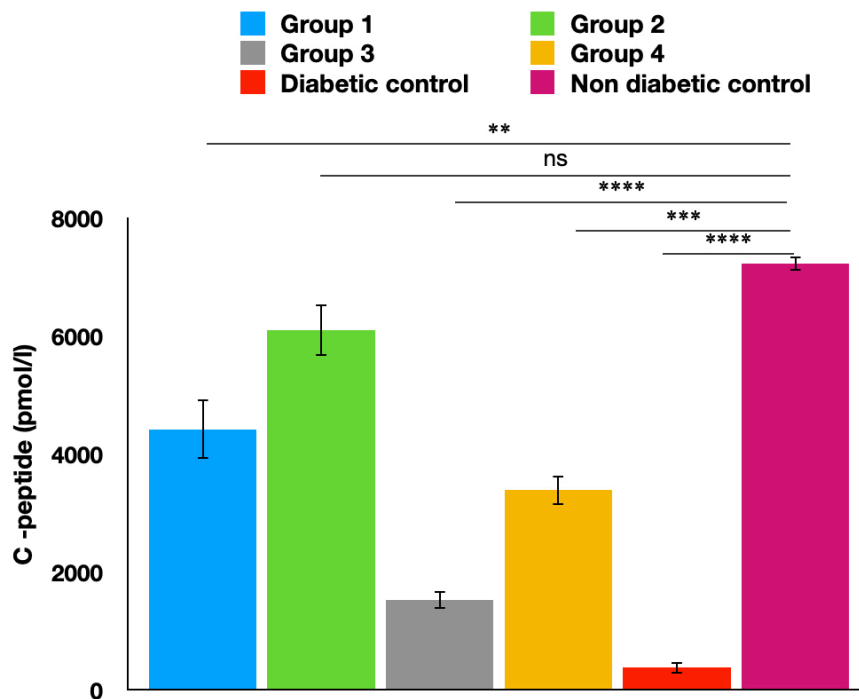


Figure 4.47 C-peptide concentration in blood serum of rats (One way ANOVA  $**p < 0.01$ ,  $***p < 0.001$ ,  $****p < 0.0001$ ).

reduced to  $360 \pm 30$  mg/dl (Fig 4.46 A&B). Serum C-peptide levels showed a higher C-peptide expression in animals transplanted with islets-IPTD (group2) followed by group 1. Stem cell differentiated ILCs on IPTD also showed an increased amount of C-peptide than the diabetic control group (Fig 4.47).

### 4.6.3 Architecture of implant

After 60 days of implantation, animals were sacrificed and constructs were retrieved. The implants were retrieved easily and no tissue adhesion was observed. In groups transplanted without IPTD, a size reduction of the construct was observed

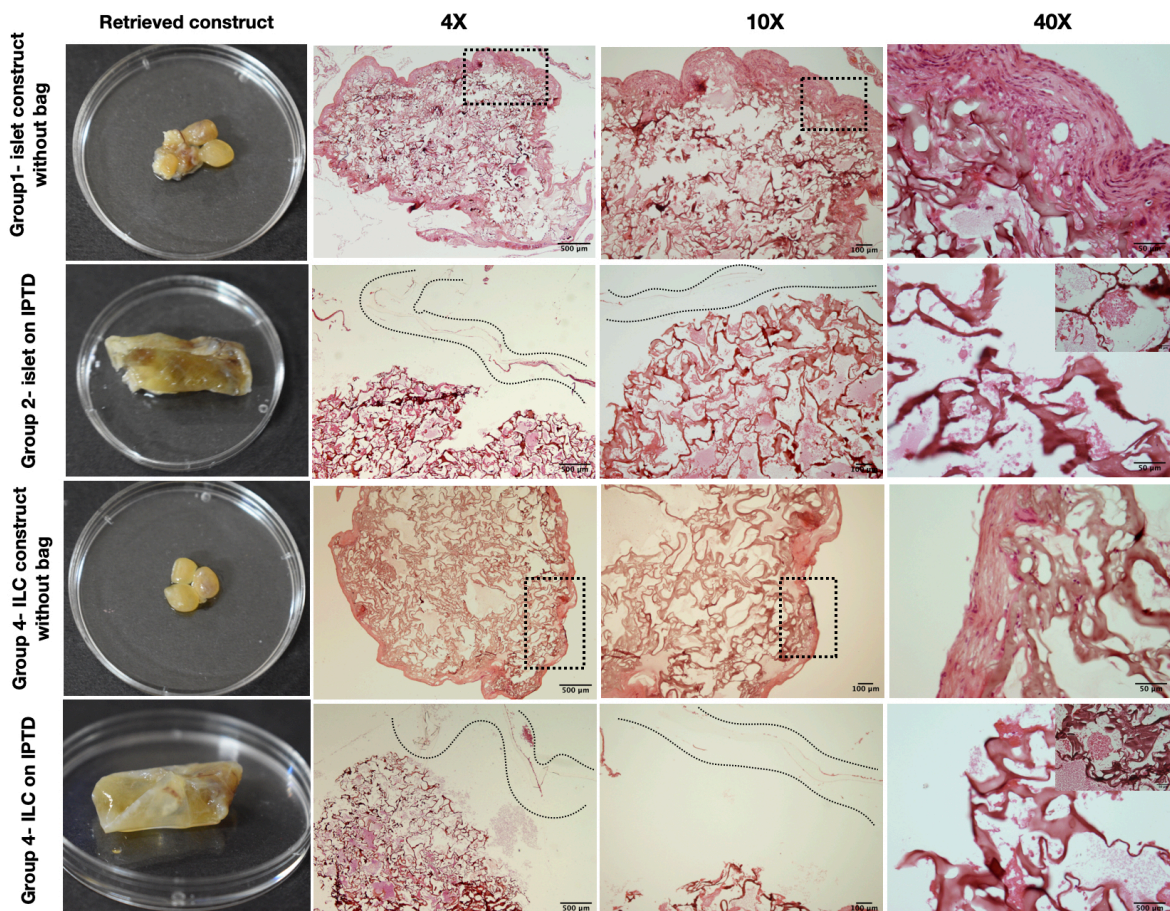


Figure 4.48 Hematoxylin and eosin staining of retrieved construct.

that may be attributed to degradation of the scaffold. Histological analysis showed no fibrotic tissue formation and also no cell penetration through the IPTD. H&E staining images showed that in group 1 and 2 a thick fibrotic layer was observed. And in groups 2 and 4, no fibrotic layer was observed around IPTD and both these groups maintained the spherical morphology of islets (Fig 4.48).

#### 4.6.4 Foreign body reaction on implant

Earlier studies report the development of strong innate immune-mediated foreign-body reactions (FBRs) caused by the implants employed in these studies lead

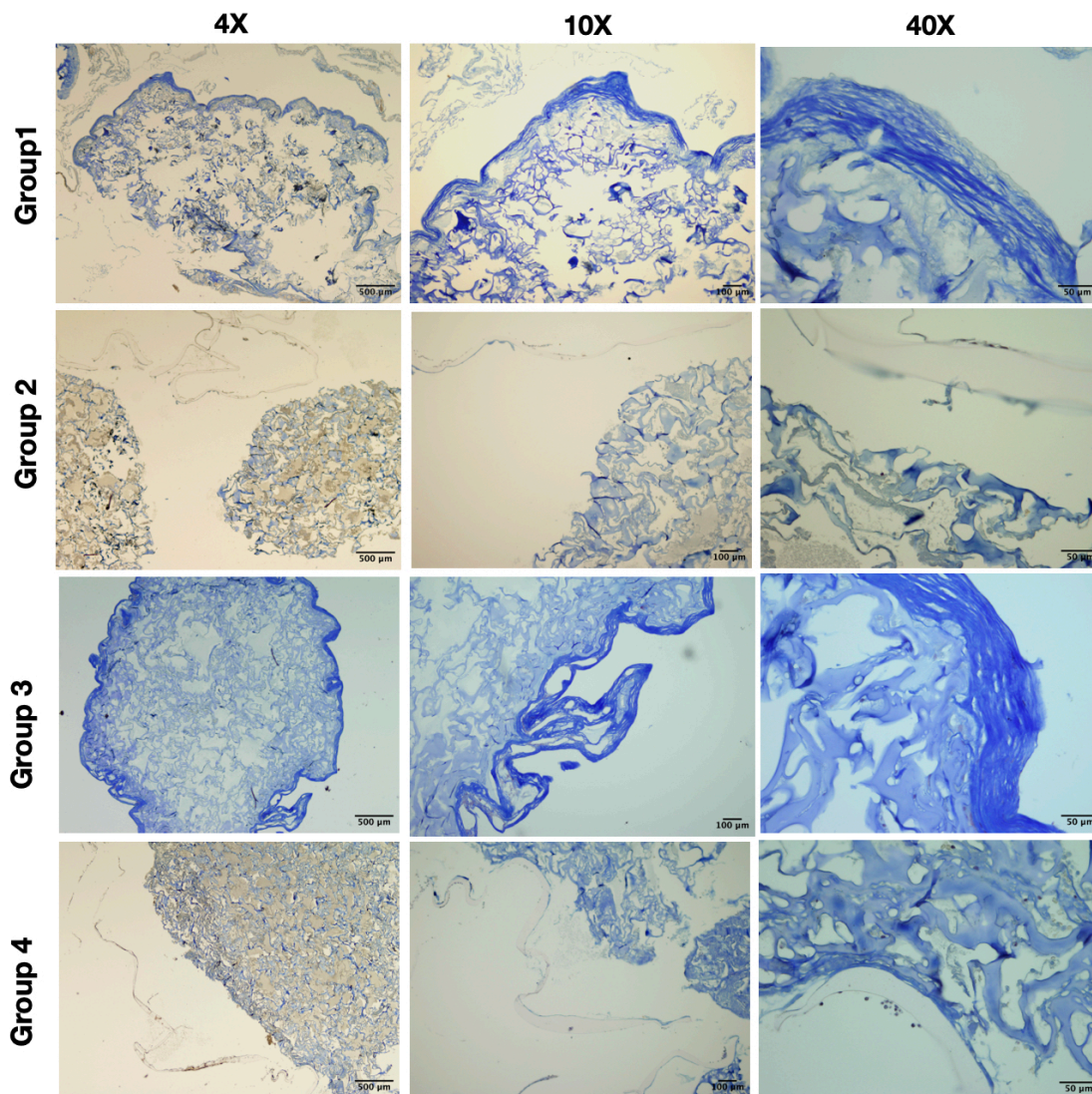


Figure 4.49 Trichrome staining of retrieved constructs.

biomaterial for cell encapsulation implant devices should have low macrophage recruitment and fibrosis at the material-tissue interface and be able to create neovasculature along its surface to sustain encapsulated cells with oxygen and nutrients. Earlier reports suggest that the implants used in these studies elicited severe innate immune-mediated foreign body reactions (FBRs) leading to fibrotic deposition followed by nutritional isolation and necrosis of the donor tissue (Anderson et al., 2008). Here we also attempted to study the fibrotic deposition using trichrome staining. In both groups 1 and 2, deposition of a thick fibrotic layer of thickness  $80 \pm 12 \mu\text{m}$  was observed. This result correlates with the blood glucose regulation in which the glucose levels of bag of group 1 was brought down to the normal range within 14 days after implantation. After one month, normoglycemia

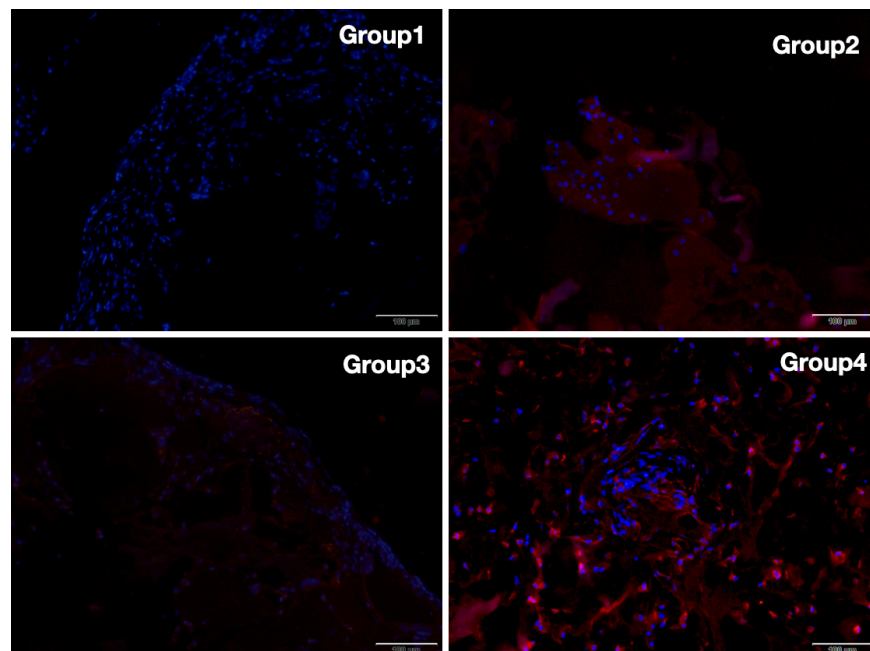


Figure 4.50 Showing insulin immunofluorescence staining of retrieved constructs.

was reversed back to hyperglycemia. This may be due to the destruction of islets/ ILCs by host immune reaction or due to the deposition of the thick fibrotic layer that limited the diffusion of insulin and glucose. In groups implanted with PTD, the formation of the fibrotic layer was limited to  $<10\ \mu\text{m}$  further increasing the function of IPTD (Fig 4.49).

## CHAPTER 5 - DISCUSSION

Transplantation of pancreatic islets has proven to be an effective treatment for T1DM (Shapiro et al., 2000). However, it has major disadvantages associated with the unavailability of donor islets, islet loss during transplantation, and continuous supply of immunosuppressants, etc. This led to the development of tissue-engineered islet-like clusters (ILCs) in which ILCs were differentiated from stem cells on a three-dimensional scaffold that mimics the native islet microenvironment and can be transplanted into the T1DM patients (Chao et al., 2008) (Jiang et al., 2007) (Nair et al., 2020) (Navarro-Tableros et al., 2019). However, in the clinical transplantation of stem cell-derived ILCs, teratoma formation from undifferentiated stem cells, as well as the immune rejection by the transplanted ILCs are the major concerns (Steele et al., 2014). Therefore, the encapsulation of transplanted ILCs in a polymeric immunoprotective device will ensure the safe delivery of ILCs and give protection from the host immune response. In this study, a combinatorial approach for the successful islet transplantation has been developed wherein, islet or stem cell derived islet was cultured on 3D scaffold systems and is again encapsulated in a 3D printed immunoisolation bag for the safe and functional delivery of transplanted cells and the feasibility of the developed system in the reversal of hyperglycaemia of diabetic rats was also tested.

### ***5.1 Fabrication and characterization of scaffolds***

Biomaterial scaffolds are the template within which cells and the biological molecules are added to create a functional tissue replacement. And ideal scaffold for

islet tissue engineering should be highly porous to accommodate the large islet clusters or stem cell derived ILCs with diameter ranging from 50-250 $\mu$ m diameter (Aloysious and Nair, 2014). Apart from porosity, scaffold should not be cytotoxic, carcinogenic or teratogenic. It should be biocompatible and biodegradable and have tailorable degradation and mechanical properties. Natural and synthetic polymers like collagen, gelatine, alginate, poly- $\epsilon$ -caprolactone (PCL), poly(l)-actic acid (PLA), poly-glycolic acid (PLG) etc are available for the fabrication of scaffolds (Shimojo et al., 2020) (Dhandayuthapani et al., 2011). To design a successful tissue engineered construct which engraft tissue cells that capable of functional restoration of defected tissue, it is important to control the structural properties of a scaffold up to nano scale level (Shimojo et al., 2020). For the current study, we have fabricated two different scaffold system fabricated via two different fabrication method for islet tissue engineering. First is a wet electrospun scaffold made of a synthetic polymer PCL and the second scaffold system consist of two natural polymers dextran and gelatin and the scaffold is fabricated via freeze drying.

### **5.1.1 Fabrication and characterisation of wet electrospun scaffold**

The average size of the pancreatic islet is around 80-150  $\mu$ m diameter and the size of stem cell-derived islets also depends on the pore size of the scaffold (Aloysious and Nair, 2014). Hence, for islet tissue engineering, the scaffold should be highly porous to maintain the spherical morphology of islets and pores should be interconnected to facilitate maximum diffusion of oxygen and nutrients. Various reports suggest that culturing islets or stem cell derived ILCs on a 3D system rather

than 2D culture plates increased the viability and functionality of cells (Ojaghi et al., 2019). Formation of ILCs on 2D surface often creates larger ILCs with less viability and functionality (Anitha et al., 2020). In order to create smaller ILCs with higher insulin production, porosity of the scaffold is a key factor (Wilson et al., 2022). Various fabrication techniques are available for the production of scaffold system for islet tissue engineering. Electrospinning is one of the versatile techniques commonly used for the fabrication of ECM mimicking fibrous matrices (Owida et al., 2022). Although, the small pore size and closely packed nanofibers of the conventional electrospun scaffold limit cell penetration and may cause the formation of large ILCs with poor viability and insulin production (Vaquette and Cooper-White, 2011). It is essential to fabricate highly porous 3D scaffolds with ECM-imitating architecture since the scaffold's porosity is a crucial factor in the formation of ILCs of the desired cluster size. Over the years, various attempts have been made to generate highly porous scaffolds by electrospinning such as wet electrospinning. In wet electrospinning, fibers are collected on a liquid bath unlike the rotating or stationary collectors in conventional electrospinning (Lee et al., 2012)

For the fabrication of wet electrospun scaffold, polycaprolactone (PCL) is selected since it is a widely used polymer for tissue engineering applications. It is an FDA approved polymer with better biocompatibility and good mechanical properties (Mondal et al., 2016). PCL scaffold was fabricated by wet electrospinning. Due to the presence of the liquid collecting medium, the fibers are loosely packed creating a larger inter fibrillar distance giving porosity to the scaffold (Yokoyama et al., 2009).

Compared to conventional electrospun scaffold, wet electrospun scaffold showed increased porosity consistent with other results. With wet electrospinning, we achieved a 50% increase in the porosity than the conventional electrospinning.

To make the scaffold hydrophilic and to enhance the cell attachment we conjugated an ECM protein collagen I to the scaffold. For that, the PCL was aminolysed with hexadamine. One of the two NH<sub>2</sub> groups in hexadamine reacts with PCL's ester group to generate a -CONH bond during aminolysis, while the other one is left unreacted on the surface to form an amide bond with collagen I's -COO group (Li and Lee, 2020). According to previous reports, mesenchymal stem cells' adhesion, survival, and functionality were increased by collagen I conjugation After collagen conjugation the hydrophilicity of the material was increased which favours cell attachment (Vrana et al., 2007). Even after aminolysis and collagen conjugation by EDC-NHS method, scaffold maintained the porosity and pore architecture.

### **5.1.2 Fabrication and protein conjugation of dextran dialdehyde-gelatin scaffold**

Previous reports suggest that scaffold made of two natural polymers, dextran dialdehyde and gelatin cross linked via Schiff's base reaction, is ideal scaffold for islet tissue engineering because their gelatin content helps in islet attachment and its dextran dialdehyde has a potential angiogenic effect which helps during islet transplantation (Aloysious and Nair, 2014). So we chose the dextran dialdehyde and gelatin (DEXGEL) scaffold as our second system.

Signalling between the extracellular matrix and cell affects many functions like cellular maintenance, differentiation, proliferation, cell survival, etc. During islet

isolation by enzymatic digestion, the basement membrane of the islet is damaged or lost leading to decreased functionality and viability during transplantation (Stendahl et al., 2009). Many reports suggest that the microenvironment of the islet has a major role in maintaining the islet architecture and functional viability, and it is known that the islet basement membrane is composed largely of collagen IV, laminin, and fibronectin etc. Restoring the islet microenvironment with these ECM proteins will be beneficial for the better functioning of islets (Yap et al., 2013). In this study, to mimic the islet microenvironment, we conjugated two ECM protein collagen IV and laminin to the free carboxyl residue of gelatin on the DEXGEL scaffold by EDC-NHS mechanism.

The porosity and the pore architecture of the scaffold were maintained after ECM protein conjugation. A DEXGEL scaffold is highly porous and the pore is interconnected which allow the free flow of nutrients and oxygen. Pore diameter of DEXGEL scaffold was 100-300 $\mu$ m which remained the same after protein conjugation. There should be a balance between the hydrophilicity and hydrophobicity of the material for better cell attachment and migration. Maximum cell adhesion and growth have been reported to be observed on moderately hydrophilic materials with contact angles ranging from 50-60 $^{\circ}$ . The contact angle of DEXGEL scaffold was 62 $\pm$ 3 $^{\circ}$  and after conjugation. Even after protein conjugation the C-DEXGEL scaffold exhibited moderately hydrophilic nature that is favorable for tissue engineering applications. A decrease in swelling and degradation was observed after protein conjugation by EDC-NHS method contributing to the

mechanical integrity of the scaffold. The degradation profile of DEXGEL and C-DEXGEL scaffold is slow comparable to that of the formation of ILCs.

## ***5.2 ADMSC isolation and characterisation and differentiation into ILC on scaffolds***

### **5.2.1 ADMSC isolation and characterization**

Stem cell derived ILCs are the alternative cell source of beta cells for the treatment of diabetes mellitus. Among the embryonic stem cells, iPSCs and various adult stem cells, ADMSC shows promising results in generating ILCs (Enderami et al., 2018). The isolated mesenchymal cells from rat adipose tissue were analysed for their plastic adherence property, expression of positive and negative markers and multi lineage differentiation potency according to The Society of Cellular therapy (ICST) (Dominici et al., 2006). The isolated cells exhibited spindle shaped fibroblastic morphology and had plastic adherence properties confirmed by cytoskeleton staining actin and vimentin. Adipose derived mesenchymal stem cells exhibit several surface markers including CD29, CD44, CD54, CD55, CD90, CD90, CD105, CD106, CD 146 etc (Chamberlain et al., 2007). Immunofluorescence analysis revealed that the isolated cells expressed CD70, CD90 and CD105 and the FACS analysis also confirmed the expression of these markers and 80% are positive for CD80, 76% expressed CD 90 and 70% expressed CD105. Both immunofluorescence and FACS confirms the absence of hematopoietic markers CD34/45 (Bayati et al., 2013). Furthermore, multi potency of the isolated cells was confirmed by their potential to osteogenic, chondrogenic and adipogenic lineages

consistent with our previous reports. Our results corroborate with previous reports (Schmelzer et al., 2019) suggest that the isolated cells are mesenchymal stem cells.

### **5.2.2 Differentiation of ADMSC into ILCs**

Type I diabetes mellitus (T1Dm) is an autoimmune disease characterized by the destruction of insulin-producing pancreatic cells by auto antibodies which results in insulin deficiency leading to elevated blood glucose levels and associated complications (Yau et al., 2000b). A major treatment strategy includes exogenous insulin administration after monitoring the blood glucose level, but it cannot effectively attain the same level of control achieved by exogenous insulin secretion. As a result, the patients undergoing such treatment often suffer from hypoglycemia and prolonged hyperglycemia induced diabetic retinopathy, nephropathy, neuropathy, cardiovascular diseases, diabetic foot ulcers, etc. (Tan et al., 2019). Transplantation of pancreatic islets from the cadaveric pancreas has proven to be an effective treatment for T1DM (Shapiro et al., 2017). However, it has major disadvantages associated with the unavailability of donor islets, islet loss during transplantation, and continuous supply of immunosuppressants, etc. This led to the development of tissue-engineered islet-like clusters (ILCs) in which ILCs were differentiated from stem cells on a three-dimensional scaffold that mimics the native islet microenvironment and can be transplanted into the T1DM patients (Dang Le et al., 2022) (Kanafi et al., 2013a) (Sandilya and Singh, 2021) (Kim et al., 2016).

Our earlier reports confirmed the efficiency of differentiating adipose derived mesenchymal stem cells into insulin producing islet like clusters. Here, we could

generate ILCs from ADMSCs using our previously reported protocol (Aloysious and Nair, 2014) (Anitha et al., 2020). In the differentiation process, mesenchymal stem cells of endodermic origin are converted in to islet like clusters of endodermic lineage in a serum free medium supplemented with different cocktails of growth factors and biomolecules for 21 days (Chandra et al., 2009). During the first three days of differentiation, growth factor activin A along with  $\beta$ -mercaptoethanol induces cells to endodermic lineage by activating transcription factors such as SOX-17, HNF-3 and TCF-2. In the next stage, cells were supplemented with transcription factors specific for pancreatic endoderm such as PSDX-1 and NGN-3 were activated by FGF, EGF, L-glutamine and non-essential amino acids. In the final stage of differentiation, nicotinamide, activin and betacellulin for the maturation and hormone synthesis of differentiated pancreatic endocrine cells (Chandra et al., 2011). In 2D differentiation, cell clustering was observed by day 10 and mature islet like clusters were observed by day 21. At the end point of differentiation, the cells stained positive for endocrine hormones insulin, glucagon and somatostatin. The size of formed ILCs is a major factor deciding the viability and hormone secretion. Larger islets tend to lose its viability by central core necrosis by hypoxia (Komatsu et al., 2017). The size of the islets formed in 2D differentiation are  $<300 \mu\text{m}$  diameter. In order to tailor the size of formed islets, it is necessary to culture them on 3D matrix with controlled pore size. Previous reports suggest that when stem cells were differentiated on 3D matrix with controlled pore size, smaller islets with increased viability and functionality were formed (Anitha et al., 2020).

### **5.2.3 Generation of ILCs on wet electrospun PCL scaffold**

ADMSCs were seeded and differentiated into ILCs following the same pattern of differentiation as in 2D. The generation of ILCs on the wet electrospun collagen coated CPCL scaffold was compared with PCL scaffold without any modification and collagen coated conventional electrospun 2D sheets. After 24 hrs of seeding, cells MSCs were attached and spread on the scaffold. At the end of differentiation from SEM images, spherical islets like clusters with size  $70 \pm 20 \mu\text{m}$  diameter was observed on CPCL scaffold and the clusters are anchored to the electrospun fibers. Previous reports suggest that, smaller islets are more superior in terms of viability and functionality that will increase the degree of success after transplantation (MacGregor et al., 2006) (Zorzi et al., 2015). Due to the lack of cell attachment moieties, ILCs on the PCL seems to be disintegrated and detached from the scaffold. Moreover, due to the limited pore size due to high fibre density, cell infiltration in the electrospun 2D sheets were limited leading to the formation of larger clusters on their surface. The size of the ILCs on the electrospun sheet was  $300 \pm 10 \mu\text{m}$  in diameter. Due to the large size, supply of oxygen in the core of the clusters were limited leading to the necrosis of cells in the centre of clusters (Komatsu et al., 2017) which is evident from live dead images. Negligible dead cells were observed in ILC formed on CPCL scaffold.

Insulin secretion of ILCs on CPLC scaffold showed 1.4-fold increase in insulin secretion than larger ILCs formed on electrospun sheets. This result is consistent with the previous reports in which, hypoxic condition in larger islets affect

the insulin secretion. pO<sub>2</sub> level 7mmHg leads to low oxygen tension and low glucose supply to the core of larger islets decreases the insulin secretion (Garcia-Contreras et al., 2017). Key pancreatic endocrine indicators including Pdx1 and Nkx6.1 were expressed by ILCs formed on the CPCL scaffold and electrospun sheet. The differentiation of ADMSCs to ILCs is confirmed by the co-expression of these two markers, which is only present in pancreatic beta cells (Rezania et al., 2014). A 68-fold increase in the insulin gene expression was seen in ILCs on CPCL scaffold than on electrospun sheet. The higher insulin protein expression of the wet electrospun samples seen in the glucose challenge assay was further supported by the gene expression results. In comparison to the electrospun sheet, the expression of Pdx1, Nkx6.1, and GLUT2 increased significantly in the CPCL scaffold. Despite the fact that glucagon and somatostatin expression was insignificant between groups. Immunofluorescence staining of insulin hormone at the end of differentiation also confirms the formation of ILCs on both scaffolds.

#### **5.2.4 Generation of ILCs on C-DEXGEL scaffold**

Here also for the differentiation, the same protocol for 2D and wet electrospun scaffold was used. Previous studies have reported that ECM plays a role in the development and differentiation of islet cells. In our study, we differentiated rat adipose stem cells into ILCs using ECM protein conjugated biodegradable 3D scaffold. To maintain the function and differentiation, pancreatic beta cells need a cell responsive matrix (Thivolet et al., 1985). A functional cellular response must therefore be elicited by the matrix exposed to these cells, which may be facilitated by

the inclusion of bimolecular recognition components into the scaffold analogous to those of the native cell matrix. Therefore, it is quite interesting to make scaffolds biomimetic through selective surface changes as opposed to nonspecific matrix components (Salvatori et al., 2014). In this study, we have conjugated two ECM components of the native pancreas such as collagen IV and laminin to make the scaffold more biomimetic. During the developmental stage islet express different integrins that bind to the ECM protein which further regulate the development and maturation of islet cells. Here we hypothesise that, ECM molecule laminin and collagen IV expressed on the C-DEXGEL scaffold heavily influence the migration and differentiation of ILCs with better insulin secretion.

Both DEXGEL and extra cellular matrix protein coated C-DEXGEL supported the attachment and growth of ADMSCs. From live dead images, after 24 hrs of culture, all of the cells are viable and negligible dead cells were observed. Live dead staining of ILCs also showed no dead cells. Peripheral actin condensation during the cluster formation was observed during differentiation. In undifferentiated conditions, the long thin actin fibers that maintain the spindle form of mesenchymal stem has shown peripheral actin condensation comparable to that of islet cells (Gallego-Perez et al., 2010).

### ***5.3 Islet isolation and culture on scaffolds***

#### **5.3.1 Islet isolation**

Islets were isolated from rat pancreas by collagenase V digestion according to our perviously reported protocol (Aloysious and Nair, 2014). After collecting the

tissue from euthanised rat, pancreas was chopped into small pieces in increase the surface area for enzyme action. Isolated islets had spherical morphology with size ranging from 50-250  $\mu\text{m}$  diameters. Purity of the isolated islet was determined by dithizone staining which is a valuable method to identify the islet cells (Pisania et al., 2010). In dithizone staining, the isolated islet appeared crimson red color by chelating the zinc granules in the  $\beta$ -cells as previous reports. The isolated islet also stained positive for insulin and in live dead staining the cells after enzymatic treatment appeared viable in calcein AM/ ethidium bromide staining. Hence, we confirmed the viability and functionality of isolated islets.

### **5.3.2 Islet on C-DEXGEL scaffold**

Islets are highly dependent on their ECM matrix for maintaining the architecture, survival and insulin secretion. Islet culture on two dimensional culture plates tends to go apoptosis after 7 days of culture (Dorrell et al., 2008). Culturing islet on three dimensional scaffolds that serves as the extra cellular matrix tend to increase viability and function of islets (Daoud et al., 2011) (Lemos et al., 2017) (Tokito et al., 2021). Isolated islets were seeded on the C-DEXGEL scaffold and effect of ECM molecule on islet attachment viability and function are compared with islet on unmodified DEXGEL scaffold. Live dead imaging after 7 days of culture showed that both DEXGEL and C-DEXGEL scaffold support the attachment and growth of islets. Even though, due to the cell attachment moieties like collagen IV and laminin, more islets cells were attached on the C-DEXGEL scaffold than DEXGEL scaffold which is evident in SEM images and Live dead staining image.

The viability of islets was more in C-DEXGEL scaffold than DEXGEL scaffold in MTT assay. Islet on C-DEXGEL scaffold also secreted more insulin than the unmodified scaffold which is also correlate with the gene expression studies. There are previous reports which suggest the role of ECM molecules such as collagen IV, laminin, fibronectin, vitronectin, etc in increasing insulin secretion and viability of islets. Collagen IV is abundant in the islet peripheral matrix and determines the cell fate, maintaining islet architecture and increased cell survival (Weber et al., 2008) (Yap et al., 2013). Laminins promote the production of hormones and transcription factors including PDX1, insulin 1, insulin 2, glucagon, somatostatin, and GLUT-2. Additionally, they activate the crucial metabolic regulator's protein kinase B (Akt) and extracellular signal-regulated kinase (ERK), which can cause the differentiation of precursor cells into beta cells. Moreover, the combination of collagen IV with a specific sequence of laminins has been shown to increase glucose-stimulated insulin secretion in islet cells (Llacua et al., 2016) (Rozario and DeSimone, 2010). Overall, these results indicated that the conjugation of collagen IV and laminin as a coating on the DEXGEL scaffold increases cell attachment and insulin hormone secretion.

#### ***5.4 Fabrication and characterization of immunoprotection membrane***

To achieve successful islet transplantation for T1DM, encapsulation of transplanted pancreatic construct in a protective polymeric membrane is necessary to create a barrier between the transplanted construct and the autoantibodies of the recipient's immune system and serve as an optimal cell encapsulation device that is biocompatible, non-biodegradable, and stable. It should facilitate the mass transfer to

maintain the viability and functionality of transplanted cells and also allow the transfer of insulin and glucose to maintain normoglycaemia. Apart from this, it needs to have a well-controlled pore size to exclude the penetration of immune cells, autoantibodies, and pro-inflammatory cytokines (Hu and de Vos, 2019) (O'Sullivan et al., 2011) (Ohgawara, 2000). There have been numerous reports over the years regarding the macro and microencapsulation devices for islet transplantation with varying degrees of success. Previously, Polymer-based encapsulation devices such as those made of polycaprolactone (PCL) based nanoporous encapsulation were used as long-term immunoprotection devices (Chang et al., 2017) (Niyitray et al., 2015). However, the small pores size and biodegradability of PCL make it less efficient for long-term clinical applications. Similarly, a nanofiber-integrated cell encapsulation device (NICE device) was reported to prevent cell escape and reported to maintain normoglycemia over a longer period of time but failed to obtain controlled nanopores are the critical defects to be used in clinical islet transplantation studies (Wang et al., 2021). Here, we have fabricated by 3D printed nanoporous immunoprotection macroencapsulation membranes of PU-PVP semi-IPN owing to their physical and mechanical properties, biocompatibility and nonbiodegradability unlike many natural polymers with endotoxin contaminations. There are previous reports suggesting the use of PU-PVP for the fabrication of nanoporous immunoisolation membranes that could be used for islet transplantation (Muthyala et al., 2011).

#### **5.4.1 Synthesis of PU-PVP semi IPN**

A polymeric network made up of two or more polymers is known as an IPN when at least one of the polymers is polymerized or cross-linked in the presence of other (Soon-Shiong, 1996). Polyurethanes are highly hydrophobic material which limits its function in biomedical applications. To make it more biocompatible by increasing its hydrophilicity, semi IPN of PU with n-vinylpyrrolidone is synthesized in the ratio 90/10 as reported elsewhere (Nair, 1995). There several reports regarding the use of PU-PVP semi IPNs as immunoisolation membranes in islet transplantation studies (Kanafi et al., 2013) (Muthyala et al., 2011). PU was hydrophobic but after the formation of IPN with PVP the hydrophilicity was increased to  $71 \pm 1^0$ , which is ideal for biomedical application. There is no significant difference between the mechanical properties of the PU and PU-PVP was observed. Cytotoxicity analysis by direct contact assay, MTT and live dead assay revealed that the synthesized PU-PVP is non cytotoxic and supported the attachment and growth of L929 cells.

#### **5.4.2 Fabrication of 3D printed Immunoisolation bag**

There-dimensional (3D) printing is an advanced technology to fabricate scaffolds with high accuracy and precision and to develop intricately detailed complex biological structures as per the computerized CAD design ((Peltola et al., 2008). It is an additive manufacturing technique in which scaffold is manufactured via layer-by-layer process and using this technique scaffold with millimeter to nanometer size range can be achieved (Hribar et al., 2013). It allows the direct fabrication of complicated shapes with high resolution for the production of

customisable medical devices. In the past decade's various studies with the use of 3D printing for the fabrication complex scaffolds with interconnected pores for the diffusion of oxygen and structures which mimic the native ECM tissues has been reported (Hsieh et al., 2018). In this study, we have adopted a solution based direct 3D printing technology for the fabrication of immunoisolation bags.

Here we adopted a top down approach for creating nano pores in which, first we created larger pores with 1.12 mm<sup>2</sup> and it is further narrowed down to 200±50 nm by decreasing the infill density of subsequent layers. 12% PU-PVP solution in chloroform was found to be printable and the printed lines were continuing and created a solid structure after the evaporation of solvent. The printing speed is standardized to 8mm/s that allowed the solvent evaporation and drying of printed layer preventing the fusing of consecutive layers printed. After printing the complete structure, the thickness of the membrane was 0.05 mm and are highly flexible, found to be mechanically stable that is suitable for the its use as immunoisolation membrane.

The function of the transplanted cells encapsulated in this nanoporous membrane is highly depends on the mass transfer. The pores should be small enough to prevent the penetration of immune cells and immunoglobulins but also allow the free diffusion of glucose and nutrients which are in the order of 10-100 nm diameter. Smaller pore size may often lead to hypoxia induced islet loss inside the immunoisolation device. So there should be a balance between the pore size and nutrient diffusion to prevent this. AFM analysis confirmed the pore size of the 3D

printed membrane to be  $200\pm 50$   $\mu\text{m}$  which is consistent with the previous reports in preventing immune cells and maintaining the functionality and viability of transplanted cells. The diffusion studies of molecules across the membrane revealed that the membrane is permeable to glucose and insulin with 10 minutes, 50% of insulin and glucose is diffused through the membrane that will be necessary for maintaining glucose homeostasis when implanted. The nanoporous membrane also reduced the diffusion of immunoglobulins in accordance with the previous reports (Chang et al., 2017).

#### **5.4.3 Fabrication of Immunoprotective Pancreatic Transplantation Device (IPTD)**

After the diffusion studies of molecules across the 3D printed nanoporous membranes, immunoprotective pancreatic transplantation device (IPTD) was fabricated as mentioned in section 3.5. Results suggest that, the islets and ILCs encapsulated in the IPTD were viable and functional and showed no significant difference with C-DEXGEL scaffold.

#### ***5.5. In vivo evaluation of tissue engineered construct***

Pancreatic islet transplantation offers effective treatment for type 1 diabetic patients with impaired hypoglycemia and severe hyperglycemic events. According to the International islet transplantation registry, In 90's the success of islet transplantation was 41% and only 11% achieved insulin dependent 1 year post transplantation which is insufficient to consider this as a generalized treatment for T1D (Anazawa et al., 2019), when all seven of the treated patients attained and

maintained insulin independence, the "Edmonton Protocol" was hailed as a major step forward towards islet transplantation with steroid free immunosuppressant (Shapiro et al., 2006). This studies revealed that the strategy was effective in restoring long-term endogenous insulin secretion and glycemic stability in T1D patients, however insulin independence was not long-lasting due to the severe islet dysfunction and destruction occurs because of the host inflammatory and immune reactions to the implant as well as the liver's unfavorable location. Around 60% of the islets may lose during engraftment. Capillary bed blockage causes hypoxia, which in turn causes the surrounding tissue to release inflammatory cytokines as islet emboli lodge in the hepatic microvasculature (Srinivasan et al., 2007).

Over the years, different methods have been adopted to increase the viability and maintaining the functionality of transplanted islets. Combining islets cells with biomaterial scaffolds and immobilizing them in imunoisolation devices increased the success of islet transplantation by protection from host immune cells and maintained the implant at the site of implantation (Zhang et al., 2022). There are various micro and macro encapsulation methods available to increase the outcome of Islet transplantation.  $\beta$ -Air is the islet transplantation device in which islet is encapsulated in oxygenated chamber made of alginate and polypropylene membrane to reduce the hypoxia and attain immune protection after transplantation (Barkai et al., 2013). In another study, mouse islet encapsulated on a silicone nanoporous membrane device with pore size 10nm was transplanted to pigs achieved normoglycemia (Song et al., 2017). Theracyte is a pouch based device which has outer membrane that enhance

vascularization and inner membrane provide immunoprotection upon transplantation of stem cell derived islet to mice (Kumagai-Braesch et al., 2013). Encaptra is also a pouch based device with semi permeable membrane that allows the growth of embryonic stem cell derived pancreatic progenitor cells (Pullen, 2018). Reports from our lab show that combined effect of immunoprotection and macroencapsulation achieved positive hypoglycaemic effect for 90 days of xenotransplantation (Muthyala et al., 2011).

In the present study, we have adopted a combinatorial approach in which ADMSCs were differentiated into ILCs on a 3D scaffold to increase the insulin secretion and viability and encapsulation of this construct in a nanoporous membrane to protect the transplanted cells from host immune response and to prevent the undifferentiated stem cell escape during transplantation. Hence, we fabricated an immuno-protective pancreatic transplantation device (IPTD) by encapsulating tissue-engineered pancreatic construct with ADMSC-derived ILCs on a protein-conjugated 3D porous scaffold encapsulated within a 3D printed nanoporous immunoprotective device made from a semi inter penetrating network of polyurethane and polyvinyl pyrrolidone (PU-PVP). The biocompatibility of the material and the transplantation site has a significant impact on the long-term performance of cell encapsulation devices (Merani et al., 2008). Previous reports suggest that less fibrotic tissue formation was observed when transplanted to the intra peritoneal space of animals (Wang et al., 2021).

The potential of IPTD seeded with islet or ILCs to reverse hyperglycemia is compared with islet or ILC seeded scaffold without any immunoprotection bag. Mature rat islet seeded IPTD showed better decrease in blood glucose level compared to other groups. The group transplanted with islet on C-DEXGEL scaffold without any immunoprotection bag showed initial decrease in blood glucose level but after 1 month of implantation, reverted back to hyperglycemia. This may either be due to the degradation of scaffold or formation of thick fibrotic layer around the transplanted construct. IPTD transplanted with stem cell derived ILCs also brought down blood glucose. After 30 days of implantation, results of the intraperitoneal glucose tolerance test which was conducted as shown in Fig 4.46 of chapter 4 reveals that, IPTD seeded with mature islets showed glucose clearance and reached plateau with 2hrs of glucose bolus compared to diabetic rat. Besides, IPTD translated with stem cell derived ILCs also showed better clearance of glucose than ILCs on C-DEXGEL scaffold without any immunoprotection bag.

Islets and ILCs preserved their morphology and architecture in group transplanted with IPTD. In groups transplanted without any immunoprotection bag, no clusters were identified and this may be due to the destruction of transplanted cells by host immune reaction. Moreover, insulin positive cells were identified only in groups transplanted with IPTD. When serum c-peptide was quantified among the transplanted groups, mature islets in IPTD showed higher concentration than other groups. ILCs on IPTD also showed better c-peptide concentration compared to diabetic control groups. These results corroborate with previous reports in which

stem cell derived ILCs showed less insulin secretion than the mature islets (Kroon et al., 2008). In H&E staining, formation of a thick fibrotic layer around the constructs without any immunoprotection bag was visible further confirmed by trichrome staining. Earlier studies report the development of strong innate immune-mediated foreign-body reactions (FBRs) caused by the implants employed in these studies lead to fibrotic deposition, nutritional isolation, and necrosis of donor tissue. An ideal biomaterial for cell encapsulation implant devices should have low macrophage recruitment and fibrosis at the material-tissue interface and be able to create neovasculature along its surface to sustain encapsulated cells with oxygen and nutrients. Earlier reports suggest that the implants used in these studies elicited severe innate immune-mediated foreign body reactions (FBRs) leading to fibrotic deposition followed by nutritional isolation and necrosis of the donor tissue (Anderson et al., 2008).

Here, the groups transplanted with mature islets and ILCs C-DEXGEL scaffold protected by 3D printed nanoporous immunoprotection membrane have shown reduction in hyperglycaemia and prolonged survival of rats and maintained islet architecture with minimal fibrotic tissue formation makes its suitable for islet transplantation in type I diabetic patients.

## CHAPTER 6 - SUMMARY AND CONCLUSIONS

Diabetes mellitus is a complex metabolic disease characterised by the impaired glucose stimulated insulin secretion. This impaired glucose metabolism occurs either due to the auto immune mediated destruction of insulin producing pancreatic  $\beta$ -cell or due to the lack of insulin secretion or insulin resistance. The long term hyperglycemia leading to numerous macro vascular and microvascular complications damaging organs like kidney, eye, heart, nerves, etc.

Oral hypoglycemic medications or insulin therapy are the major treatments for diabetes mellitus. However, these approaches are unable to mimic the physiological oscillating pattern of insulin release in order to achieve normoglycemia, which makes it impossible to prevent the long-term complications of diabetes and hypoglycemia. The goal of pancreatic islet transplantation is to produce euglycemia by following the normal pattern of insulin release. However, it has major disadvantages associated with the unavailability of donor islets, islet loss during transplantation, and continuous supply of immunosuppressants, etc. This led to the development of tissue-engineered islet-like clusters (ILCs) in which ILCs were differentiated from stem cells on a three-dimensional scaffold that mimics the native islet microenvironment and can be transplanted into the T1DM patients. However, in the clinical transplantation of stem cell-derived ILCs, teratoma formation from undifferentiated stem cells, as well as the immune rejection by the transplanted ILCs are the major concerns. Therefore, the encapsulation of transplanted ILCs in a

polymeric immunoprotective device will ensure the safe delivery of ILCs and give protection from the host immune response.

In order to address these concerns, the current study on “In vivo evaluation of tissue engineered islets derived from stem cells aided by a functionalized 3D scaffold system protected by a nanoporous immunoisolation device” was based on the hypothesis that extra cellular matrix protein conjugated 3D biomimetic scaffolds could enhance stem cell differentiation to islet-like clusters and maintain its survival and functionality when transplanted *in vivo* with 3D-printed nanoporous immunoprotection device.

Two different three dimensional polymeric scaffolds systems were fabricated that supported the growth and differentiation of adipose derived mesenchymal stem cells into insulin producing islet-like clusters (ILCs). This stem cell derived ILCs will overcome the shortage of mature islet for transplantation. Both scaffold systems were coated with extra cellular matrix proteins to increase the cell attachment and insulin secretion. Even though both scaffold systems supported the growth and functionality of differentiated ILCS, the second scaffold system made of two natural polymers were selected for further *in vivo* studies since it showed better insulin secretion than the synthetic scaffold system. The selected scaffold system also supported the attachment and maintained the spherical morphology of native islets. The conjugation of ECM proteins collagen IV and laminin to the scaffold also showed better cell attachment an insulin secretion than unmodified scaffold. Thus the

present work emphasises on the importance of cell-matrix interaction and cell-cell interaction for maintaining the viability and functionality islets.

For the safe delivery of stem cell derived islets during transplantation, the present study was intended to fabricate a macro encapsulation device that will facilitate the mass transfer and inhibit the diffusion immunoglobulins, cytokines and immune cells and for preventing the transplanted cells from host immune response. Nanoporous immunoprotection membrane was fabricated via solution based 3D printing of the synthesised semi IPN of polyurethane-polyvinylpyrrolidone. The benefit of 3D printing is that we can control size of the pores in such a way that it will allow the diffusion of glucose and insulin while excluding immune cells and immunoglobulins. Intraperitoneal pancreatic transplantation device (IPTD) was fabricated by encapsulation ILCs/islet seeded scaffold in the 3D printed membrane by heat sealing at the edges. The encapsulated cells remain viable and the functionality was confirmed by glucose challenge assay.

In vivo analysis of the tissue engineered intraperitoneal pancreatic transplantation device (IPTD) demonstrated that they could reduce the blood glucose concentration of diabetic rat model and prolong the life span of transplanted animals. The IPTD was accepted without any immune rejection when implanted. Histology of retrieved construct showed that implantation of tissue engineered construct without any immunoprotection membrane leads to the formation of thick fibrotic layer around the construct that further reduce the functionality of implant. The fibrotic layer formation on IPTD was very less did not affected the mass transfer. In groups

transplanted with IPTD, the islet/ILCs exhibited spherical morphology and expressed insulin hormone. This study also revealed the intraperitoneal cavity as a better implantation site for future islet transplantation studies since the fibrotic layer formation was very less in IPTD. Nevertheless, the approach of the use of the immunoprotective pancreatic transplantation device maintaining the viability and functionality of the differentiated islets encapsulated within an ECM coated scaffold seems to be a promising islet transplantation therapeutic option.

## **Future Perspectives**

In the current study, only the effect of ECM molecules on increasing insulin synthesis was studied. Though our approach of the use of the immunoprotective pancreatic transplantation device maintaining the viability and functionality of the differentiated islets encapsulated within an ECM coated scaffold seems to be a promising islet transplantation therapeutic option. The study could be extended to the other strategies for enhancing insulin secretion by co-culturing with endothelial cells, treatment with small molecule such a harmine and miRNA treatment to increase insulin secretion. Further studies are to be conducted to scale down the porosity of 3D immunoprotection bags to completely prevent the immunoglobulin and cytokine diffusion since the ideal porosity reported is 10-50 nm in diameter. The transplantation studies also need to be carried out in a higher animal model such as pig and/or dogs.

## REFERENCES

- Abadpour S, Wang C, Niemi EM, et al. (2021) Tissue Engineering Strategies for Improving Beta Cell Transplantation Outcome. *Current Transplantation Reports* 8(3): 205–219. DOI: 10.1007/s40472-021-00333-2.
- Ahmed A (2002) history of diabetes mellitus. *Saudi medical journal* 23: 486–491.
- Aloysious N and Nair PD (2014) Enhanced Survival and Function of Islet-Like Clusters Differentiated from Adipose Stem Cells on a Three-Dimensional Natural Polymeric Scaffold: An *In Vitro* Study. *Tissue Engineering Part A* 20(9–10): 1508–1522. DOI: 10.1089/ten.tea.2012.0615.
- Amer LD, Mahoney MJ and Bryant SJ (2014) Tissue Engineering Approaches to Cell-Based Type 1 Diabetes Therapy. *Tissue Engineering. Part B, Reviews* 20(5): 455–467. DOI: 10.1089/ten.teb.2013.0462.
- Anazawa T, Okajima H, Masui T, et al. (2019) Current state and future evolution of pancreatic islet transplantation. *Annals of Gastroenterological Surgery* 3(1). Wiley-Blackwell: 34. DOI: 10.1002/ags3.12214.
- Anderson JM, Rodriguez A and Chang DT (2008) Foreign body reaction to biomaterials. *Seminars in Immunology* 20(2). Innate and Adaptive Immune Responses in Tissue Engineering: 86–100. DOI: 10.1016/j.smim.2007.11.004.
- Anitha R, Vaikkath D, Shenoy SJ, et al. (2020a) Tissue-engineered islet-like cell clusters generated from adipose tissue-derived stem cells on three-dimensional electrospun scaffolds can reverse diabetes in an experimental rat model and the role of porosity of scaffolds on cluster differentiation. *Journal of Biomedical Materials Research Part A* 108(3): 749–759. DOI: 10.1002/jbm.a.36854.
- Anitha R, Vaikkath D, Shenoy SJ, et al. (2020b) Tissue-engineered islet-like cell clusters generated from adipose tissue-derived stem cells on three-dimensional electrospun scaffolds can reverse diabetes in an experimental rat model and the role of porosity of scaffolds on cluster differentiation. *Journal*

*of Biomedical Materials Research Part A* 108(3): 749–759. DOI: 10.1002/jbm.a.36854.

Anitha R, Vaikkath D, Shenoy SJ, et al. (2020c) Tissue-engineered islet-like cell clusters generated from adipose tissue-derived stem cells on three-dimensional electrospun scaffolds can reverse diabetes in an experimental rat model and the role of porosity of scaffolds on cluster differentiation. *Journal of Biomedical Materials Research Part A* 108(3): 749–759. DOI: 10.1002/jbm.a.36854.

Bahar SG and Devulapally P (2022) Pancreas Transplantation. In: *StatPearls*. Treasure Island (FL): StatPearls Publishing. Available at: <http://www.ncbi.nlm.nih.gov/books/NBK562338/> (accessed 28 December 2022).

Barkai U, Weir GC, Colton CK, et al. (2013) Enhanced oxygen supply improves islet viability in a new bioartificial pancreas. *Cell Transplantation* 22(8): 1463–1476. DOI: 10.3727/096368912X657341.

Bayati V, Hashemitabar M, Gazor R, et al. (2013) Expression of surface markers and myogenic potential of rat bone marrow- and adipose-derived stem cells: a comparative study. *Anatomy & Cell Biology* 46(2): 113–121. DOI: 10.5115/acb.2013.46.2.113.

Bloomgarden ZT (2008) Approaches to Treatment of Type 2 Diabetes. *Diabetes Care* 31(8): 1697–1703. DOI: 10.2337/dc08-zb08.

Casanova D and en nombre de Grupo Español de Trasplante de Páncreas (2017) Pancreas transplantation: 50 years of experience. *Cirugia Espanola* 95(5): 254–260. DOI: 10.1016/j.ciresp.2017.02.005.

Chamberlain G, Fox J, Ashton B, et al. (2007) Concise review: mesenchymal stem cells: their phenotype, differentiation capacity, immunological features, and potential for homing. *Stem Cells (Dayton, Ohio)* 25(11): 2739–2749. DOI: 10.1634/stemcells.2007-0197.

Chandra V, G S, Phadnis S, et al. (2009) Generation of pancreatic hormone-expressing islet-like cell aggregates from murine adipose tissue-derived stem cells. *Stem Cells (Dayton, Ohio)* 27(8): 1941–1953. DOI: 10.1002/stem.117.

- Chandra V, G S, Muthyala S, et al. (2011) Islet-Like Cell Aggregates Generated from Human Adipose Tissue Derived Stem Cells Ameliorate Experimental Diabetes in Mice. *PLOS ONE* 6(6). Public Library of Science: e20615. DOI: 10.1371/journal.pone.0020615.
- Chang R, Faleo G, Russ HA, et al. (2017) Nanoporous Immunoprotective Device for Stem-Cell-Derived  $\beta$ -Cell Replacement Therapy. *ACS Nano* 11(8): 7747–7757. DOI: 10.1021/acsnano.7b01239.
- Chao KC, Chao KF, Fu YS, et al. (2008) Islet-Like Clusters Derived from Mesenchymal Stem Cells in Wharton’s Jelly of the Human Umbilical Cord for Transplantation to Control Type 1 Diabetes. *PLOS ONE* 3(1). Public Library of Science: e1451. DOI: 10.1371/journal.pone.0001451.
- Cheng JYC, Raghunath M, Whitelock J, et al. (2011) Matrix Components and Scaffolds for Sustained Islet Function. *Tissue Engineering Part B: Reviews* 17(4). Mary Ann Liebert, Inc., publishers: 235–247. DOI: 10.1089/ten.teb.2011.0004.
- Da Silva Xavier G (2018) The Cells of the Islets of Langerhans. *Journal of Clinical Medicine* 7(3): 54. DOI: 10.3390/jcm7030054.
- Dang Le Q, Rodprasert W, Kuncorojakti S, et al. (2022) In vitro generation of transplantable insulin-producing cells from canine adipose-derived mesenchymal stem cells. *Scientific Reports* 12(1). 1. Nature Publishing Group: 9127. DOI: 10.1038/s41598-022-13114-3.
- Daoud J, Petropavlovskaja M, Rosenberg L, et al. (2010) The effect of extracellular matrix components on the preservation of human islet function in vitro. *Biomaterials* 31(7): 1676–1682. DOI: 10.1016/j.biomaterials.2009.11.057.
- Daoud JT, Petropavlovskaja MS, Patapas JM, et al. (2011) Long-term in vitro human pancreatic islet culture using three-dimensional microfabricated scaffolds. *Biomaterials* 32(6): 1536–1542. DOI: 10.1016/j.biomaterials.2010.10.036.
- Desai T and Shea LD (2017) Advances in islet encapsulation technologies. *Nature Reviews Drug Discovery* 16(5). 5. Nature Publishing Group: 338–350. DOI: 10.1038/nrd.2016.232.

- Dhandayuthapani B, Yoshida Y, Maekawa T, et al. (2011) Polymeric Scaffolds in Tissue Engineering Application: A Review. *International Journal of Polymer Science* 2011. Hindawi: e290602. DOI: 10.1155/2011/290602.
- Dominici M, Le Blanc K, Mueller I, et al. (2006) Minimal criteria for defining multipotent mesenchymal stromal cells. The International Society for Cellular Therapy position statement. *Cytotherapy* 8(4): 315–317. DOI: 10.1080/14653240600855905.
- Dorrell C, Abraham SL, Lanxon-Cookson KM, et al. (2008) Isolation of major pancreatic cell types and long-term culture-initiating cells using novel human surface markers. *Stem Cell Research* 1(3): 183–194. DOI: 10.1016/j.scr.2008.04.001.
- Elnashar M, Vaccarezza M and Al-Salami H (n.d.) Cutting-edge biotechnological advancement in islet delivery using pancreatic and cellular approaches. *Future Science OA* 7(3): FSO660. DOI: 10.2144/fsoa-2020-0105.
- Enderami SE, Kehtari M, Abazari MF, et al. (2018) Generation of insulin-producing cells from human induced pluripotent stem cells on PLLA/PVA nanofiber scaffold. *Artificial Cells, Nanomedicine, and Biotechnology* 46(sup1). Taylor & Francis: 1062–1069. DOI: 10.1080/21691401.2018.1443466.
- Galicía-García U, Benito-Vicente A, Jebari S, et al. (2020) Pathophysiology of Type 2 Diabetes Mellitus. *International Journal of Molecular Sciences* 21(17): 6275. DOI: 10.3390/ijms21176275.
- Gallego-Perez D, Higuera-Castro N, Sharma S, et al. (2010) High throughput assembly of spatially controlled 3D cell clusters on a micro/nanoplatfom. *Lab on a Chip* 10(6). Royal Society of Chemistry: 775–782. DOI: 10.1039/B919475D.
- Gamble A, Pepper AR, Bruni A, et al. (2018) The journey of islet cell transplantation and future development. *Islets* 10(2). Taylor & Francis: 80–94. DOI: 10.1080/19382014.2018.1428511.
- García-Contreras M, Tamayo-García A, Pappan KL, et al. (2017) A Metabolomics Study of the Effects of Inflammation, Hypoxia, and High Glucose on Isolated

Human Pancreatic Islets. *Journal of proteome research* 16(6): 2294–2306. DOI: 10.1021/acs.jproteome.7b00160.

Genuth SM, Palmer JP and Nathan DM (2018) Classification and Diagnosis of Diabetes. In: Cowie CC, Casagrande SS, Menke A, et al. (eds) *Diabetes in America*. 3rd ed. Bethesda (MD): National Institute of Diabetes and Digestive and Kidney Diseases (US). Available at: <http://www.ncbi.nlm.nih.gov/books/NBK568014/> (accessed 28 December 2022).

Giraldo JA, Weaver JD and Stabler CL (2010) Enhancing Clinical Islet Transplantation through Tissue Engineering Strategies. *Journal of Diabetes Science and Technology* 4(5): 1238–1247.

Gomes MF, Amorim JB, ChrystianeGiannasi L, et al. (2017) *Biomaterials for Tissue Engineering Applications in Diabetes Mellitus*. IntechOpen. DOI: 10.5772/intechopen.69719.

Gruessner RWG (2022) The current state of clinical islet transplantation. *The Lancet Diabetes & Endocrinology* 10(7). Elsevier: 476–478. DOI: 10.1016/S2213-8587(22)00138-3.

Guo T and Hebrok M (2009) Stem Cells to Pancreatic  $\beta$ -Cells: New Sources for Diabetes Cell Therapy. *Endocrine Reviews* 30(3): 214–227. DOI: 10.1210/er.2009-0004.

Hackett E, Gallagher A and Jacques N (n.d.) Type 1 diabetes: pathophysiology and diagnosis. Available at: <https://pharmaceutical-journal.com/article/ld/type-1-diabetes-pathophysiology-and-diagnosis> (accessed 28 December 2022).

Hadavi E (2018) A tissue engineering approach towards treatment of type 1 diabetes. DOI: 10.3990/1.9789463610872.

Hoffman LS, Fox TJ, Anastasopoulou C, et al. (2022) Maturity Onset Diabetes in the Young. In: *StatPearls*. Treasure Island (FL): StatPearls Publishing. Available at: <http://www.ncbi.nlm.nih.gov/books/NBK532900/> (accessed 28 December 2022).

Hogrebe NJ, Maxwell KG, Augsornworawat P, et al. (2021) Generation of insulin-producing pancreatic  $\beta$  cells from multiple human stem cell lines. *Nature*

*Protocols* 16(9). 9. Nature Publishing Group: 4109–4143. DOI: 10.1038/s41596-021-00560-y.

Hribar KC, Soman P, Warner J, et al. (2013) Light-assisted direct-write of 3D functional biomaterials. *Lab on a Chip* 14(2). The Royal Society of Chemistry: 268–275. DOI: 10.1039/C3LC50634G.

Hsieh C-T, Liao C-Y, Dai N-T, et al. (2018) 3D printing of tubular scaffolds with elasticity and complex structure from multiple waterborne polyurethanes for tracheal tissue engineering. *Applied Materials Today* 12: 330–341. DOI: 10.1016/j.apmt.2018.06.004.

Hu S and de Vos P (2019) Polymeric Approaches to Reduce Tissue Responses Against Devices Applied for Islet-Cell Encapsulation. *Frontiers in Bioengineering and Biotechnology* 7. Available at: <https://www.frontiersin.org/articles/10.3389/fbioe.2019.00134> (accessed 28 December 2022).

Jiang J, Au M, Lu K, et al. (2007) Generation of insulin-producing islet-like clusters from human embryonic stem cells. *Stem Cells (Dayton, Ohio)* 25(8): 1940–1953. DOI: 10.1634/stemcells.2006-0761.

Jun I, Han H-S, Edwards JR, et al. (2018) Electrospun Fibrous Scaffolds for Tissue Engineering: Viewpoints on Architecture and Fabrication. *International Journal of Molecular Sciences* 19(3): 745. DOI: 10.3390/ijms19030745.

Kaku K (2010) Pathophysiology of Type 2 Diabetes and Its Treatment Policy. 53(1).

Kanafi MM, Rajeshwari YB, Gupta S, et al. (2013a) Transplantation of islet-like cell clusters derived from human dental pulp stem cells restores normoglycemia in diabetic mice. *Cytotherapy* 15(10): 1228–1236. DOI: 10.1016/j.jcyt.2013.05.008.

Kanafi MM, Rajeshwari YB, Gupta S, et al. (2013b) Transplantation of islet-like cell clusters derived from human dental pulp stem cells restores normoglycemia in diabetic mice. *Cytotherapy* 15(10): 1228–1236. DOI: 10.1016/j.jcyt.2013.05.008.

- Karamanou M, Protogerou A, Tsoucalas G, et al. (2016) Milestones in the history of diabetes mellitus: The main contributors. *World Journal of Diabetes* 7(1). Baishideng Publishing Group Inc.: 1–7. DOI: 10.4239/wjd.v7.i1.1.
- Karnieli O, Izhar-Prato Y, Bulvik S, et al. (2007) Generation of insulin-producing cells from human bone marrow mesenchymal stem cells by genetic manipulation. *Stem Cells (Dayton, Ohio)* 25(11): 2837–2844. DOI: 10.1634/stemcells.2007-0164.
- Khazaei M, Khazaei F, Niromand E, et al. (2022) Tissue engineering approaches and generation of insulin-producing cells to treat type 1 diabetes. *Journal of Drug Targeting* 0(0). Taylor & Francis: 1–18. DOI: 10.1080/1061186X.2022.2107653.
- Kim Y, Kim Hyeongseok, Ko UH, et al. (2016) Islet-like organoids derived from human pluripotent stem cells efficiently function in the glucose responsiveness in vitro and in vivo. *Scientific Reports* 6(1). 1. Nature Publishing Group: 35145. DOI: 10.1038/srep35145.
- Kochar IS and Jain R (2021) Pancreas transplant in type 1 diabetes mellitus: the emerging role of islet cell transplant. *Annals of Pediatric Endocrinology & Metabolism* 26(2): 86–91. DOI: 10.6065/apem.2142012.006.
- Komatsu H, Cook C, Wang C-H, et al. (2017) Oxygen environment and islet size are the primary limiting factors of isolated pancreatic islet survival. *PLOS ONE* 12(8). Public Library of Science: e0183780. DOI: 10.1371/journal.pone.0183780.
- Krentz AJ and Bailey CJ (2005) Oral antidiabetic agents: current role in type 2 diabetes mellitus. *Drugs* 65(3): 385–411. DOI: 10.2165/00003495-200565030-00005.
- Kroon E, Martinson LA, Kadoya K, et al. (2008) Pancreatic endoderm derived from human embryonic stem cells generates glucose-responsive insulin-secreting cells in vivo. *Nature Biotechnology* 26(4): 443–452. DOI: 10.1038/nbt1393.
- Kumagai-Braesch M, Jacobson S, Mori H, et al. (2013) The TheraCyte™ Device Protects against Islet Allograft Rejection in Immunized Hosts. *Cell*

- Transplantation* 22(7). SAGE Publications Inc: 1137–1146. DOI: 10.3727/096368912X657486.
- Kumar N, Joisher H and Ganguly A (2017) Polymeric Scaffolds for Pancreatic Tissue Engineering: A Review. *The Review of Diabetic Studies : RDS* 14(4): 334–353. DOI: 10.1900/RDS.2017.14.334.
- Kuwabara R, Hu S, Smink AM, et al. (2022) Applying Immunomodulation to Promote Longevity of Immunoisolated Pancreatic Islet Grafts. *Tissue Engineering Part B: Reviews* 28(1). Mary Ann Liebert, Inc., publishers: 129–140. DOI: 10.1089/ten.teb.2020.0326.
- Lakhtakia R (2013) The History of Diabetes Mellitus. *Sultan Qaboos University Medical Journal* 13(3): 368–370.
- Lee J, Lee SY, Jang J, et al. (2012) Fabrication of Patterned Nanofibrous Mats Using Direct-Write Electrospinning. *Langmuir* 28(18). American Chemical Society: 7267–7275. DOI: 10.1021/la3009249.
- Lemos NE, Brondani L de A, Dieter C, et al. (2017) Use of additives, scaffolds and extracellular matrix components for improvement of human pancreatic islet outcomes in vitro: A systematic review. *Islets* 9(5): 73–86. DOI: 10.1080/19382014.2017.1335842.
- Li B (2017) Construction of Artificial Islet Tissue with Functional Scaffolds for Stem Cells Differentiated into Insulin- Secreting Cells. *Current Research in Diabetes & Obesity Journal* 3(5). DOI: 10.19080/CRDOJ.2017.03.555621.
- Li S and Lee B-K (2020) Electrospinning of circumferentially aligned polymer nanofibers floating on rotating water collector. *Journal of Applied Polymer Science* 137(22): 48759. DOI: 10.1002/app.48759.
- Llacua A, de Haan BJ, Smink SA, et al. (2016) Extracellular matrix components supporting human islet function in alginate-based immunoprotective microcapsules for treatment of diabetes. *Journal of Biomedical Materials Research Part A* 104(7): 1788–1796. DOI: 10.1002/jbm.a.35706.

- Lucier J and Weinstock RS (2022) Diabetes Mellitus Type 1. In: *StatPearls*. Treasure Island (FL): StatPearls Publishing. Available at: <http://www.ncbi.nlm.nih.gov/books/NBK507713/> (accessed 28 December 2022).
- MacGregor RR, Williams SJ, Tong PY, et al. (2006) Small rat islets are superior to large islets in in vitro function and in transplantation outcomes. *American Journal of Physiology-Endocrinology and Metabolism* 290(5). American Physiological Society: E771–E779. DOI: 10.1152/ajpendo.00097.2005.
- Matsumoto S and Shimoda M (2020) Current situation of clinical islet transplantation from allogeneic toward xenogeneic. *Journal of Diabetes* 12(10): 733–741. DOI: 10.1111/1753-0407.13041.
- Maxwell KG and Millman JR (2021) Applications of iPSC-derived beta cells from patients with diabetes. *Cell Reports Medicine* 2(4): 100238. DOI: 10.1016/j.xcrm.2021.100238.
- Mondal D, Griffith M and Venkatraman SS (2016) Polycaprolactone-based biomaterials for tissue engineering and drug delivery: Current scenario and challenges. *International Journal of Polymeric Materials and Polymeric Biomaterials* 65(5). Taylor & Francis: 255–265. DOI: 10.1080/00914037.2015.1103241.
- Moore SJ, Gala-Lopez BL, Pepper AR, et al. (2015) Bioengineered stem cells as an alternative for islet cell transplantation. *World Journal of Transplantation* 5(1): 1–10. DOI: 10.5500/wjt.v5.i1.1.
- Muthyala S, Raj VRR, Mohanty M, et al. (2011) The reversal of diabetes in rat model using mouse insulin producing cells – A combination approach of tissue engineering and macroencapsulation. *Acta Biomaterialia* 7(5): 2153–2162. DOI: 10.1016/j.actbio.2011.01.036.
- Nair GG, Tzanakakis ES and Hebrok M (2020) Emerging routes to the generation of functional  $\beta$ -cells for diabetes mellitus cell therapy. *Nature Reviews Endocrinology* 16(9). 9. Nature Publishing Group: 506–518. DOI: 10.1038/s41574-020-0375-3.

- Nair PD (1995) A polyurethane–polyvinylpyrrolidone interpenetrating polymer network for mammalian cell encapsulation. *Current Science* 68(11). Current Science Association: 1126–1129.
- Navarro-Tableros V, Gai C, Gomez Y, et al. (2019) Islet-Like Structures Generated In Vitro from Adult Human Liver Stem Cells Revert Hyperglycemia in Diabetic SCID Mice. *Stem Cell Reviews and Reports* 15(1): 93–111. DOI: 10.1007/s12015-018-9845-6.
- Nyitray CE, Chang R, Faleo G, et al. (2015) Polycaprolactone Thin-Film Micro- and Nanoporous Cell-Encapsulation Devices. *ACS Nano* 9(6): 5675–5682. DOI: 10.1021/acsnano.5b00679.
- Ohgawara H (2000) Strategies for immunoisolation in islet transplantation: challenges for the twenty-first century. *Journal of Hepato-Biliary-Pancreatic Surgery* 7(4): 374–379. DOI: 10.1007/s005340070032.
- Ojaghi M, Soleimanifar F, Kazemi A, et al. (2019) Electrospun poly-l-lactic acid/polyvinyl alcohol nanofibers improved insulin-producing cell differentiation potential of human adipose-derived mesenchymal stem cells. *Journal of Cellular Biochemistry* 120(6): 9917–9926. DOI: 10.1002/jcb.28274.
- O’Sullivan ES, Vegas A, Anderson DG, et al. (2011a) Islets Transplanted in Immunoisolation Devices: A Review of the Progress and the Challenges that Remain. *Endocrine Reviews* 32(6): 827–844. DOI: 10.1210/er.2010-0026.
- O’Sullivan ES, Vegas A, Anderson DG, et al. (2011b) Islets transplanted in immunoisolation devices: a review of the progress and the challenges that remain. *Endocrine Reviews* 32(6): 827–844. DOI: 10.1210/er.2010-0026.
- Owida HA, Al-Nabulsi JI, Alnaimat F, et al. (2022) Recent Applications of Electrospun Nanofibrous Scaffold in Tissue Engineering. *Applied Bionics and Biomechanics* 2022. Hindawi: e1953861. DOI: 10.1155/2022/1953861.
- Pan G, Mu Y, Hou L, et al. (2019) Examining the therapeutic potential of various stem cell sources for differentiation into insulin-producing cells to treat diabetes. *Annales d’Endocrinologie* 80(1): 47–53. DOI: 10.1016/j.ando.2018.06.1084.

- Paschou SA, Papadopoulou-Marketou N, Chrousos GP, et al. (2017) On type 1 diabetes mellitus pathogenesis. *Endocrine Connections* 7(1): R38–R46. DOI: 10.1530/EC-17-0347.
- Pathak S, Pham TT, Jeong J-H, et al. (2019) Immunoisolation of pancreatic islets via thin-layer surface modification. *Journal of Controlled Release* 305: 176–193. DOI: 10.1016/j.jconrel.2019.04.034.
- Peltola SM, Melchels FPW, Grijpma DW, et al. (2008) A review of rapid prototyping techniques for tissue engineering purposes. *Annals of Medicine* 40(4): 268–280. DOI: 10.1080/07853890701881788.
- Pisania A, Weir GC, O’Neil JJ, et al. (2010) Quantitative analysis of cell composition and purity of human pancreatic islet preparations. *Laboratory Investigation; a Journal of Technical Methods and Pathology* 90(11): 1661–1675. DOI: 10.1038/labinvest.2010.124.
- Plows JF, Stanley JL, Baker PN, et al. (2018) The Pathophysiology of Gestational Diabetes Mellitus. *International Journal of Molecular Sciences* 19(11): 3342. DOI: 10.3390/ijms19113342.
- Pullen LC (2018) Stem Cell–Derived Pancreatic Progenitor Cells Have Now Been Transplanted into Patients: Report from IPITA 2018. *American Journal of Transplantation* 18(7): 1581–1582. DOI: 10.1111/ajt.14954.
- Raikwar SP and Zavazava N (2009) Insulin Producing Cells Derived from Embryonic Stem Cells: Are We There Yet? *Journal of cellular physiology* 218(2): 256–263. DOI: 10.1002/jcp.21615.
- Rezania A, Bruin JE, Arora P, et al. (2014) Reversal of diabetes with insulin-producing cells derived in vitro from human pluripotent stem cells. *Nature Biotechnology* 32(11): 1121–1133. DOI: 10.1038/nbt.3033.
- Rodprasert W, Nantavisai S, Pathanachai K, et al. (2021) Tailored generation of insulin producing cells from canine mesenchymal stem cells derived from bone marrow and adipose tissue. *Scientific Reports* 11(1). 1. Nature Publishing Group: 12409. DOI: 10.1038/s41598-021-91774-3.

- Rozario T and DeSimone DW (2010) The extracellular matrix in development and morphogenesis: A dynamic view. *Developmental Biology* 341(1). Special Section: Morphogenesis: 126–140. DOI: 10.1016/j.ydbio.2009.10.026.
- S M, Ja S, M S, et al. (2011) *Regenerative Medicine and Tissue Engineering for the Treatment of Diabetes*. IntechOpen. DOI: 10.5772/22808.
- Salg GA, Giese NA, Schenk M, et al. (2019) The emerging field of pancreatic tissue engineering: A systematic review and evidence map of scaffold materials and scaffolding techniques for insulin-secreting cells. *Journal of Tissue Engineering* 10: 2041731419884708. DOI: 10.1177/2041731419884708.
- Salvatori M, Katari R, Patel T, et al. (2014) Extracellular Matrix Scaffold Technology for Bioartificial Pancreas Engineering. *Journal of Diabetes Science and Technology* 8(1): 159–169. DOI: 10.1177/1932296813519558.
- Sandilya S and Singh S (2021) Development of islet organoids from human induced pluripotent stem cells in a cross-linked collagen scaffold. *Cell Regeneration* 10(1): 38. DOI: 10.1186/s13619-021-00099-z.
- Sapra A and Bhandari P (2022) Diabetes Mellitus. In: *StatPearls*. Treasure Island (FL): StatPearls Publishing. Available at: <http://www.ncbi.nlm.nih.gov/books/NBK551501/> (accessed 28 December 2022).
- Schmelzer E, McKeel DT and Gerlach JC (2019) Characterization of Human Mesenchymal Stem Cells from Different Tissues and Their Membrane Encasement for Prospective Transplantation Therapies. *BioMed Research International* 2019. Hindawi: e6376271. DOI: 10.1155/2019/6376271.
- Shapiro AMJ, Lakey JRT, Ryan EA, et al. (2000) Islet Transplantation in Seven Patients with Type 1 Diabetes Mellitus Using a Glucocorticoid-Free Immunosuppressive Regimen. *New England Journal of Medicine* 343(4). Massachusetts Medical Society: 230–238. DOI: 10.1056/NEJM200007273430401.
- Shapiro AMJ, Ricordi C, Hering BJ, et al. (2006) International trial of the Edmonton protocol for islet transplantation. *The New England Journal of Medicine* 355(13): 1318–1330. DOI: 10.1056/NEJMoa061267.

- Shapiro AMJ, Pokrywczynska M and Ricordi C (2017) Clinical pancreatic islet transplantation. *Nature Reviews Endocrinology* 13(5). 5. Nature Publishing Group: 268–277. DOI: 10.1038/nrendo.2016.178.
- Shimojo AAM, Rodrigues ICP, Perez AGM, et al. (2020) Scaffolds for Tissue Engineering: A State-of-the-Art Review Concerning Types, Properties, Materials, Processing, and Characterization. In: Li B, Moriarty TF, Webster T, et al. (eds) *Racing for the Surface: Antimicrobial and Interface Tissue Engineering*. Cham: Springer International Publishing, pp. 647–676. DOI: 10.1007/978-3-030-34471-9\_23.
- Silver B, Ramaiya K, Andrew SB, et al. (2018) EADSG Guidelines: Insulin Therapy in Diabetes. *Diabetes Therapy* 9(2): 449–492. DOI: 10.1007/s13300-018-0384-6.
- Sim EZ, Shiraki N and Kume S (2021) Recent progress in pancreatic islet cell therapy. *Inflammation and Regeneration* 41(1): 1. DOI: 10.1186/s41232-020-00152-5.
- Smink AM and de Vos P (2018) Therapeutic Strategies for Modulating the Extracellular Matrix to Improve Pancreatic Islet Function and Survival After Transplantation. *Current Diabetes Reports* 18(7): 39. DOI: 10.1007/s11892-018-1014-4.
- Smink AM, de Haan BJ, Lakey JRT, et al. (2018) Polymer scaffolds for pancreatic islet transplantation — Progress and challenges. *American Journal of Transplantation* 18(9): 2113–2119. DOI: 10.1111/ajt.14942.
- Song S, Blaha C, Moses W, et al. (2017) An intravascular bioartificial pancreas device (iBAP) with silicon nanopore membranes (SNM) for islet encapsulation under convective mass transport. *Lab on a Chip* 17(10). Royal Society of Chemistry: 1778–1792. DOI: 10.1039/C7LC00096K.
- Soon-Shiong P (1996) Encapsulated islet cell therapy for the treatment of diabetes: Intraperitoneal injection of islets. *Journal of Controlled Release* 39(2). Proceedings of the Seventh International Symposium on Recent Advances in Drug Delivery Systems: 399–409. DOI: 10.1016/0168-3659(95)00151-4.

- Srinivasan P, Huang GC, Amiel SA, et al. (2007) Islet cell transplantation. *Postgraduate Medical Journal* 83(978): 224–229. DOI: 10.1136/pgmj.2006.053447.
- Steele JAM, Hallé J-P, Poncelet D, et al. (2014) Therapeutic cell encapsulation techniques and applications in diabetes. *Advanced Drug Delivery Reviews* 67–68. Cell encapsulation and drug delivery: 74–83. DOI: 10.1016/j.addr.2013.09.015.
- Stendahl JC, Kaufman DB and Stupp SI (2009) Extracellular Matrix in Pancreatic Islets: Relevance to Scaffold Design and Transplantation. *Cell transplantation* 18(1): 1–12.
- Swinnen SG, Hoekstra JB and DeVries JH (2009) Insulin Therapy for Type 2 Diabetes. *Diabetes Care* 32(Suppl 2): S253–S259. DOI: 10.2337/dc09-S318.
- Tan SY, Mei Wong JL, Sim YJ, et al. (2019) Type 1 and 2 diabetes mellitus: A review on current treatment approach and gene therapy as potential intervention. *Diabetes & Metabolic Syndrome: Clinical Research & Reviews* 13(1): 364–372. DOI: 10.1016/j.dsx.2018.10.008.
- Thivolet CH, Chatelain P, Nicoloso H, et al. (1985) Morphological and functional effects of extracellular matrix on pancreatic islet cell cultures. *Experimental Cell Research* 159(2): 313–322. DOI: 10.1016/S0014-4827(85)80005-7.
- Thota S and Akbar A (2022) Insulin. In: *StatPearls*. Treasure Island (FL): StatPearls Publishing. Available at: <http://www.ncbi.nlm.nih.gov/books/NBK560688/> (accessed 28 December 2022).
- Tiwari P (2015) Recent Trends in Therapeutic Approaches for Diabetes Management: A Comprehensive Update. *Journal of Diabetes Research* 2015. Hindawi: e340838. DOI: 10.1155/2015/340838.
- Tokito F, Shinohara M, Maruyama M, et al. (2021) High density culture of pancreatic islet-like 3D tissue organized in oxygen-permeable porous scaffolds with external oxygen supply. *Journal of Bioscience and Bioengineering* 131(5): 543–548. DOI: 10.1016/j.jbiosc.2020.12.009.

- Townsend SE and Gannon M (2019) Extracellular Matrix–Associated Factors Play Critical Roles in Regulating Pancreatic  $\beta$ -Cell Proliferation and Survival. *Endocrinology* 160(8): 1885–1894. DOI: 10.1210/en.2019-00206.
- Triolo TM and Bellin MD (2021) Lessons from Human Islet Transplantation Inform Stem Cell-Based Approaches in the Treatment of Diabetes. *Frontiers in Endocrinology* 12. Available at: <https://www.frontiersin.org/articles/10.3389/fendo.2021.636824> (accessed 28 December 2022).
- Van Belle TL, Coppieters KT and Von Herrath MG (2011) Type 1 Diabetes: Etiology, Immunology, and Therapeutic Strategies. *Physiological Reviews* 91(1). American Physiological Society: 79–118. DOI: 10.1152/physrev.00003.2010.
- Vaquette C and Cooper-White JJ (2011) Increasing electrospun scaffold pore size with tailored collectors for improved cell penetration. *Acta Biomaterialia* 7(6): 2544–2557. DOI: 10.1016/j.actbio.2011.02.036.
- Vrana NE, Builles N, Kocak H, et al. (2007) EDC/NHS cross-linked collagen foams as scaffolds for artificial corneal stroma. *Journal of Biomaterials Science. Polymer Edition* 18(12): 1527–1545.
- Wang X, Maxwell KG, Wang K, et al. (2021) A nanofibrous encapsulation device for safe delivery of insulin-producing cells to treat type 1 diabetes. *Science Translational Medicine* 13(596). American Association for the Advancement of Science: eabb4601. DOI: 10.1126/scitranslmed.abb4601.
- Weber LM, Hayda KN and Anseth KS (2008) Cell–Matrix Interactions Improve  $\beta$ -Cell Survival and Insulin Secretion in Three-Dimensional Culture. *Tissue Engineering Part A* 14(12). Mary Ann Liebert, Inc., publishers: 1959–1968. DOI: 10.1089/ten.tea.2007.0238.
- Wei R, Yang J, Hou W, et al. (2013) Insulin-Producing Cells Derived from Human Embryonic Stem Cells: Comparison of Definitive Endoderm- and Nestin-Positive Progenitor-Based Differentiation Strategies. *PLOS ONE* 8(8). Public Library of Science: e72513. DOI: 10.1371/journal.pone.0072513.
- Weiss M, Steiner DF and Philipson LH (2000) Insulin Biosynthesis, Secretion, Structure, and Structure-Activity Relationships. In: Feingold KR, Anawalt B, Boyce A, et al. (eds) *Endotext*. South Dartmouth (MA): MDText.com, Inc.

Available at: <http://www.ncbi.nlm.nih.gov/books/NBK279029/> (accessed 14 November 2022).

Wieland FC, van Blitterswijk CA, van Apeldoorn A, et al. (2021) The functional importance of the cellular and extracellular composition of the islets of Langerhans. *Journal of Immunology and Regenerative Medicine* 13: 100048. DOI: 10.1016/j.regen.2021.100048.

Wilson J, Rahul VG, Thomas LV, et al. (2022) Three-dimensional wet electrospun scaffold system for the differentiation of adipose-derived mesenchymal stem cells to islet-like clusters. *Journal of Tissue Engineering and Regenerative Medicine* 16(12): 1276–1283. DOI: 10.1002/term.3366.

Witkowski P, Philipson LH, Buse JB, et al. (2022) Islets Transplantation at a Crossroads - Need for Urgent Regulatory Update in the United States: Perspective Presented During the Scientific Sessions 2021 at the American Diabetes Association Congress. *Frontiers in Endocrinology* 12. Available at: <https://www.frontiersin.org/articles/10.3389/fendo.2021.789526> (accessed 28 December 2022).

Yap WT, Salvay DM, Silliman MA, et al. (2013) Collagen IV-Modified Scaffolds Improve Islet Survival and Function and Reduce Time to Euglycemia. *Tissue Engineering. Part A* 19(21–22): 2361–2372. DOI: 10.1089/ten.tea.2013.0033.

Yau M, Maclaren NK and Sperling MA (2000a) Etiology and Pathogenesis of Diabetes Mellitus in Children and Adolescents. In: Feingold KR, Anawalt B, Boyce A, et al. (eds) *Endotext*. South Dartmouth (MA): MDText.com, Inc. Available at: <http://www.ncbi.nlm.nih.gov/books/NBK498653/> (accessed 28 December 2022).

Yau M, Maclaren NK and Sperling MA (2000b) Etiology and Pathogenesis of Diabetes Mellitus in Children and Adolescents. In: Feingold KR, Anawalt B, Boyce A, et al. (eds) *Endotext*. South Dartmouth (MA): MDText.com, Inc. Available at: <http://www.ncbi.nlm.nih.gov/books/NBK498653/> (accessed 28 December 2022).

Yokoyama Y, Hattori S, Yoshikawa C, et al. (2009) Novel wet electrospinning system for fabrication of spongiform nanofiber 3-dimensional fabric. *Materials Letters - MATER LETT* 63: 754–756. DOI: 10.1016/j.matlet.2008.12.042.

- Yuan S, Xiong G, Wang X, et al. (2012) Surface modification of polycaprolactone substrates using collagen-conjugated poly(methacrylic acid) brushes for the regulation of cell proliferation and endothelialisation. *Journal of Materials Chemistry* 22(26). The Royal Society of Chemistry: 13039–13049. DOI: 10.1039/C2JM31213A.
- Zhang Q, Gonelle-Gispert C, Li Y, et al. (2022a) Islet Encapsulation: New Developments for the Treatment of Type 1 Diabetes. *Frontiers in Immunology* 13. Available at: <https://www.frontiersin.org/articles/10.3389/fimmu.2022.869984> (accessed 28 December 2022).
- Zhang Q, Gonelle-Gispert C, Li Y, et al. (2022b) Islet Encapsulation: New Developments for the Treatment of Type 1 Diabetes. *Frontiers in Immunology* 13. Available at: <https://www.frontiersin.org/articles/10.3389/fimmu.2022.869984> (accessed 28 December 2022).
- Zorzi D, Phan T, Sequi M, et al. (2015) Impact of Size in Pancreatic Islet Transplantation and Potential Interventions to Improve Outcome. *Cell transplantation* 24(1): 11–23. DOI: 10.3727/096368913X673469.

## LIST OF PUBLICATIONS

**Wilson, J.**, Rahul, V.G., Thomas, L.V. and Nair, P.D., 2022. Three-dimensional wet electrospun scaffold system for the differentiation of adipose-derived mesenchymal stem cells to islet-like clusters. *Journal of Tissue Engineering and Regenerative Medicine*, 16(12), pp.1276-1283.

Prasad, A.S., **Wilson, J.** and Thomas, L.V., 2023. Designer injectable matrices of photocrosslinkable carboxymethyl cellulose methacrylate based hydrogels as cell carriers for gel type autologous chondrocyte implantation (GACI). *International Journal of Biological Macromolecules*, 224, pp.465-482.

VG, R., **Wilson, J.**, V. Thomas, L. and Nair, P.D., 2022. Assessing the 3D Printability of an Elastomeric Poly (caprolactone-co-lactide) Copolymer as a Potential Material for 3D Printing Tracheal Scaffolds. *ACS omega*, 7(8), pp.7002-7011.

Sreenivasan, P., **Wilson, J.**, Nair, P.D. and Thomas, L.V., 2020. Polycaprolactone solution-based ink for designing microfluidic channels on paper via 3D printing platform for biosensing application. *Polymers for Advanced Technologies*, 31(5), pp.1139-1149.

Mohan, N., **Wilson, J.**, Joseph, D., Vaikkath, D. and Nair, P.D., 2015. Biomimetic fiber assembled gradient hydrogel to engineer glycosaminoglycan enriched and mineralized cartilage: An in vitro study. *Journal of Biomedical Materials Research Part A*, 103(12), pp.3896-3906.

**Wilson J.**, V.G Rahul, V.S Harikrishnan, Thomas L, Anil Kumar T.V, Nair P.D. A tissue engineered pancreatic transplantation device for the safe delivery of stem cell derived islet-like clusters to treat type 1 diabetes mellitus (under preparation).

**Wilson J.**, Nair P.D. Cell based therapy for Type I Diabetes mellitus: Recent advances (under preparation).

## **CONFERENCES AND TRAININGS**

- Attended asian biomaterials congress (ABMC-2017) held from October 25-27, 2017 at Trivandrum.
- Workshop on “ Application of Flow Cytometry in Health and Disease” conducted on 28<sup>th</sup>-31<sup>st</sup> Oct 2017 by The Cytometry Society of India.
- Presented a poster entitled “Three dimensional polymeric matrices encapsulating mesenchymal stem cells for augmenting the differentiation in to Islet like clusters” at Biomet 2018, Vellore Institute of Technology held on 26-28 July 2018.
- Given an oral presentation entitled “Bio-polymeric scaffold enhances 3-d differentiation of mesenchymal stem cells in to islet-like clusters” at 6<sup>th</sup> international conference on natural polymers in MG University held on 7-9 December 2018.
- Given an oral presentation on the abstract entitled “Functionalised three dimensional scaffold system for enhanced insulin secretion of mesenchymal stem cell derived islet like clusters” at the International e-Conference on Biopolymers (APA bioforum-2022) organised jointly by Asian Polymer Association (APA) and Indian Chitin and Chitosan society from 14-16 July 2022.

## **AWARD**

- Won the student oral contest, for the abstract entitled “Functionalised three dimensional scaffold system for enhanced insulin secretion of mesenchymal stem cell derived islet like clusters” presented at the International e-Conference on Biopolymers (APA bioforum-2022) organised jointly by Asian Polymer Association (APA) and Indian Chitin and Chitosan society from 14-16 July 2022.